GEOMETRIC PERFORMANCE OF THE GLOBAL POSITIONING SYSTEM

A. H. Bogen

Aerospace Corporation

Prepared for:

Air Force Systems Command

21 June 1974

Approved by

G. M. Hatch, Director
Satellite Office
NAVSTAR/GPS
Advanced Orbital Systems Division
Systems Engineering Operations

Publication of this report does not constitute Air Force approval of the report's findings or conclusions. It is published only for the exchange and stimulation of ideas.

WALTER J. LARKIN, Captain, USAF
Director, Configuration Management

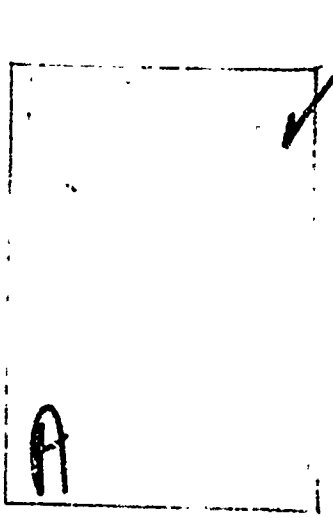

UNCLASSIFIED

SECUPITY CLASSIFICATION OF THIS PAGE *(When Data Entered)*

AD783 210

REPORT DOCUMENTATION PAGE		READ INSTRUCTIONS BEFORE COMPLETING FORM
1 REPORT NUMBER SAMSO-TR-74-169	2. GOVT ACCESSION NO.	3. RECIPIENT'S CATALOG NUMBER
4. TITLE *(and Subtitle)* GEOMETRIC PERFORMANCE OF THE GLOBAL POSITIONING SYSTEM		5. TYPE OF REPORT & PERIOD COVERED Final
		6. PERFORMING ORG. REPORT NUMBER TR-0074(4461-02)-2
7. AUTHOR(s) A. H. Bogen		8. CONTRACT OR GRANT NUMBER(s) F04701-73-C-0074
9. PERFORMING ORGANIZATION NAME AND ADDRESS The Aerospace Corporation El Segundo, Calif. 90245		10. PROGRAM ELEMENT, PROJECT, TASK AREA & WORK UNIT NUMBERS
11. CONTROLLING OFFICE NAME AND ADDRESS Space and Missile Systems Organization Air Force Systems Command Los Angeles, Calif. 90045		12. REPORT DATE 21 June 1974
		13. NUMBER OF PAGES ~~109~~ 111
14 MONITORING AGENCY NAME & ADDRESS*(if different from Controlling Office)*		15. SECURITY CLASS. *(of this report)* Unclassified
		15a. DECLASSIFICATION/DOWNGRADING SCHEDULE

16. DISTRIBUTION STATEMENT *(of this Report)*

Approved for public release; distribution unlimited

17. DISTRIBUTION STATEMENT *(of the abstract entered in Block 20, if different from Report)*

18. SUPPLEMENTARY NOTES

19. KEY WORDS *(Continue on reverse side if necessary and identify by block number)*

GDOP
Global Positioning System
Near real-time navigation
Satellite-induced Doppler
Visibility; user/ground station

20 ABSTRACT *(Continue on reverse side if necessary and identify by block number)*

This report is intended to identify and evaluate some of the factors affecting the Global Positioning System navigation performance for the satellite configurations, as well as system design issues related to the orbital geometry. The report addresses the user visibility, ground station visibility, satellite-induced Doppler, geometric dilution of precision, selection of satellites for optimum navigation conditions, and satellite eclipses. The levels of nominal geometric performance which can be achieved are establish established

DD FORM 1473 (FACSIMILE)

UNCLASSIFIED

SECURITY CLASSIFICATION OF THIS PAGE *(When Data Entered)*

CONTENTS

FIGURES

FIGURES (Continued)

FIGURES (Continued)

TABLES

1. INTRODUCTION

The Global Positioning System (GPS) navigation program is divided into two development phases that employ 4- and 9-satellite configurations, respectively. The operational GPS (Phase III) configuration consists of 24 satellites. In each of these configurations the navigation signals are generated and transmitted by the satellites. The reception of four navigation signals from different satellites enables the system user to almost instantaneously calculate his position and velocity in three dimensions. The user may also navigate by using three or two satellites if an accurate altimeter and/or clock is available to him.

The most significant performance parameter of the GPS is the degree of navigation accuracy which can be obtained by the user. The ability to navigate and the attainable navigation accuracy is intimately coupled with the choice of orbit configuration.

It is the purpose of this report to identify and evaluate some of the factors affecting the GPS navigation performance for each of the development phases and system design issues related to the orbital geometry. This report addresses the user visibility, ground station visibility, satellite-induced Doppler, geometric dilution of precision (GDOP), selection of satellites for optimum navigation conditions, and satellite eclipses. The report establishes the levels of nominal geometric performance which can be achieved.

2. CONSTRAINTS AND CONDITIONS FOR REAL-TIME NAVIGATION

2.1 FACTORS AFFECTING PERFORMANCE

The GPS satellite navigation system enables the system user to navigate in near real time by calculation of position and velocity based upon pseudorange and pseudorange rate measurements from each of four satellites in view.

To determine position and velocity, the user cross-correlates the pseudorandom phase-shift-keyed (PSK) codes generated in the receiver with the codes of the navigation signals emitted by the satellites. The user measures the relative phases between the local codes and a reference code driven by the receiver frequency reference, and establishes an apparent range called a pseudorange. Since the user frequency reference is not synchronized to satellite time, the measurements are pseudoranges. They are offset from the true geometrical ranges by the receiver oscillator bias (which is common to all four pseudoranges). At the same time, the user is also measuring range rate in each channel which is obtained by extracting the Doppler from the signal carriers. Disregarding signal propagation delays and other effects, these range measurements are accurate to the extent the satellite and user clocks (or oscillators) are synchronized.

If the user clock is perfectly synchronized with the satellite clocks (and they in turn are synchronized with each other) and provided the positions of the satellites are known, the user will need to obtain only three range measurements to different satellites in order to calculate position. The user position is simply the intersection of the three spheres centered at the satellites having the radii of the range measurements. However, the user clocks are not normally synchronized with the satellite clocks and the user needs a minimum of four independent pseudorange measurements to different satellites to permit calculation of his position. This can be done in two ways: (1) four simultaneous and independent range measurements

provide three range differences which can be used to calculate the intersection of three hyperboloids of revolution which define the user position vector; or (2) four independent pseudorange measurements can be used to calculate the user position and the determination of system time (i.e., the three-dimensional position vector and the oscillator time bias) by the simultaneous solution of four equations.

Irrespective of the algorithm, the general navigation user who is equipped with a ranging receiver and computer requires (as a minimum) the following information to enable him to nearly instantaneously compute his position:

a. Satellite ephemerides

b. Apparent satellite clock phase with respect to system time, including electronic group delay effects

c. Ionospheric and tropospheric group delays, measured or modeled.

In addition, the following conditions must exist:

a. A minimum of four satellites must be simultaneously visible to the dynamic user who is not equipped with external aids

b. The satellites' positions relative to the user must provide a geometry (GDOP) which results in good navigation accuracy

c. An adequate satellite RF signal strength and quality must be available to the user to permit navigation signal acquisition and user-satellite range measurements.

Depending upon the time required for signal acquisition, it becomes important to know how long signal lock can be maintained using the same satellites before the orbital geometry (and navigation accuracy) deteriorates and the extent of this deterioration.

2.2 NAVIGATION ACCURACY AND GEOMETRIC DILUTION OF PRECISION

Navigation accuracy is here defined to be the estimated statistics of the error magnitudes in the user position vector, where the estimate of these errors contains the correlated dependence between the error sources

(e.g., satellite tracking, ionospheric delays, equipment group delay, multipath, and receiver noise) projected through the user satellite geometry.

The degree to which the pseudoranging errors contribute to navigation accuracy is thus magnified or diluted by the user-satellite geometry. This dilution of range measurement precision is expressed by the performance index, GDOP, which is the ratio of the position error statistics to the pseudoranging error standard deviation under the stipulation that all satellite ranging measurement errors are expressed as uncorrelated errors with equal standard deviations Thus, GDOP depends only on the geometry defined by the relative position of the satellites and the user at the time of the measurements, and is in no way dependent on the magnitude of the pseudoranging errors.

The GDOP is the most important parameter for the selection of orbit elements and the definition of constellations. The mathematical definition of GDOP used here is defined in Appendix A.

3. GLOBAL POSITIONING SYSTEM DESCRIPTION

The major segments of the GPS are: (1) the control system, (2) the space system, and (3) the user system. These segments, and the various RF links required for system operations and their interfaces, are defined in Reference 1 and depicted in Figure 1.

3.1 CONTROL SYSTEM SEGMENT

The control system, as currently envisioned for the various phases of the GPS, consists of a master control station (MCS) and several monitor stations (MS), and one or more upload stations (UL). The MCS provides for the data processing and computations required to support the navigation and tracking functions based upon the L-band measurements obtained by the monitor stations. The upload station(s) provides each satellite with the navigation data required by the user. The data for satellite memory update are transmitted by the upload station at S-band frequencies. The navigation pseudorandom noise (PRN) signals are transmitted by each satellite using two carrier frequencies in L-band (L_1 and L_2). The monitor stations obtain one-way ranges to individual satellites from the received L-band signals by correlating generated versus received PRN ranging codes using the monitor station clock as time reference. These measurements provide the basic input to the generation of the satellite ephemerides and the determination of satellite clock biases; they also enable the transfer of the MCS master time to the monitor stations.

The dual frequency one-way range measurements (L_1 and L_2) at the monitor stations also serve as the primary updating input to the spatial and temporal atmospheric group delay prediction model. The coefficients of this model, together with the satellite ephemeris, clock, and other data required for navigation, define the satellite state vector. This vector is provided to the satellite via the S-band navigation control uplink, is stored in the satellite memory, and then superimposed upon the L-band PRN ranging code for the navigator's use.

3.2 SPACE SYSTEM SEGMENT

The space system baseline consists of several satellites in 12-hour circular orbits. Each satellite carries a payload consisting of an S-band receiver, a processor-memory unit, PRN sequence generators, a data modulator, L-band transmitters, and appropriate antenna systems. The satellite L-band antennas are directed towards earth center at all times and provide adequate RF power for all users. The PRN navigation signals at L_1 and L_2 frequencies are generated in the satellites using a very stable atomic clock as frequency reference. The auxiliary navigation signal at L_2 is synchronized with the primary signal at L_1 and transmitted for the purpose of instantaneous assessment of the local signal propagation group delay by appropriately-equipped users.

3.3 USER SYSTEM SEGMENT

The user system consists of various classes of military and civilian users. The satellite L-band navigation signals are used to establish position and velocity in three dimensions for a wide range of user applications and dynamic conditions. The user is equipped with an omnidirectional antenna, a correlation receiver, a computer, and any auxiliary displays required to perform his mission.

As described earlier, the user obtains pseudorange and pseudorange-rate measurements from selected satellites in view, and extracts the navigation data superimposed upon the navigation signals. This information is provided to the user's computer. The computer processes the data and calculates the position and velocity vector information in any chosen coordinate system and may calculate system time if required.

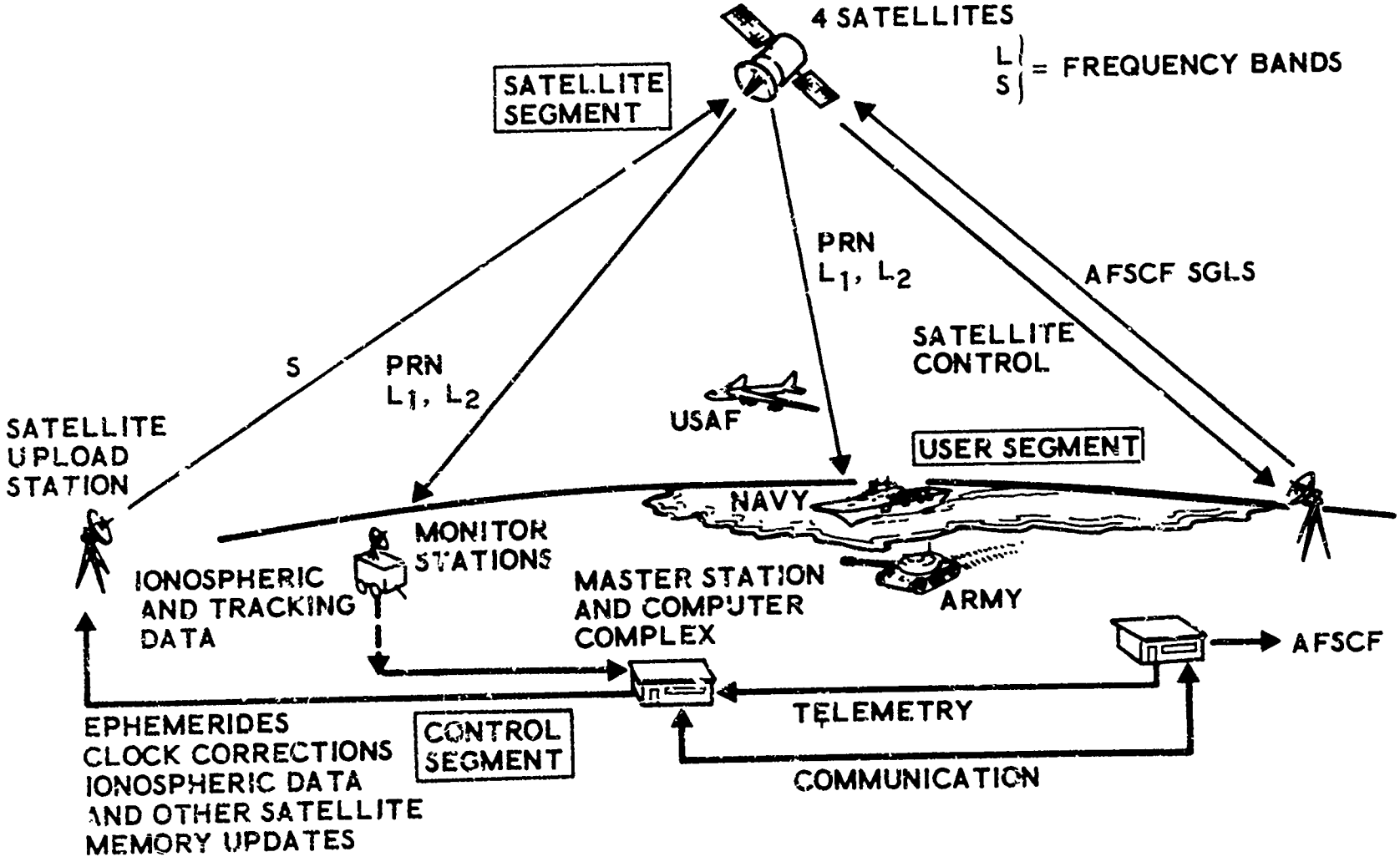

Figure 1. GPS, System Operation Interfaces

4. GPS PHASE III GEOMETRIC PERFORMANCE

4.1 SATELLITE DEPLOYMENT

The baseline GPS orbit configuration consists of 24 satellites deployed in circular 63-deg inclined, subsynchronous, 12-hour orbits. Eight satellites are uniformly distributed in each of three orbit planes whose celestial ascending nodes are separated by 120 deg. The phasing or staggering of satellites between orbit planes is such as to produce optimum navigation geometry. Table 1 defines the nominal orbit parameters, and Figure 2 indicates the relative position of the satellites in one plane and shows one of the satellite ground tracks.

A short discussion of the performance of other subsynchronous constellations leading to the selection of the above baseline is included in Section 4.3.

4.2 SATELLITE VISIBILITY

One criterion for real-time navigation is that a minimum of four satellites be simultaneously visible to a user at any time. The percent probability that a given number of satellites is simultaneously visible to a user on a global basis is shown in Figure 3. The users are uniformly distributed over the surface of the earth and the observations are uniformly distributed in time. The distribution includes all satellite observations for all user longitude and latitude positions throughout the orbit period. Because the users are uniformly distributed, the number at a given latitude decreases with the cosine of the latitude. It is seen that the number of satellites observed simultaneously is never less than 6 and never greater than 11 for a 5-deg masking (elevation) angle, and never less than 4 nor greater than 9 for a 10-deg angle. The percent cumulative distribution indicates that the probability of observing 9 or more satellites is 44.3 and 11.7 percent for the 5- and 10-deg elevation angles, respectively.

The percent cumulative probability that a given number of satellites will be observed simultaneously as a function of user latitude for all user longitude positions is shown in Figure 4. The distribution indicates that satellite visibility at higher latitudes is better than at other latitudes, and that at higher elevation angles the probability of a high number of satellite sightings is reduced at all latitudes. Figure 5 shows the cumulative distribution of the user-satellite elevation angles. This graph shows the probability that at any position and at any arbitrary time the user will observe a given satellite elevation angle or a higher elevation. It is observed that a 50 percent chance exists for users to observe satellites above 5 deg.

4.3 GDOP PERFORMANCE

The user's ability to navigate depends not only on the availability of four satellites but also on the relative positions between the user and the satellites. The GDOP is treated here as a statistical measure in a time-space domain where the users obtain fixes from four satellites at uniformly-distributed surface locations and time intervals. These uniformly-distributed fixes furnish the statistical population used for the evaluation of GDOP, based upon the particular set of four satellites which provide the minimum PDOP position error (see Appendix B). The identity of this set of satellites can be found from one of the number of combinations of satellites visible to the user, taken four at a time. Each fix is unique in that no other set of four satellites results in better navigation accuracy for that particular geographic position and time. The computational process involves the evaluation of the appropriate elements of the covariance matrix (see Appendix A) given by

$$\mathrm{COV}\left(\delta\bar{X}_u\right) = \left(G_u^T G_u\right)^{-1}$$

for each combination of visible satellites (N) taken four at a time; i.e.,

$$\binom{N}{4} = \frac{N!}{(N-4)!\ 4!}$$

With the number of satellites visible to the user and the global position-time population statistics sampling just mentioned, this computation process becomes very lengthy.

As discussed in Appendix B, the performance index PDOP is inversely proportional to the volume of the inscribed tetrahedron formed by the four user-to-satellite unit vectors. Here, the maximum volume (or minimum PDOP) is established by selecting the highest satellite in the sky and is found amongst one of the number of combinations of the remaining satellites visible to the user, taken three at a time. The PDOP is computed only for the combination having maximum volume. This selection process provides results identical to the previous approach and suggests a simple algorithm for the selection of satellites in the user computer (see Section 4.4).

The sensitivity of performance to the number of GPS satellites in each plane and the orbital inclination is discussed in the following paragraphs. Table 2 shows the position at epoch of the 3 × 7, 3 × 8, and 3 × 9 orbit constellations. It is observed that the orbit phasing and staggering between planes are symmetric about plane No. 3. These positions provide optimum geometric performance for these constellations.

Figures 6, 7, and 8 show the cumulative probability distribution of PDOP for orbit inclinations between 40 and 90 deg at 5- and 10-deg elevation angles, based upon the selection method of maximum unit vector volume indicated above. For optimum inclinations at 5-deg elevation angles, there is hardly any difference in performance between the 3 × 8 and the 3 × 9 constellations. The addition of three satellites (relative to the 3 × 8) does not provide a justifiable increase in performance; however, for the 3 × 7 constellation, the addition of three satellites greatly improves performance. At 5-deg elevation angles, the 3 × 9 constellation has an optimum inclination at approximately 55 deg that provides a PDOP performance of 4.3 or lower for 99.99 percent of time-space. Correspondingly, the 3 × 8 constellation provides for the same percentile, a PDOP of 4.4 or lower for all inclinations between 50 and 65 deg. The global geometric performance of the 3 × 8 constellation is very insensitive to the value of inclination in this region.

Since for GPS Phase I, an inclination of 63 deg has been selected to maximize on-orbit payload weight with launches from the Western Test Range, the above insensitivity appears to provide acceptable navigation performance for the 3 × 8 constellation at the 63-deg inclination.

If a 10-deg (rather than 5-deg) elevation mask is considered for the 3 × 8 constellation at an inclination of 63 deg, the resultant performance provides PDOP equal to or less than 4.3 for 99 percent of time-space. The 3 × 8 constellation at 63-deg inclination is, therefore, chosen for the GPS baseline.

Figure 9 shows the global cumulative distribution of PDOP, HDOP, VDOP, and TDOP for the GPS, 12-hour, 63-deg inclination, 24-satellite constellation defined in Table 1. It is observed that TDOP will be below a factor of 2.2 for 99.99 percent of time-space, and that for the same probability, VDOP will be equal to or less than 4.2. Figures 10 through 14 show how the various GDOPs vary with latitude. Figures 15 through 18 provide a comparison between PDOP, HDOP, VDOP, and TDOP at 5- and 10-deg masking angles. By removing all satellites between 5 and 10 deg from the statistical population, the average deterioration of approximately 10 percent occurs for about 99 percent of time-space; the system will provide inferior conditions 1 percent of the time on a global scale.

4.4 SATELLITE SELECTION

One of the more frequent questions regarding the operational use of the GPS pertains to the process of selecting and acquiring the satellite signals. Apart from the signal mechanization processes inherent in the user receiver, and the data manipulation and computer algorithms required, the time to first fix (i.e., the time consumed before the user obtains information about this position and velocity) is a significant system parameter.

Since this acquisition process includes four different satellite signals, it becomes desirable to find a method to identify the optimum set of four satellites which will provide maximum navigation accuracy for the longest possible time over a wide geographic area. It must be determined

how at any time of the day, at some arbitrary location, a user can select the optimum set of four satellites, and when selected, for how long they can be used before navigation accuracy deteriorates to an undesirable level. Since the user might be moving at a high speed, it is also of interest to know something about the geographic areas which can be supported by the same set of four satellites. The selection process clearly involves some form of almanac or computational capability accessible to the user. A proposed method to accomplish this is discussed in the following paragraphs.

The number of combinations in a population of 24 satellites, taken four at a time, is 10,626. Approximately 310 different combinations provide the identities of the optimum four satellites on a global scale at any arbitrary time. These optimum combinations will change rapidly with time due to the movement of the satellites and the user; a change in time of a few minutes and/or a change in longitude or latitude of a few degrees may cause another combination of satellites to be optimum for that time and place. It is with this in mind that a set of algorithms has been developed which might be used to identify the optimum set of four satellites and to assess the impact on navigation accuracy when the same set is used for some length of time. (The best set of four used for an instantaneous fix is not the same as the optimum set which can be used advantageously over some length of time.)

Since the volume of the tetrahedron formed by the four user-to-satellite unit vectors is inversely proportional to PDOP, the instantaneous rate of change of this volume provides a clue to the expected conditions in the future. This prognostic condition, however, would not be valid if one of the satellites disappeared from view in the meantime. Therefore, the satellite population providing the optimum set of four includes only those satellites whose elevation and velocity make them visible to the user during the projected period of use.

Appendix B describes some details of the algorithms used. Here it is assumed that ephemerides in the form of the six Keplerian elements

for all 24 satellites in the 3 × 8 GPS constellation are available in the user computer, because a prior knowledge of crude satellite ephemerides are required to enter the system in the first place. Clearly, some alternate form of the ephemerides would equally suffice. With an estimate of position and time and with appropriate subroutines (which represent basic parts of the algorithms for the navigation determination process itself), the user can easily compute the satellite position and velocity vectors and hence determine which satellites are visible. Having identified the highest satellite in the sky and eliminated those which will be below the horizon after a given time interval, an estimate of the mean geometric unit vector volume (between now and some future time) can be obtained for all the combinations available from the satellite population. Comparing the mean volumes of these combinations, the one having the maximum volume identifies the set of four satellites to be used and hence the navigation signal codes. Electronic acquisition of these signals can now begin. It is to be emphasized that the crude ephemerides identified above are not the same ephemerides that are provided to the user as part of the navigation data superimposed upon the L-band downlink navigation signal.

Figure 19 shows, for a given geographic position, how PDOP varies as a function of time when an optimum set of four satellites is selected every 30 min and signal lock is maintained for the same period of time. Sometimes the performance increases and at other times decreases due to the specific availability of the optimum set of four. For comparison, the "best" performance (i.e., the optimum for that instant in time without regard for the future) is also plotted. The difference is the performance penalty paid when the user wishes to continue using the same set of four for the time interval considered. Clearly this penalty increases as the time interval increases.

Figure 20 shows the cumulative statistical distribution of PDOP based upon navigation fixes obtained uniformly over the time-space domain on a global scale. The probability of obtaining a given performance or better is presented as a function of the time interval the user continues

using the optimum set of four satellites. Also presented, for comparison, is the best condition (see Figure 9) resulting from fixes the user can obtain for instantaneous use without any external aid. It is seen that the magnitude of system deterioration increases drastically the longer the user retains the same set. As an example, at a guaranteed performance level of PDOP ≤8, the probability of inferior navigation conditions during the orbit period is 8 percent if the same four optimum satellites are used for one hour.

For the same conditions, Figure 21 shows the length of time the optimum set of four satellites can be used for a given performance level. For a reasonable level of PDOP ≤ 5, the user has a 99 percent probability of continued use of the same satellites for 20 min. This time includes the time for satellite identification and electronic signal acquisition.

Figure 22 shows the magnitude of the global areas where the same sets of four satellites provide optimum navigation performance versus the frequency with which they occur. These areas vary in size from 20,000 to 5,000,000 sq nmi. Areas in the order of 160,000 sq nmi occur more frequently than any other size and account for 16 percent of the total time. The cumulative distribution indicates a 50 percent chance of encountering areas of 300,000 sq nmi.

Table 3 indicates the specific combination* of the four instantaneous optimum satellites as they occur for each longitude and latitude at four instances in time, 7.5 min apart. On an average for the entire globe, at any arbitrary time of the day, approximately 310 such combinations result from the selection process described above. The geographic areas for each of these combinations are seen to change in size and to move with respect to time. Adjacent areas have combination numbers which would indicate that optimum conditions can be attained when crossing the boundary

*A number between 1 and 10,626 that identifies the specific combination and particular identities of the 24 satellites visible at that instant of time, taken four at a time.

into another area by changing only one of the four satellites. As an example, the following combination numbers [K] define the satellite identities [I]:

Combination [K]	Satellite Identity [I]	Identity Change
2837	2 9 18 20	
2774	2 9 11 20	18, 11
113	1 2 9 11	20, 1
1212	1 9 10 11	2, 10

The need to acquire another satellite signal to maintain optimum condtions appears to be a strong function of user speed, present position, and heading. This "handover problem" should be a subject of later investigation.

4.5 DOPPLER

The instantaneous satellite fixes required by the user for computation of position and velocity require knowledge of the apparent velocity of the satellite. In the process of signal acquisition, the uncertainty of the carrier frequency shift attributable to the satellite range rate or Doppler must be much less than the signal bandwidth of the receiver.

Here Doppler is defined as that component of the satellite velocity vector which lies along the line of sight between the user and the satellite. The Doppler rate is the rate of change of this velocity component. Figure 23 shows the maximum Doppler contributed by the satellites and observed by users located at the indicated longitudes and latitudes. These values are symmetric in northern and southern latitudes and are the absolute maxima occurring sometime during the orbit period, assuming all the satellites to be above a 5-deg elevation angle. The largest value of Doppler is approximately ±2705 fps and the largest value of Doppler rate is approximately ±0.514 fps/sec. At the center frequency of 1575 MHz this corresponds to 4.25 kHz and 0.81 Hz/sec, respectively.

4.6 SOLAR ECLIPSES

Satellite operation during solar eclipses is a major consideration in satellite design. In particular, the duration and frequency of eclipses impose design constraints which not only affect the design of the satellite electrical system, but other subsystems as well.

Figure 24 shows the dates of solar eclipses for satellites deployed in any orbit plane whose right ascension (Ω) varies between 0 and 360 deg. The longest periods of daily eclipsing last for 45 days for satellites in the plane whose Ω = 0 deg, and occur at the equinoxes. The shortest periods last 28 days when the orbit plane is located at Ω = 180 deg. This difference is due to the different inertial orientation of the orbit planes coupled with the change of the sun declination at these times.

For all conditions, due to the zero eccentric orbits, the maximum duration of all eclipses will last slightly less than 56 min, conservatively based upon the assumption of a cylindrical shadow rather than the conic umbra. For satellites in the same orbit plane, none will be eclipsed simultaneously, but rather each satellite will be eclipsed 1.5 hours apart.

The relative inertial separation between orbit planes for this configuration is 120 deg. If it is assumed that the three orbit planes are located at Ω = 110, 230, and 350 deg, the two eclipse seasons will occur six months apart and will last for approximately 30 days for orbit planes 1 and 2 and for 42 days for plane 3. For the satellites in the different orbit planes, none of them will be eclipsed simultaneously and six periods are completely clear of eclipses. The longest such noneclipse period lasts 50 days from day 136 to 186 (May-June).

Table 1. GPS Phase III – 3 × 8 Nominal Orbit Parameters

SAT. No.	ECCENTRICITY	ARGUMENT OF PERIGEE (deg)	RA OF AN (deg)	INCLINATION (deg)	MEAN ANOMALY (deg)	PERIOD (hrs)
1	0.00	0.00	0.00	63.00	15.00	12.00
2	0.00	0.00	0.00	63.00	60.00	12.00
3	0.00	0.00	0.00	63.00	105.00	12.00
4	0.00	0.00	0.00	63.00	150.00	12.00
5	0.00	0.00	0.00	63.00	195.00	12.00
6	0.00	0.00	0.00	63.00	240.00	12.00
7	0.00	0.00	0.00	63.00	285.00	12.00
8	0.00	0.00	0.00	63.00	330.00	12.00
9	0.00	0.00	120.00	63.00	-15.00	12.00
10	0.00	0.00	120.00	63.00	30.00	12.00
11	0.00	0.00	120.00	63.00	75.00	12.00
12	0.00	0.00	120.00	63.00	120.00	12.00
13	0.00	0.00	120.00	63.00	165.00	12.00
14	0.00	0.00	120.00	63.00	210.00	12.00
15	0.00	0.00	120.00	63.00	255.00	12.00
16	0.00	0.00	120.00	63.00	300.00	12.00
17	0.00	0.00	240.00	63.00	0.00	12.00
18	0.00	0.00	240.00	63.00	45.00	12.00
19	0.00	0.00	240.00	63.00	90.00	12.00
20	0.00	0.00	240.00	63.00	135.00	12.00
21	0.00	0.00	240.00	63.00	180.00	12.00
22	0.00	0.00	240.00	63.00	225.00	12.00
23	0.00	0.00	240.00	63.00	270.00	12.00
24	0.00	0.00	240.00	63.00	315.00	12.00

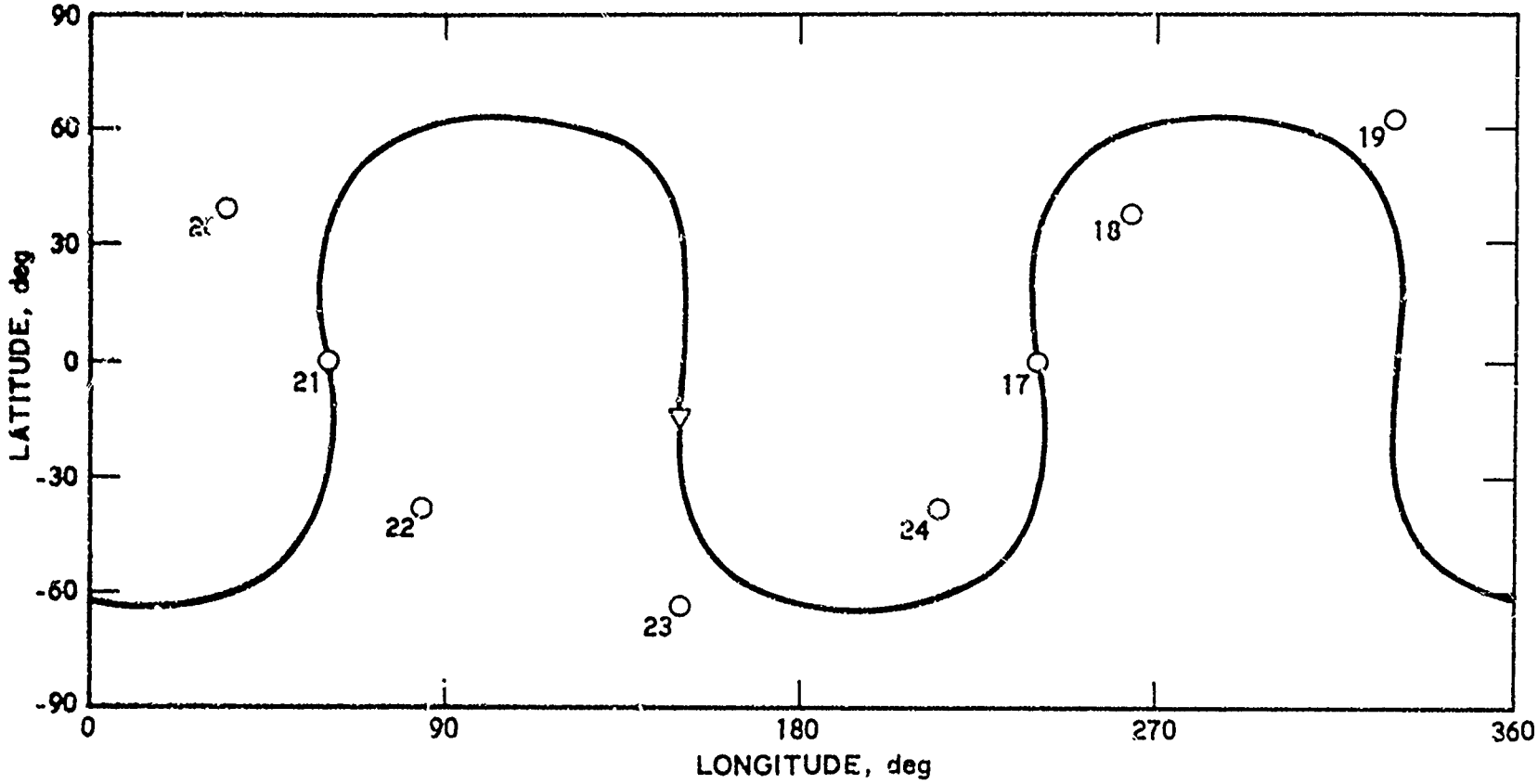

Figure 2. GPS Phase III – 3 × 8 Ground Track and Positions of Satellites in One Plane

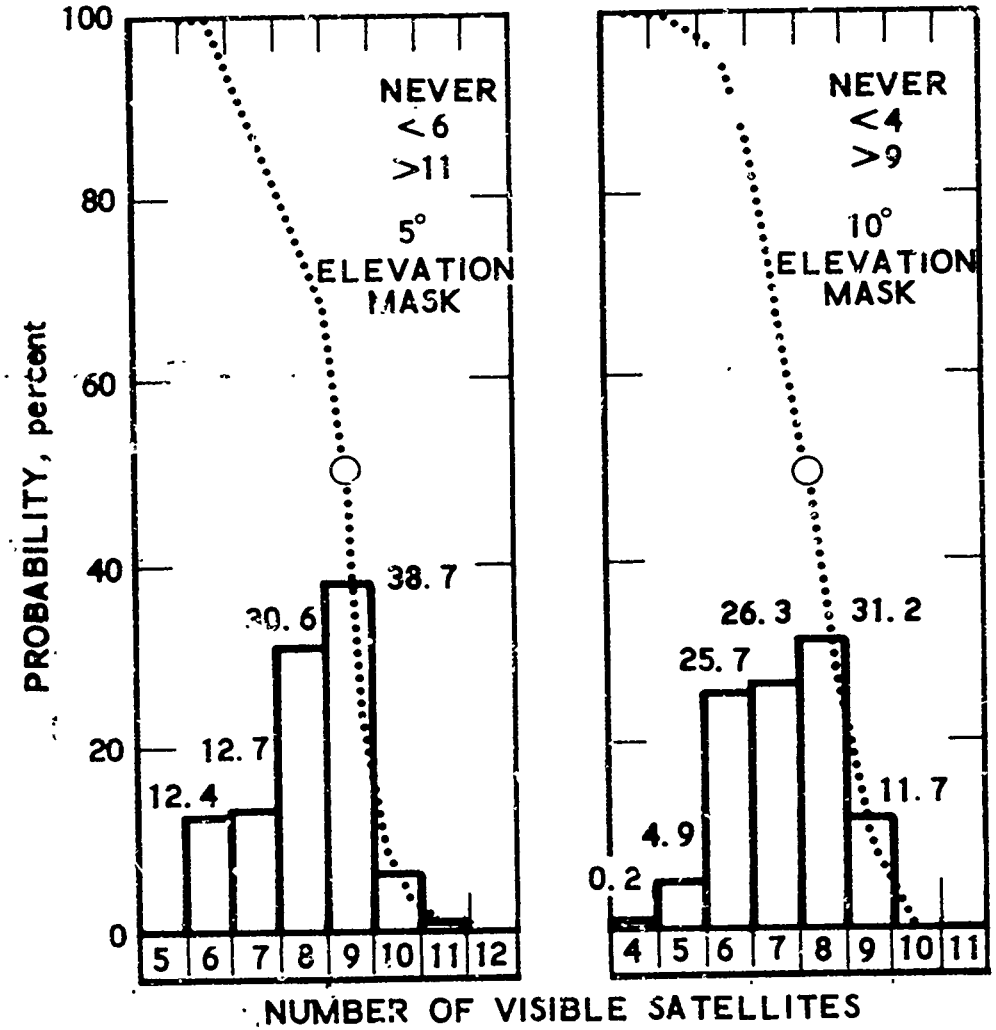

Figure 3. GPS Phase III — 3 × 8 Distribution of Global Satellite Visibility

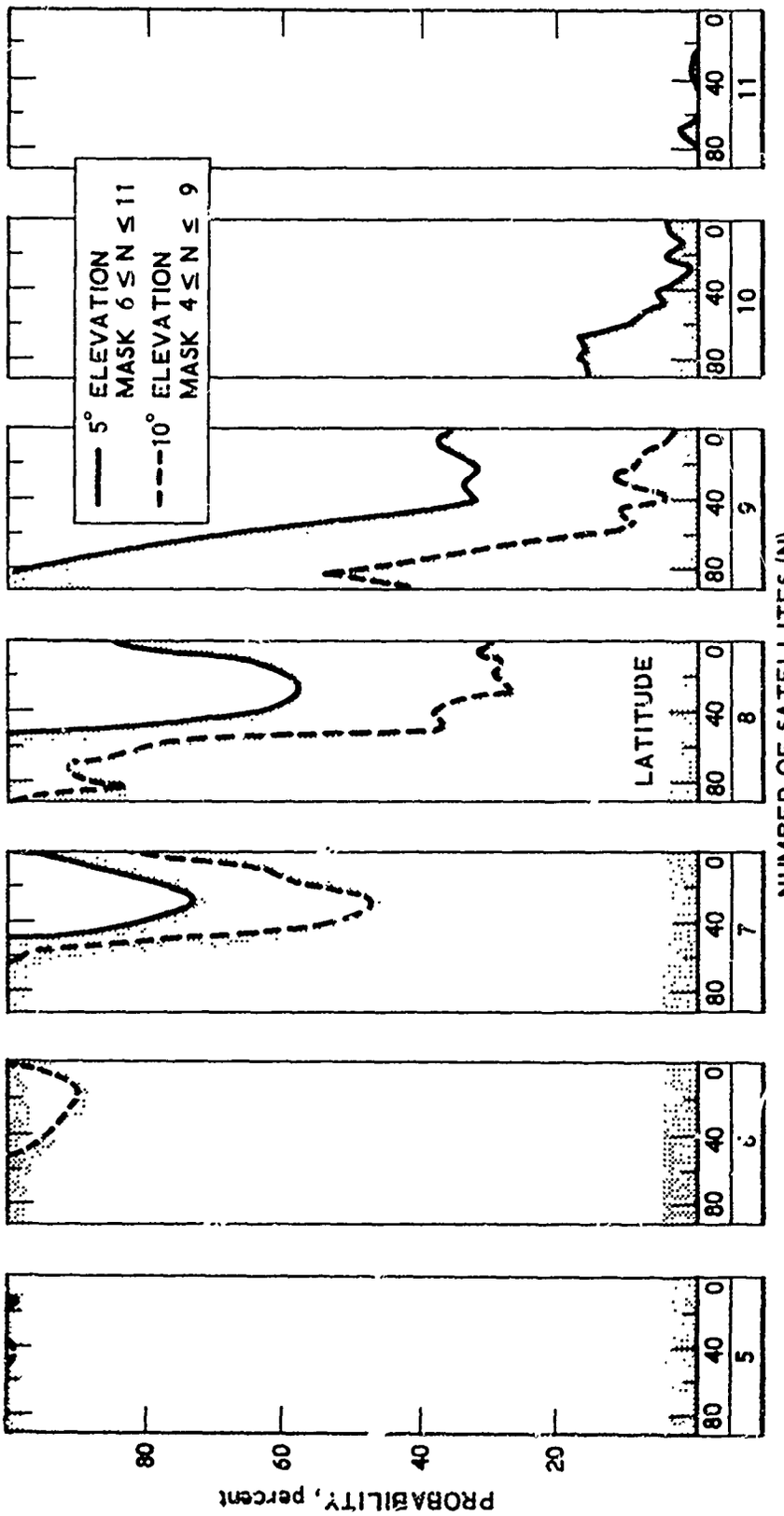

Figure 4. GPS Phase III – Probability Distribution of Global Satellite Visibility

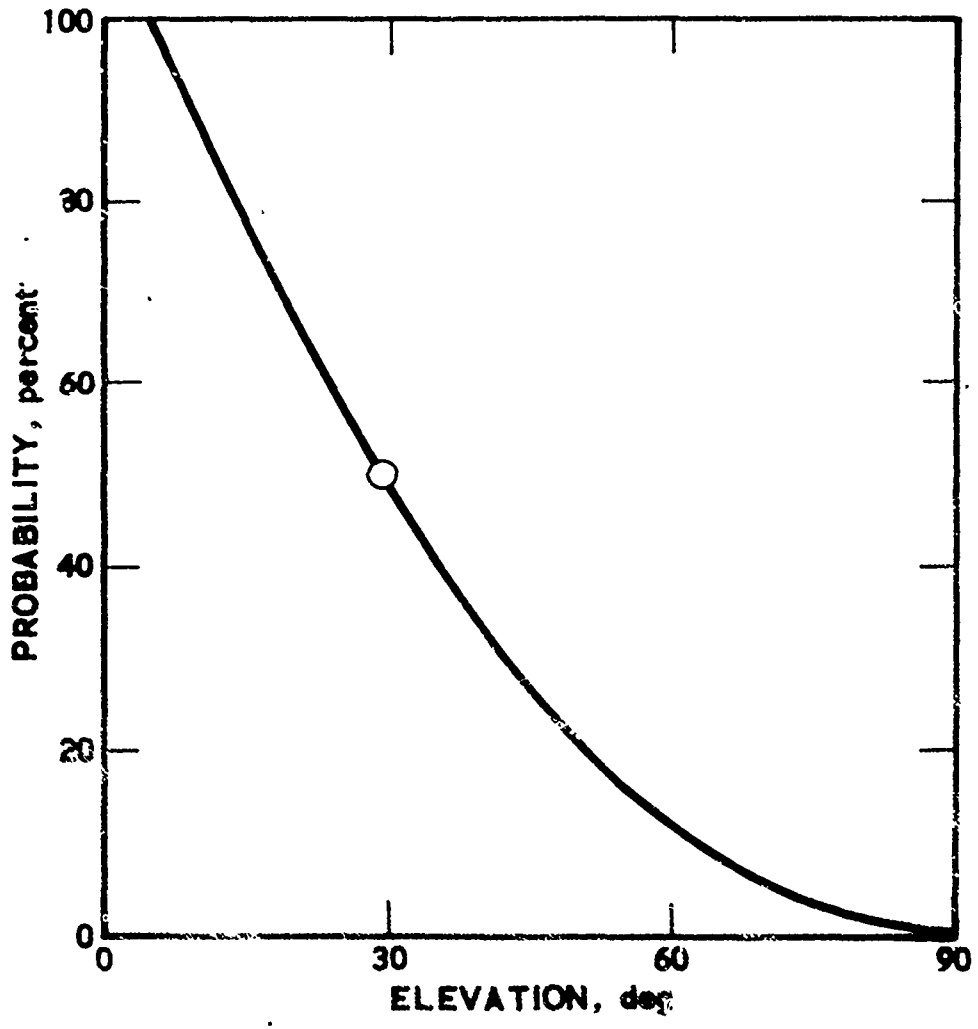

Figure 5. GPS Phase III – Cumulative User Elevation Angles for All Longitudes, Latitudes, and Times

Table 2. Positions at Epoch of the 3 × 7, 3 × 8, and 3 × 9 Satellite Constellations

Plane	ω	Ω	3 × 7		3 × 8		3 × 9	
			$\Delta\gamma$	t_o	$\Delta\gamma$	t_o	$\Delta\gamma$	t_o
1	0	0	(360/7) 51-3/7	(360/7/3) 17-1/7	(360/8) 45	(360/8/3) 15	(360/9) 40	(360/9/3) 13-1/3
2	0	120	51-3/7	(-)17-1/7	45	(-)15	40	(-)13-1/3
3	0	240	51-3/7	0	45	0	40	0

ω = argument of perigee
Ω = right ascension of ascending node
$\Delta\gamma$ = angular distance between satellites in one plane
t_o = position of a satellite relative to perigee at epoch

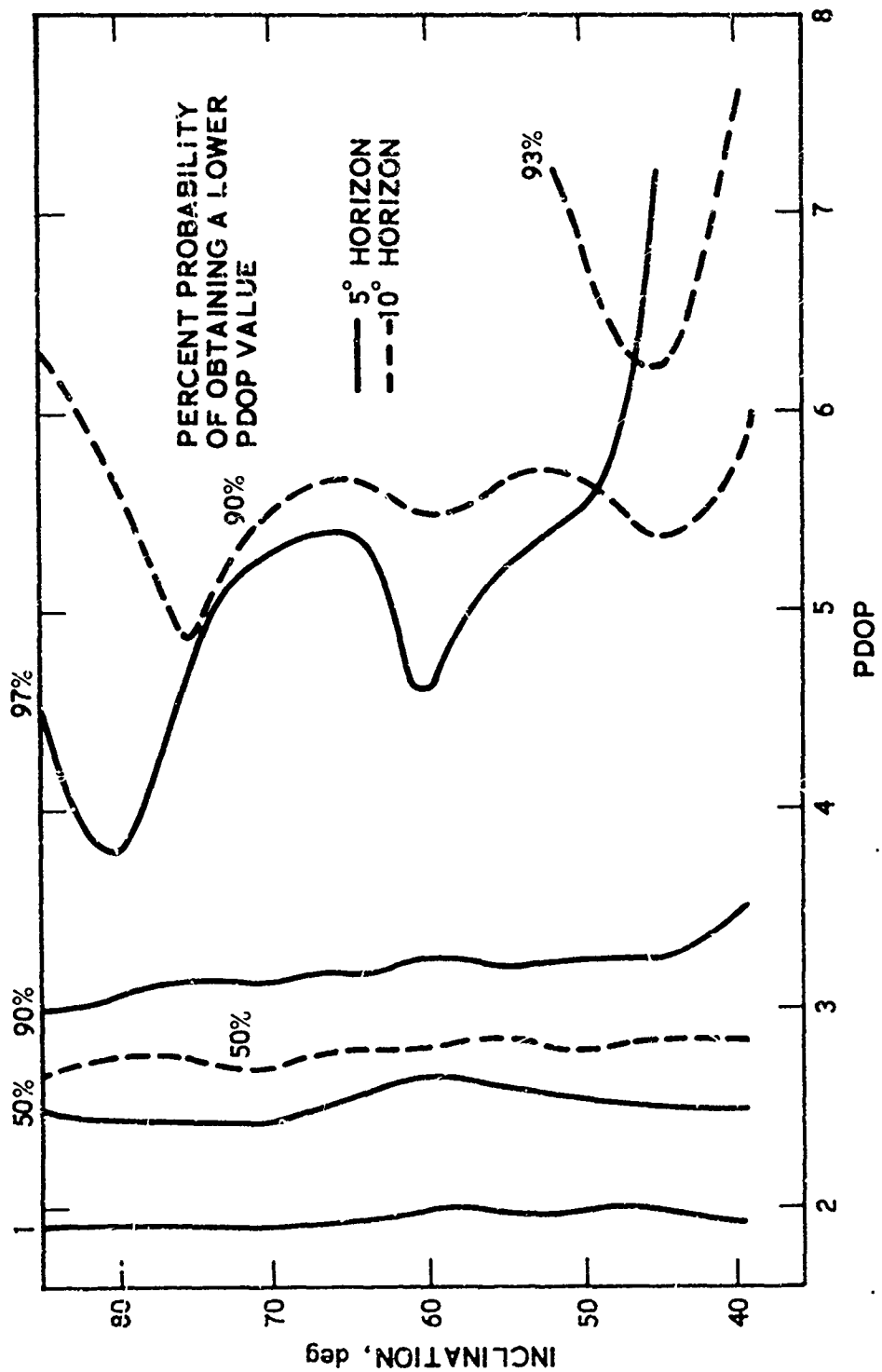

Figure 6. GPS Constellation — 3 × 7 Global Geometric Performance

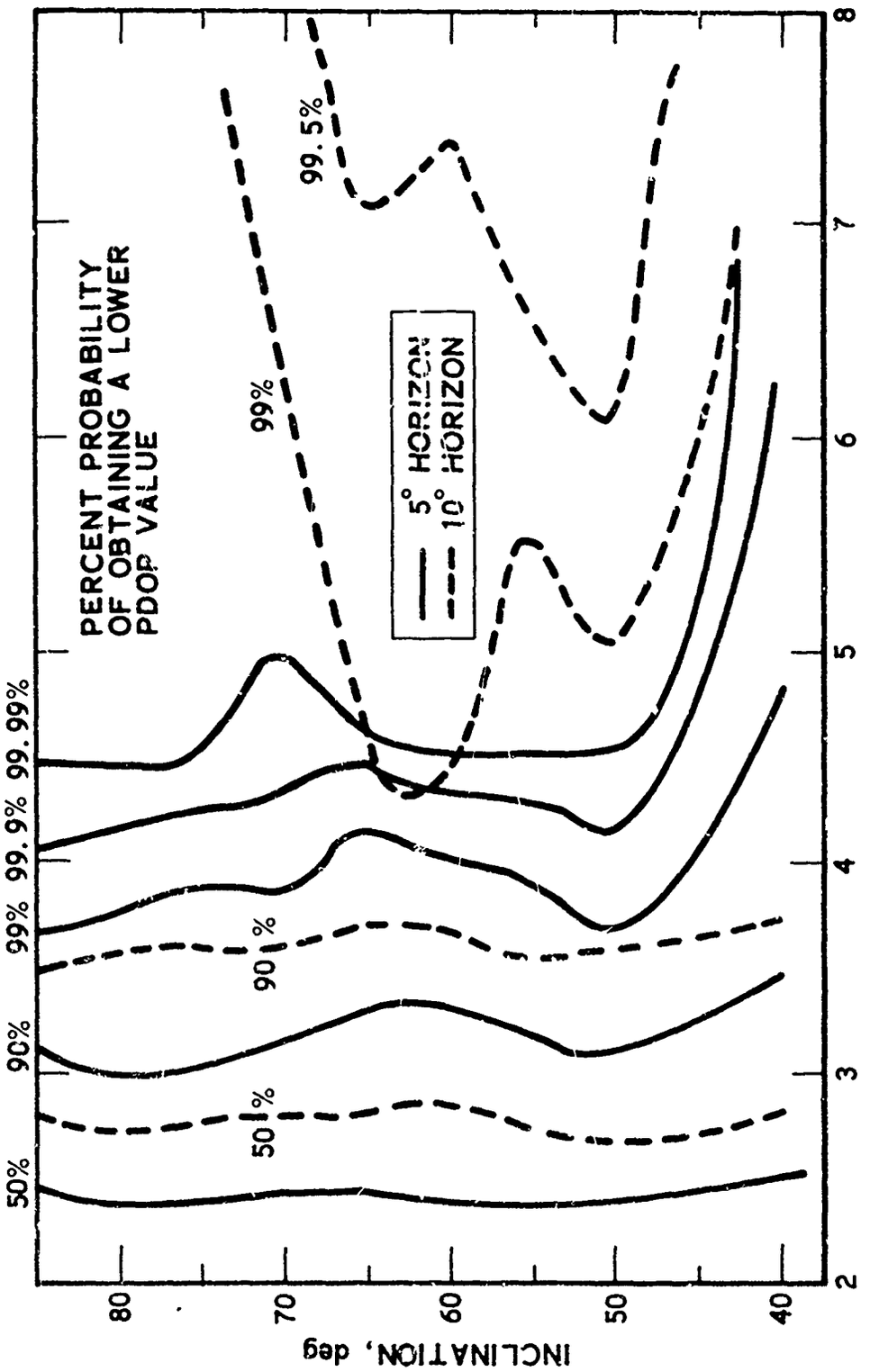

Figure 7. GPS Constellation — 3 × 8 Global Geometric Performance

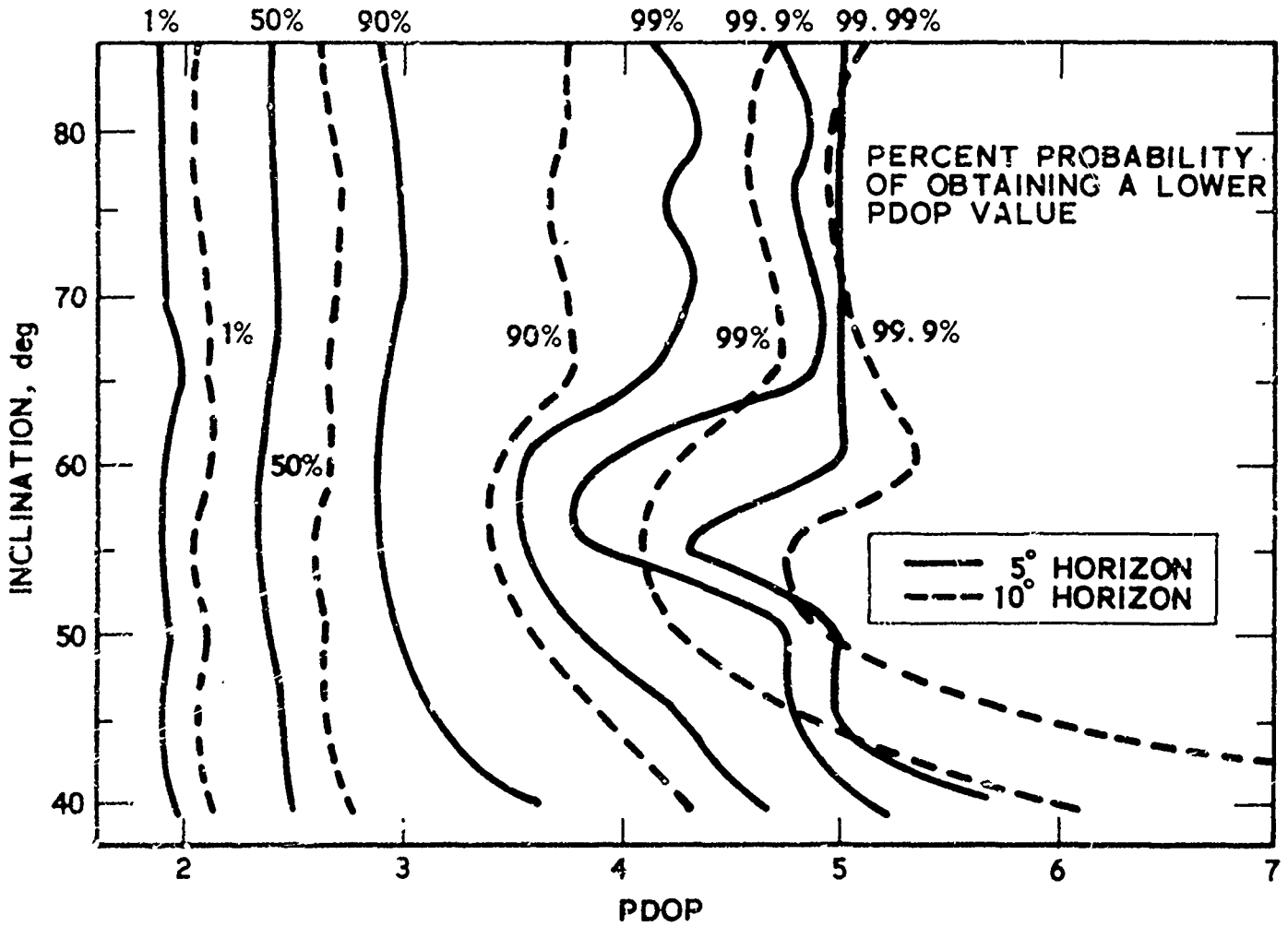

Figure 8. GPS Constellation — 3 × 9 Global Geometric Performance

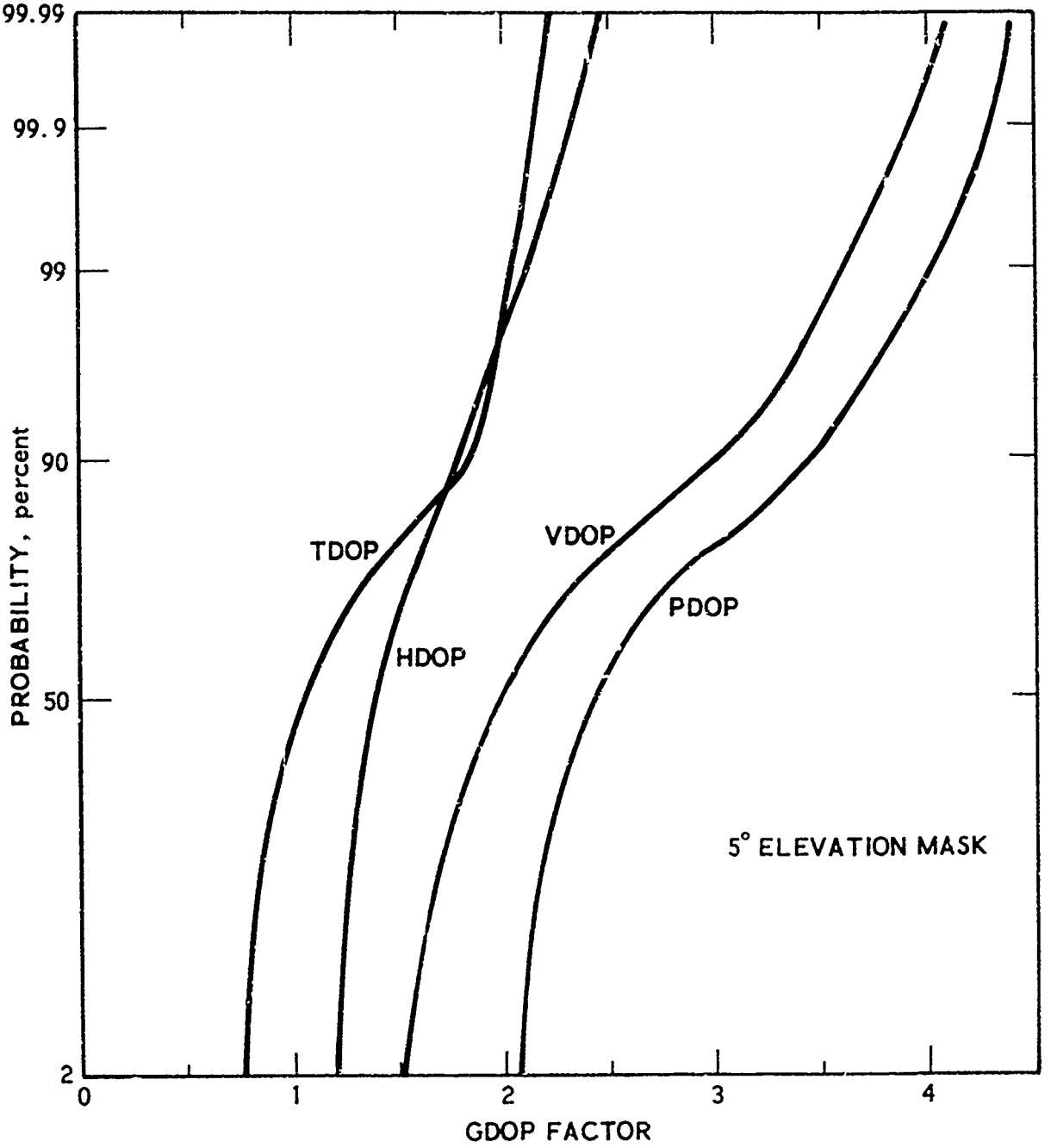

Figure 9. GPS Phase III – 3 × 8 Baseline Global Geometric Performance

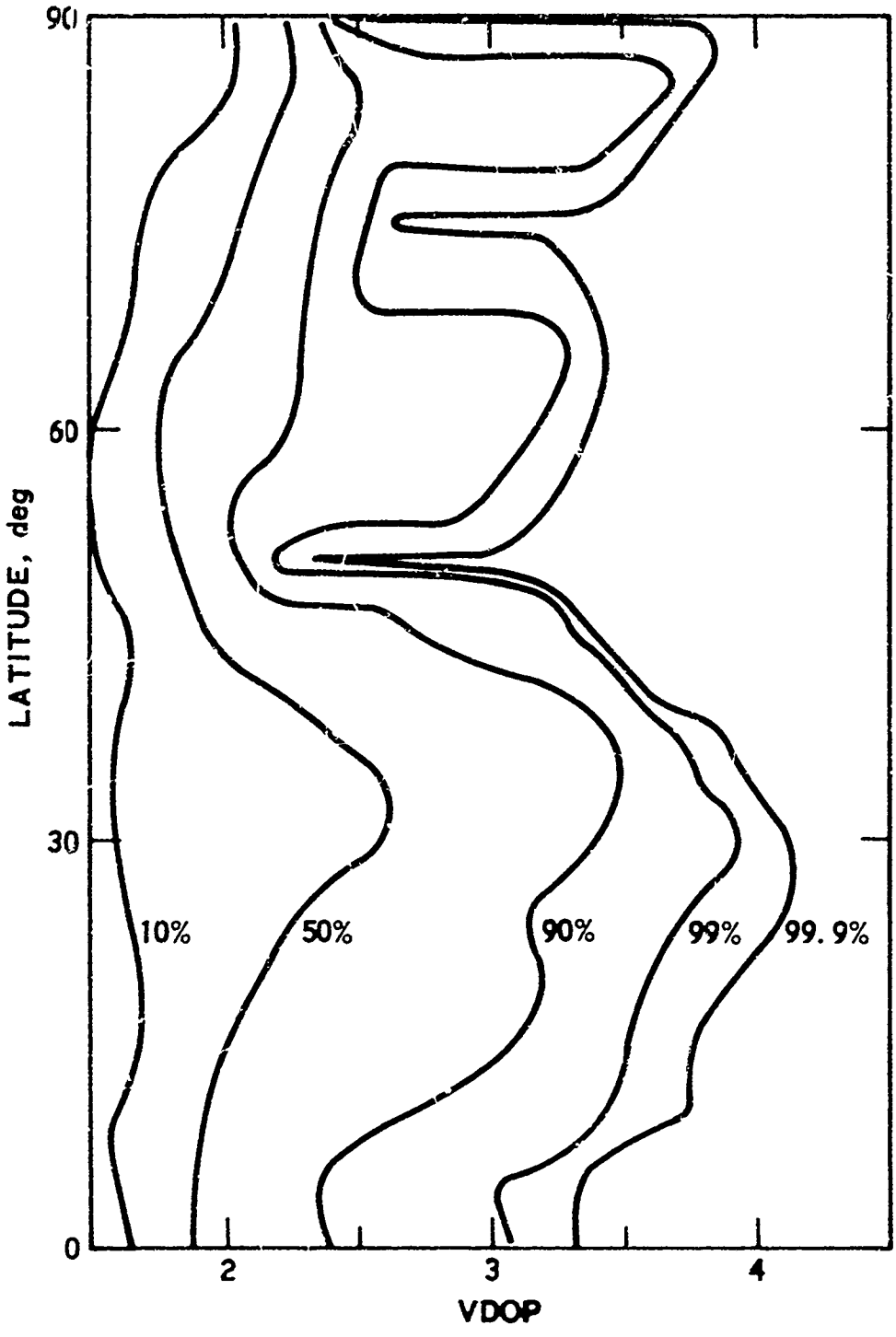

Figure 10. GPS Phase III – 3 × 8 Baseline Global Latitude Performance, VDOP

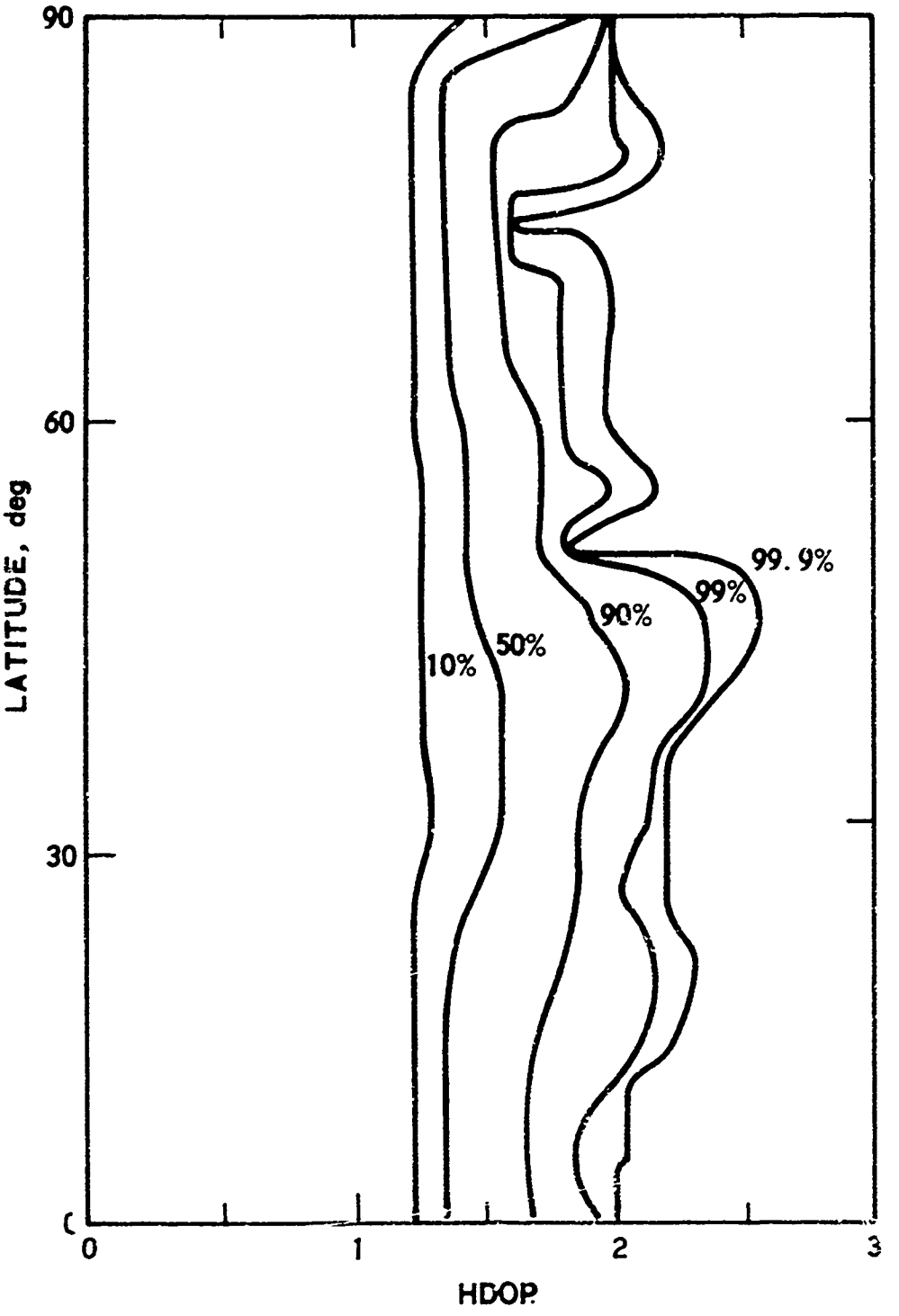

Figure 11. GPS Phase III – 3 × 8 Global Latitude Performance, HDOP

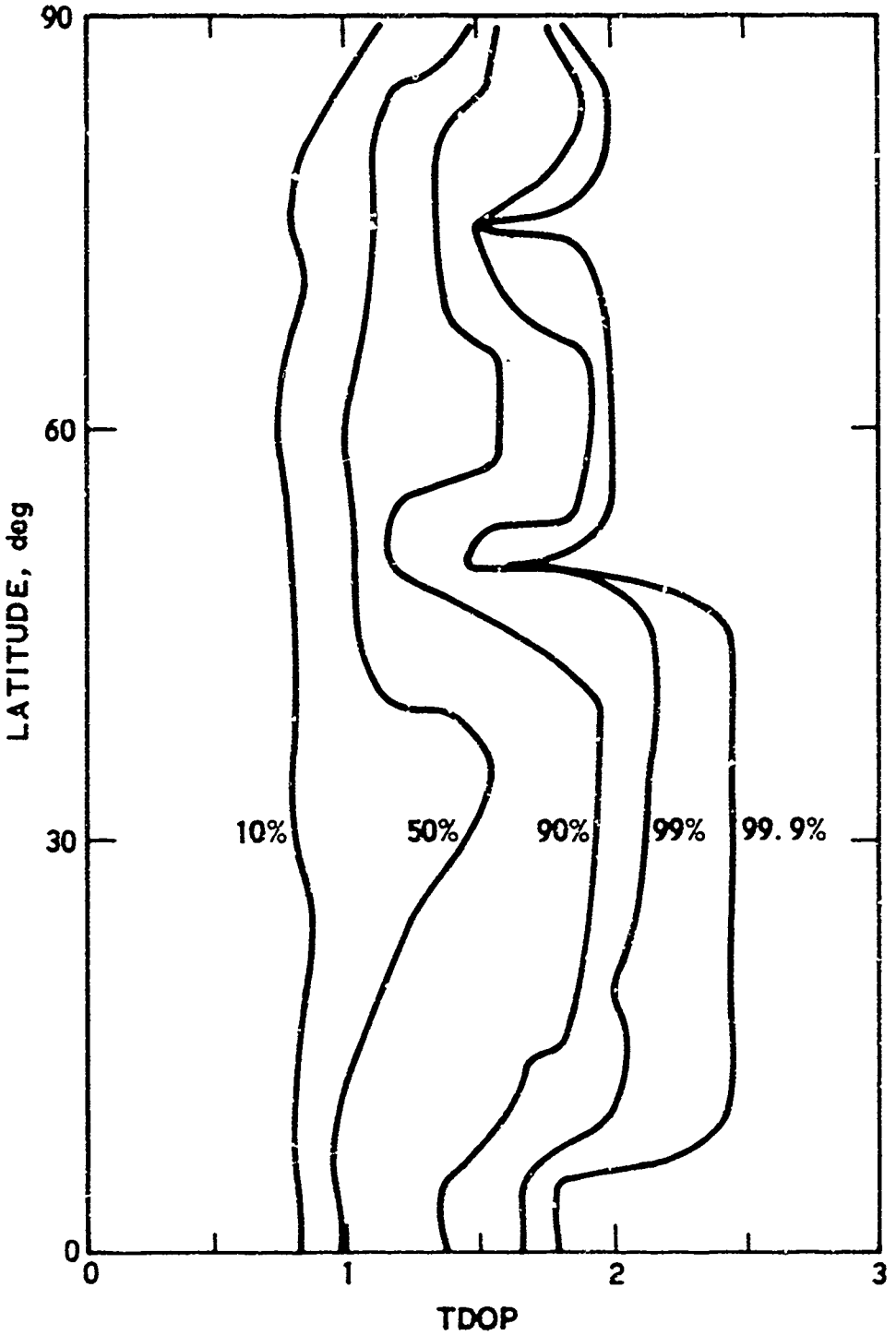

Figure 12. GPS Phase III – 3 × 8 Global Latitude Performance, TDOP

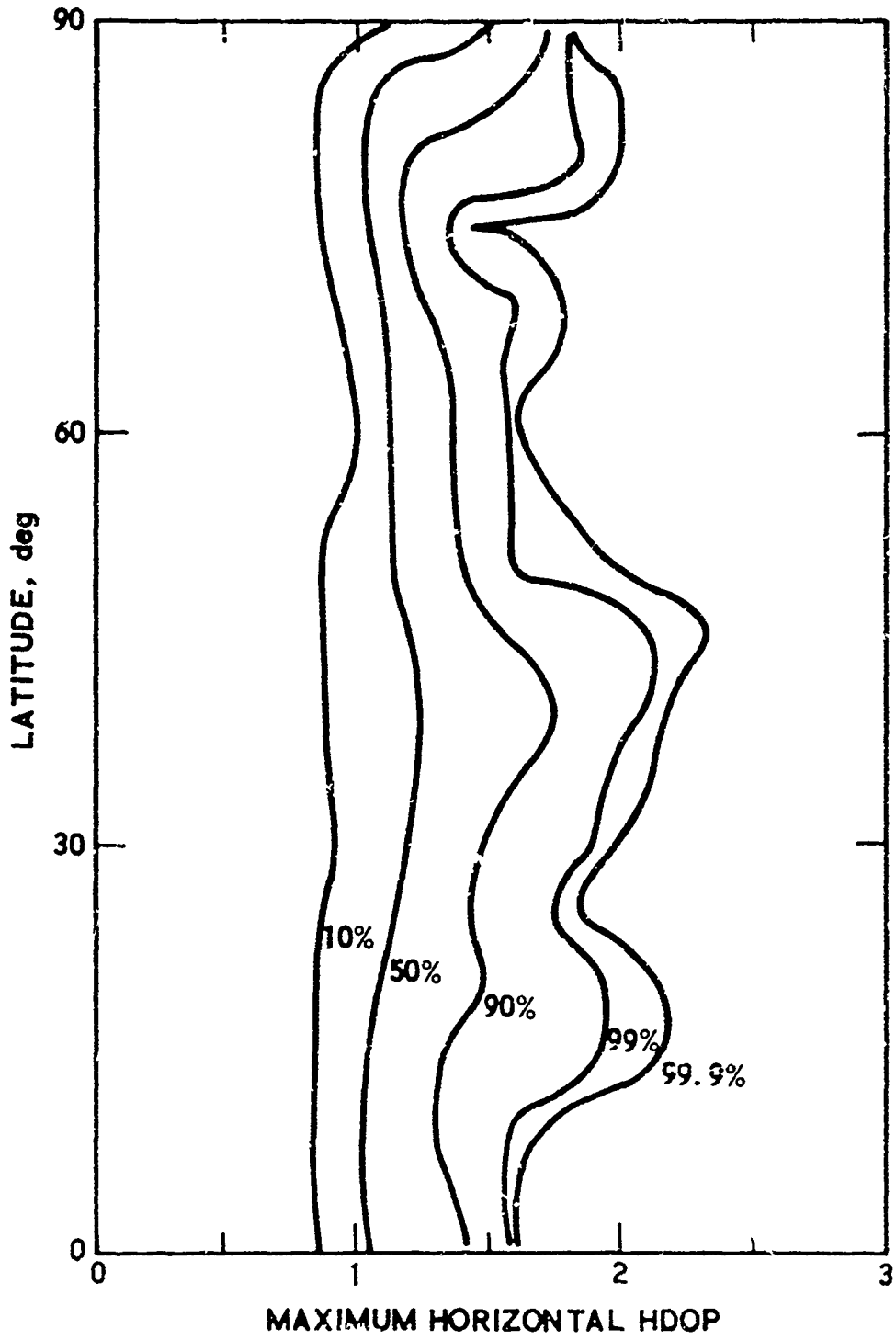

Figure 13. GPS Phase III – 3 × 8 Global Latitude Performance, Maximum Horizontal HDOP

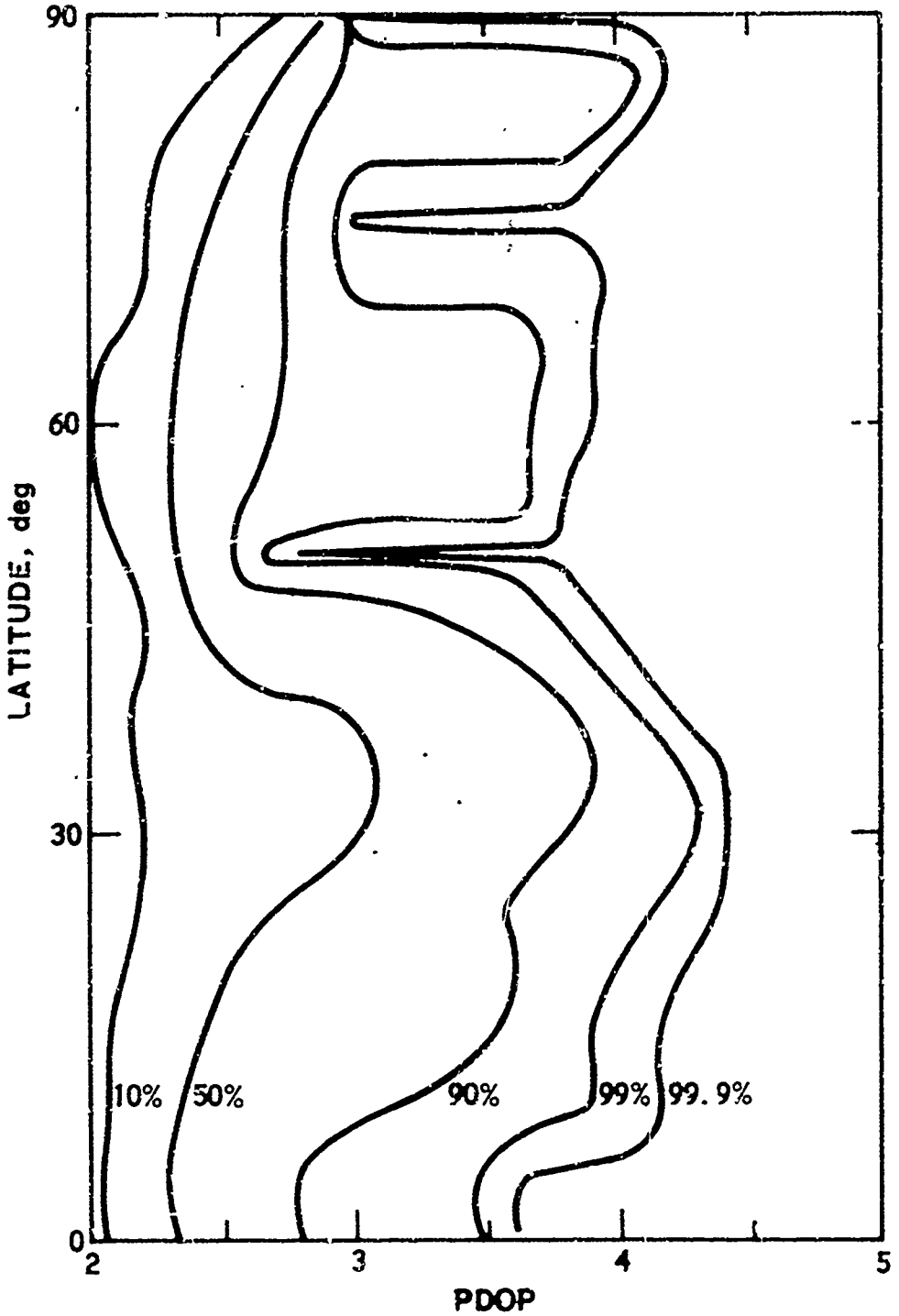

Figure 14. GPS Phase III – 3 × 8 Global Latitude Performance, PDOP

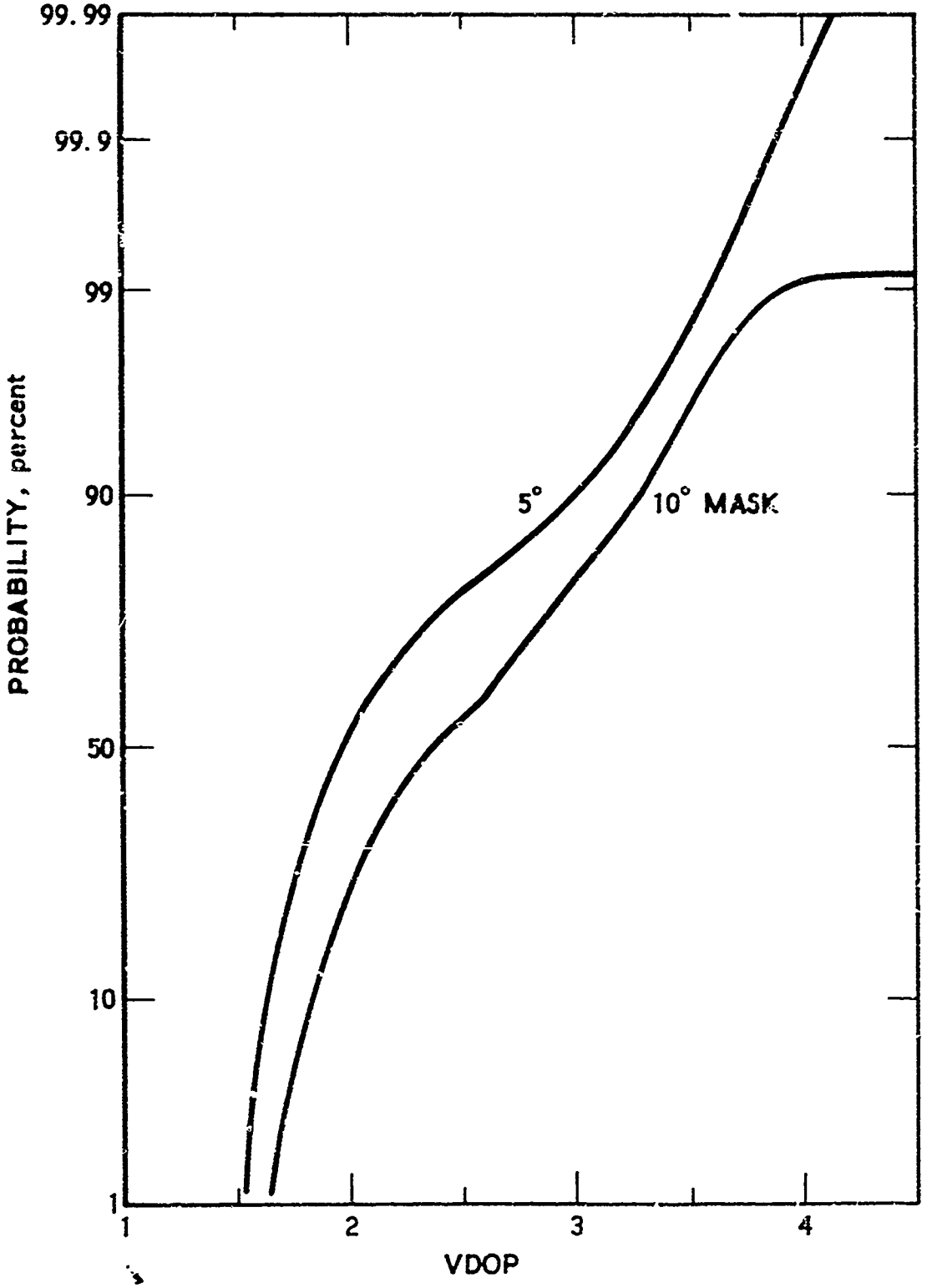

Figure 15. GPS Phase III – 3 × 8 Global Performance at 5- and 10-deg Elevation Angles, VDOP

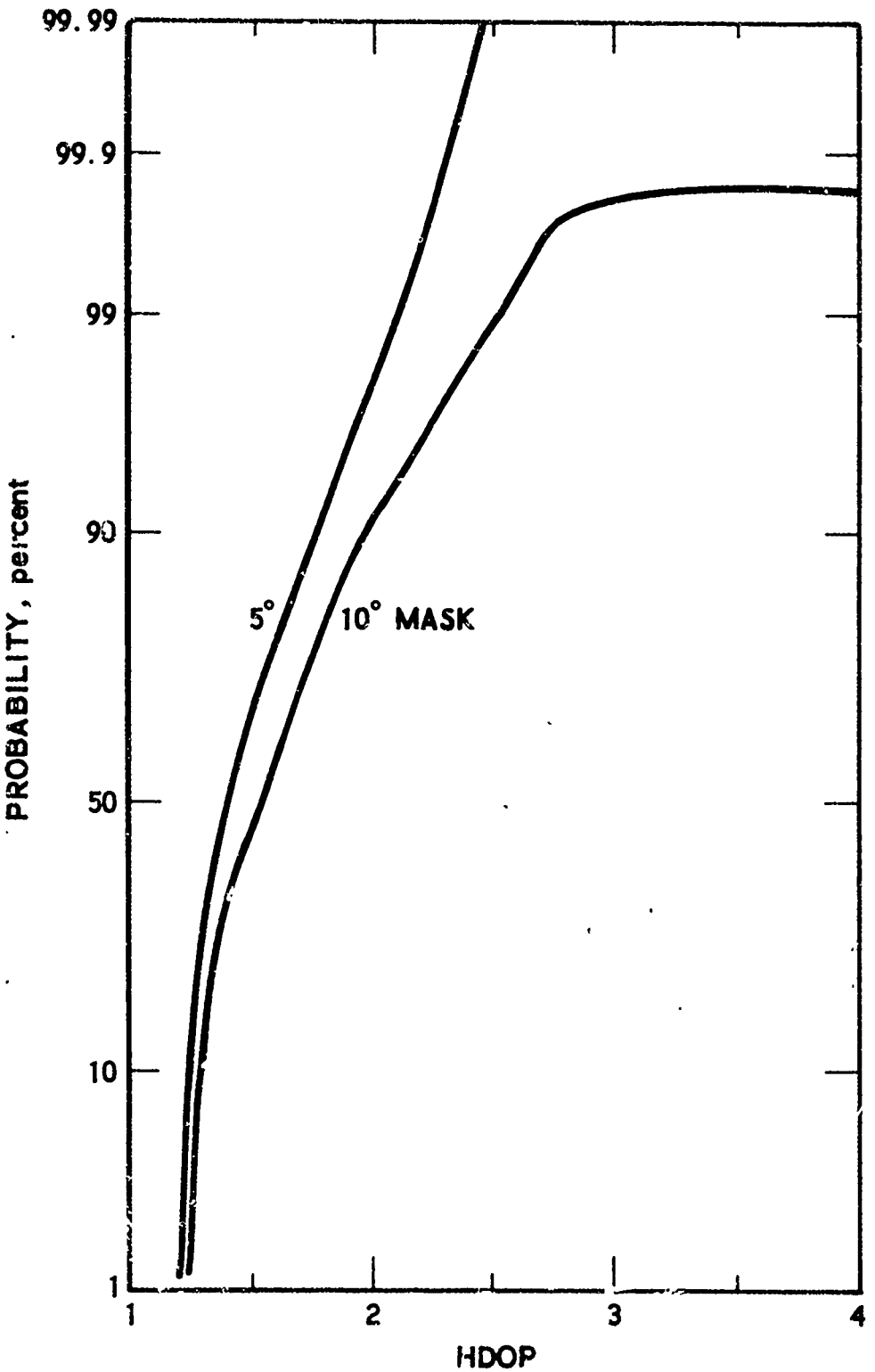

Figure 16. GPS Phase III -- 3 × 8 Global Performance at 5- and 10-deg Elevation Angles, HDOP

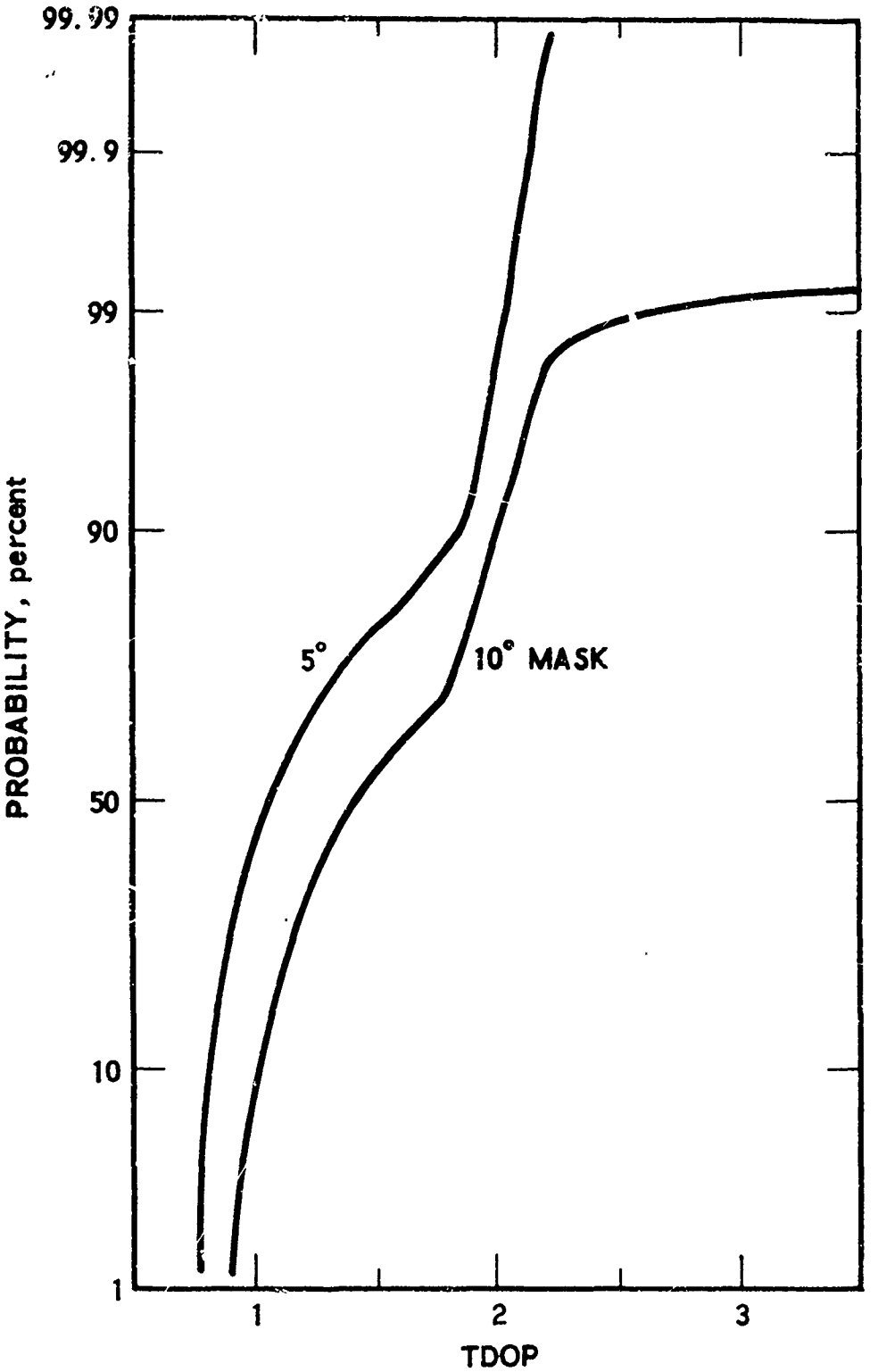

Figure 17. GPS Phase III — 3 × 8 Global Performance at 5- and 10-deg Elevation Angles, TDOP

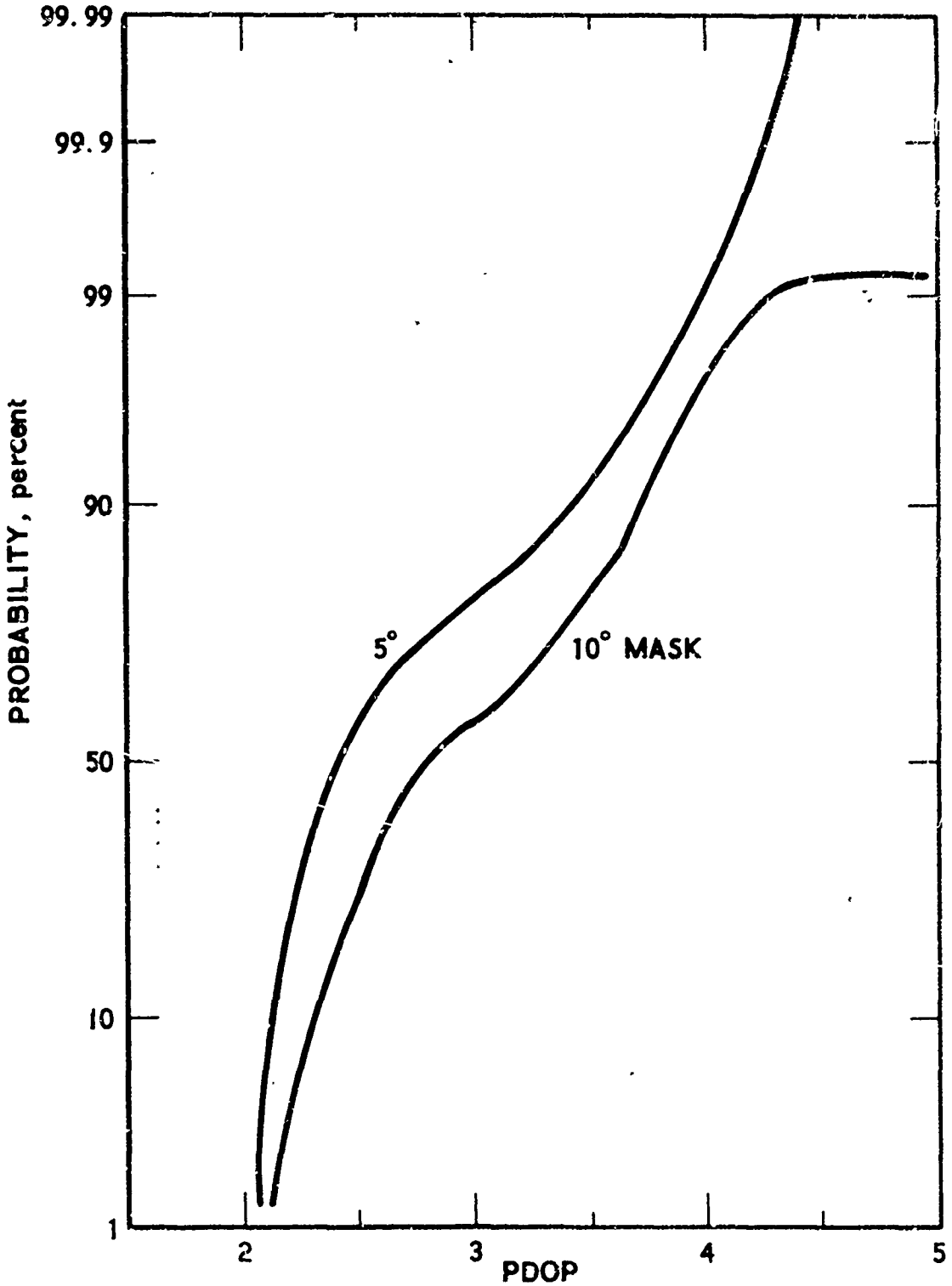

Figure 18. GPS Phase III – 3 X 8 Global Performance at 5- and 10-deg Elevation Angles, PDOP

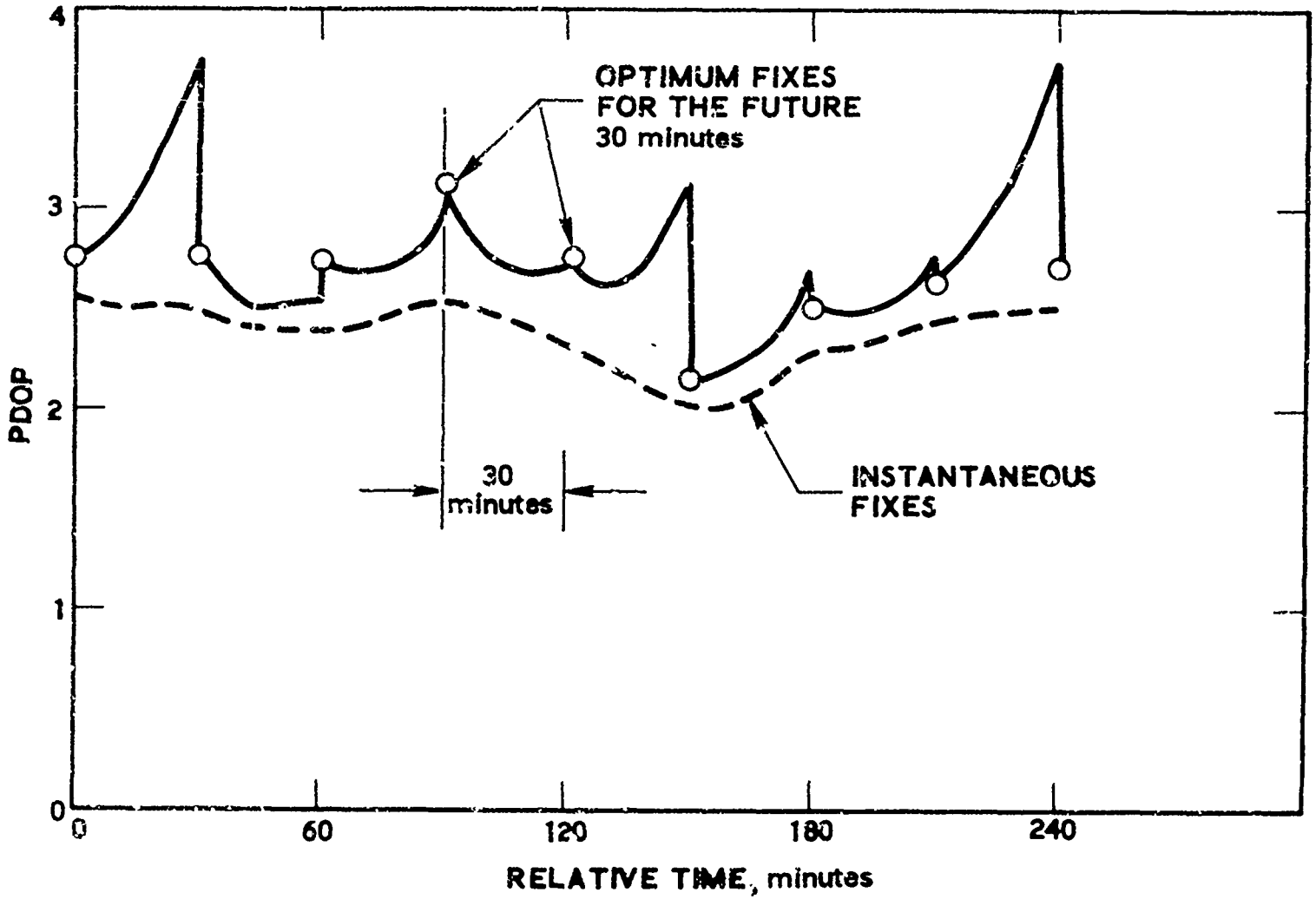

Figure 19. GPS Phase III – 3 × 8 Satellite Selection
Single Point Performance Variation

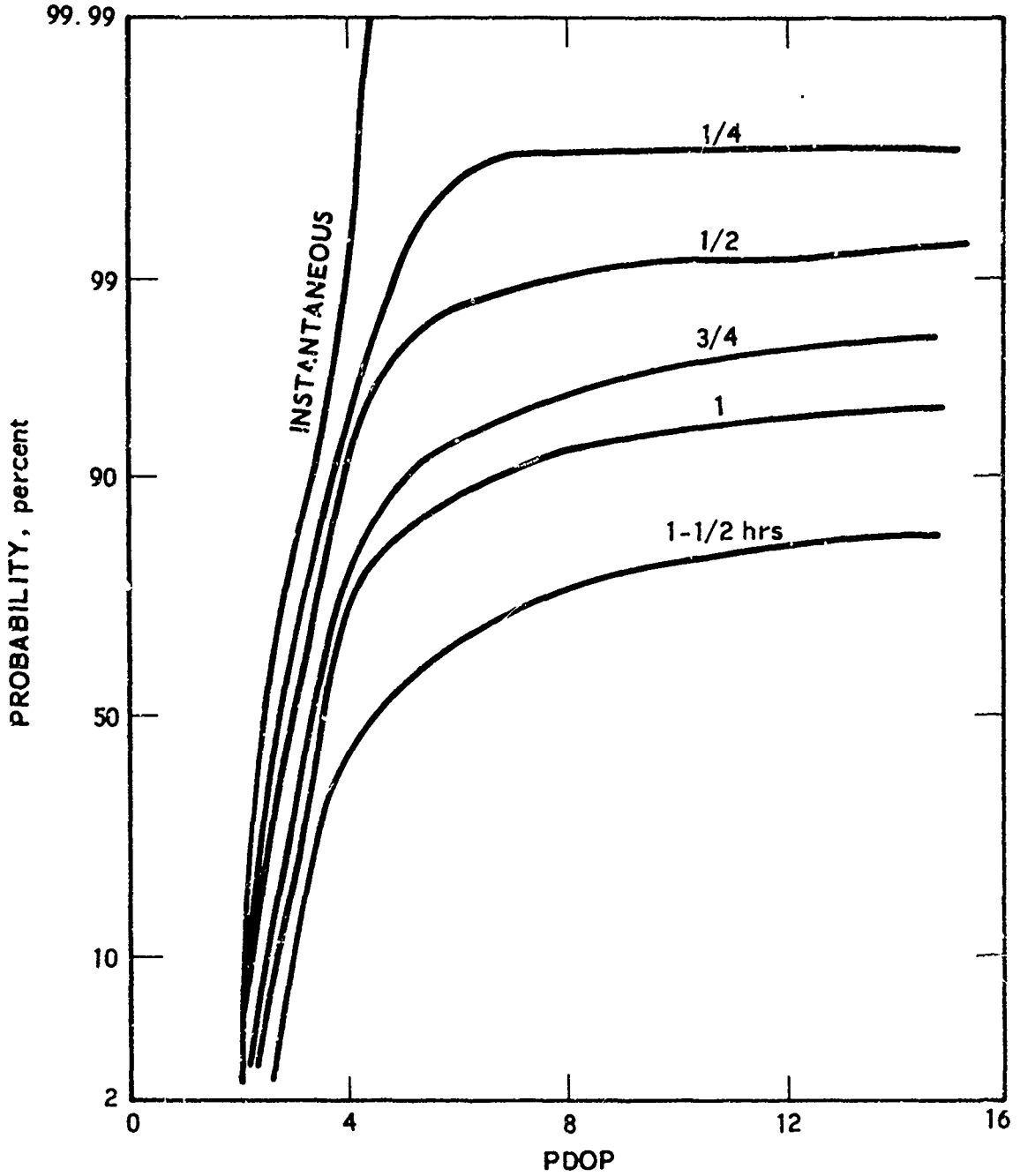

Figure 20. GPS Phase III – 3 × 8 Baseline System Performance Deterioration

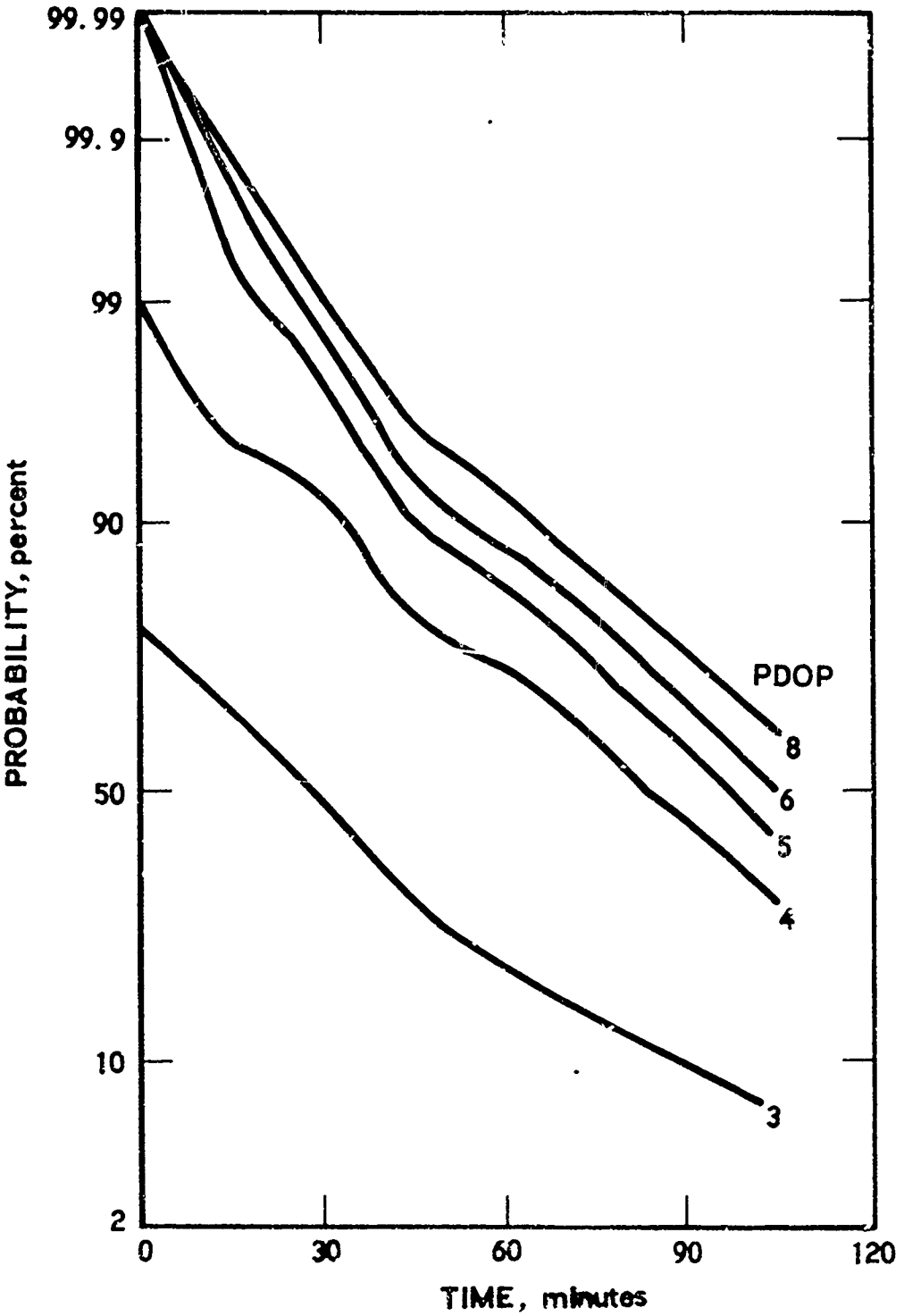

Figure 21. GPS Phase III – 3 × 8 Baseline System Performance Degradation

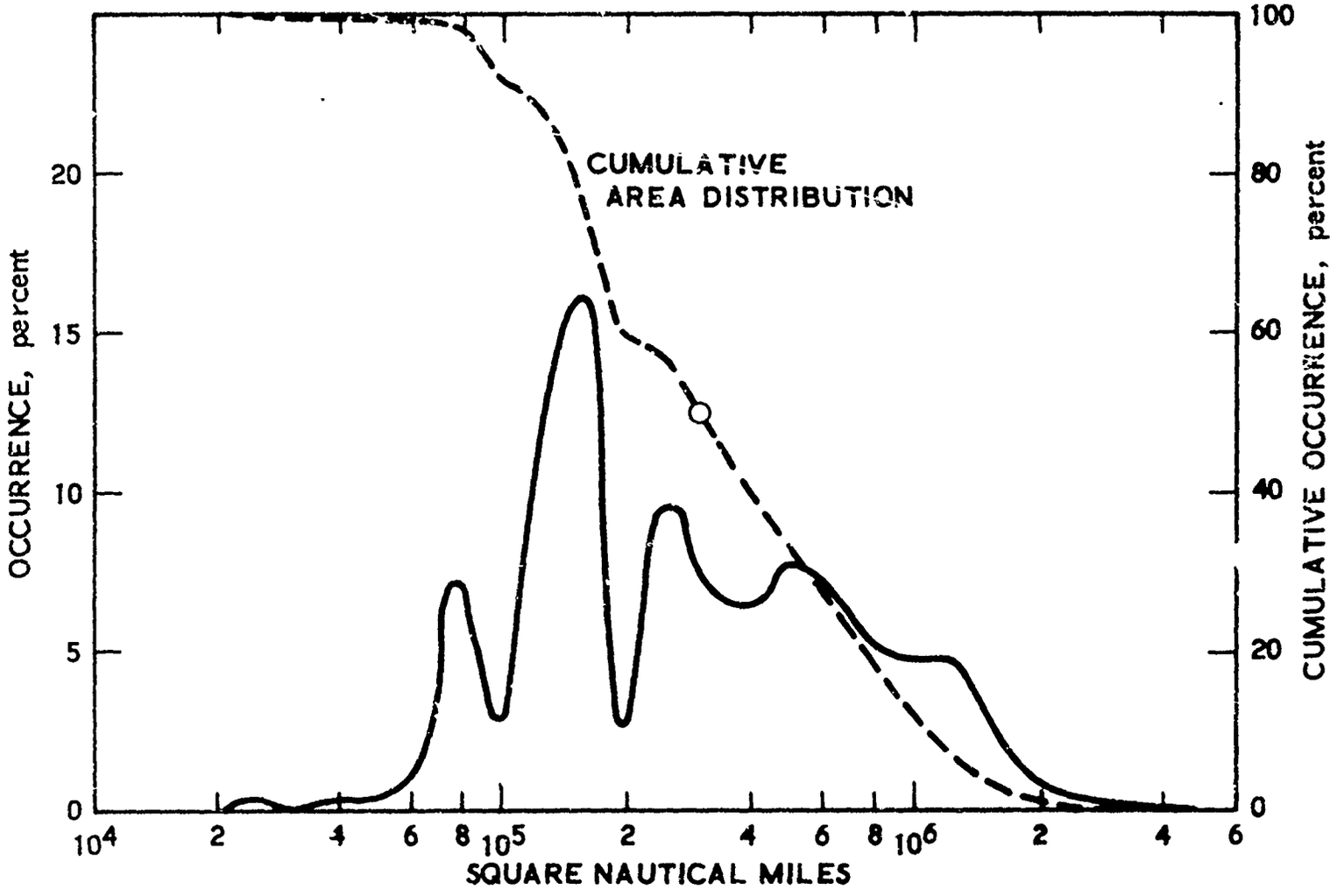

Figure 22. GPS Phase III – 3 × 8 Area Distribution of Optimum Coverage

Table 3. GPS Phase III — Satellite Selection Geographic Area Coverage

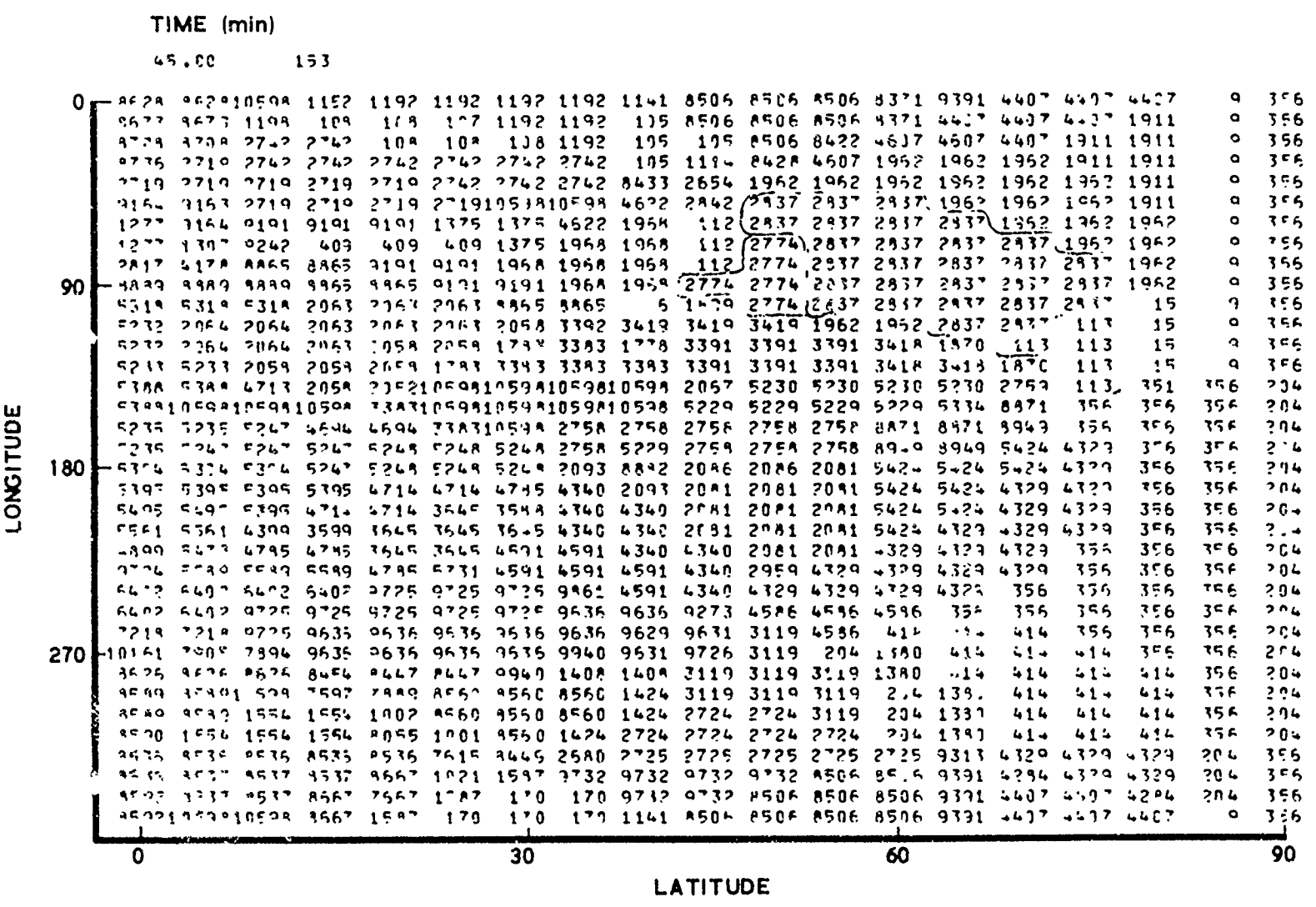

Table 3. GPS Phase III – Satellite Selection Geographic Area Coverage (continued)

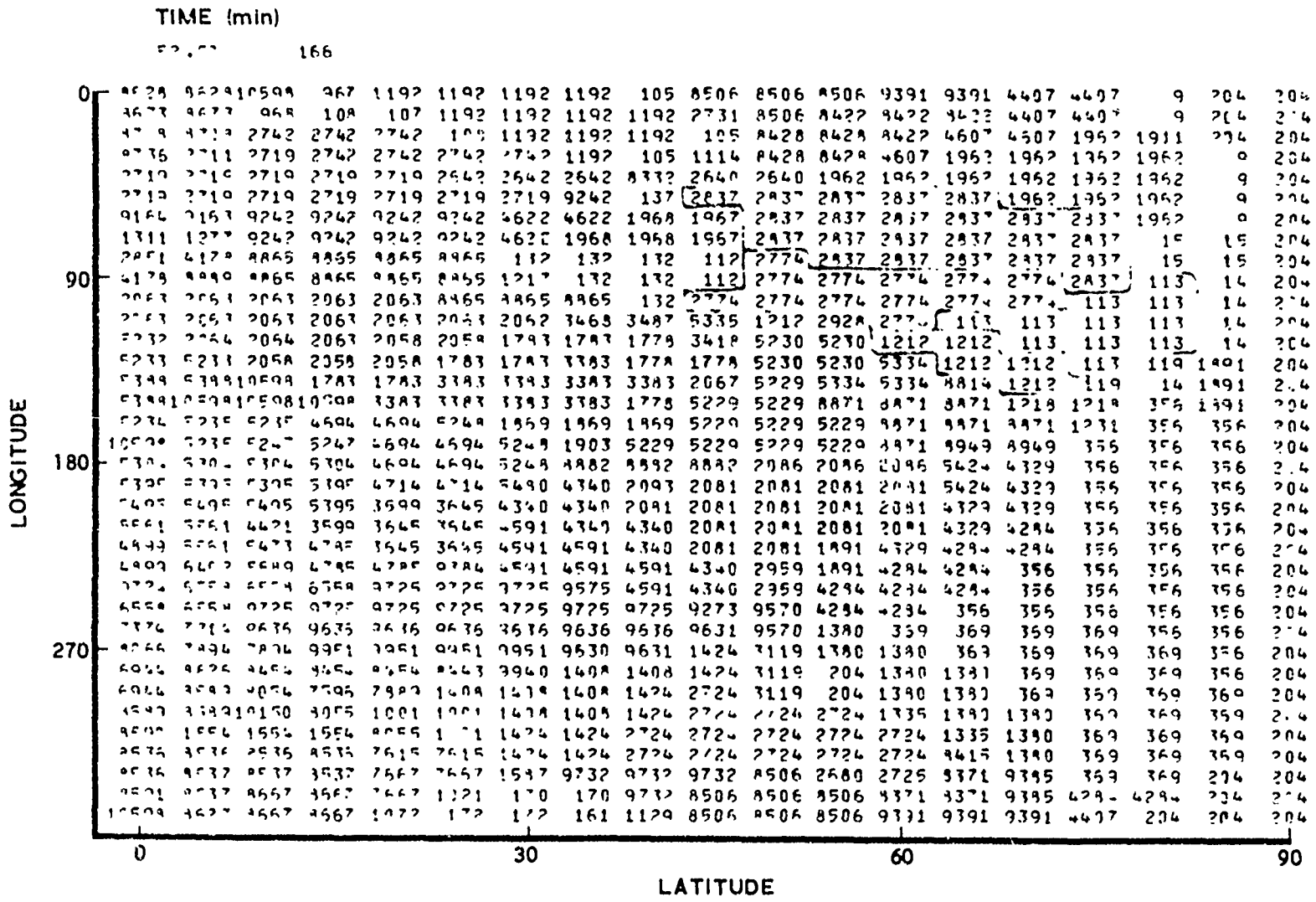

Table 3. GPS Phase III — Satellite Selection Geographic Area Coverage (continued)

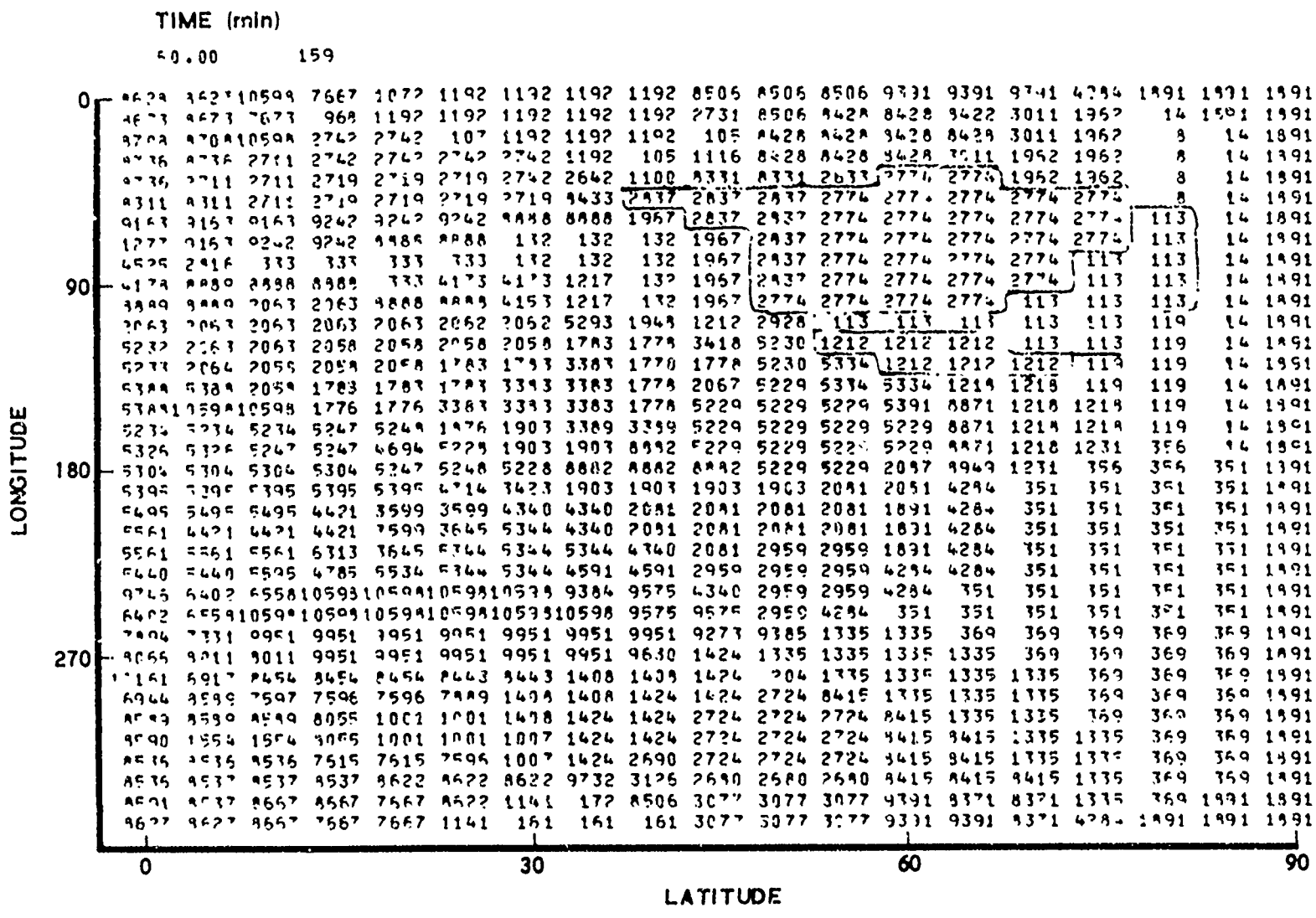

Table 3. GPS Phase III – Satellite Selection Geographic Area Coverage (continued)

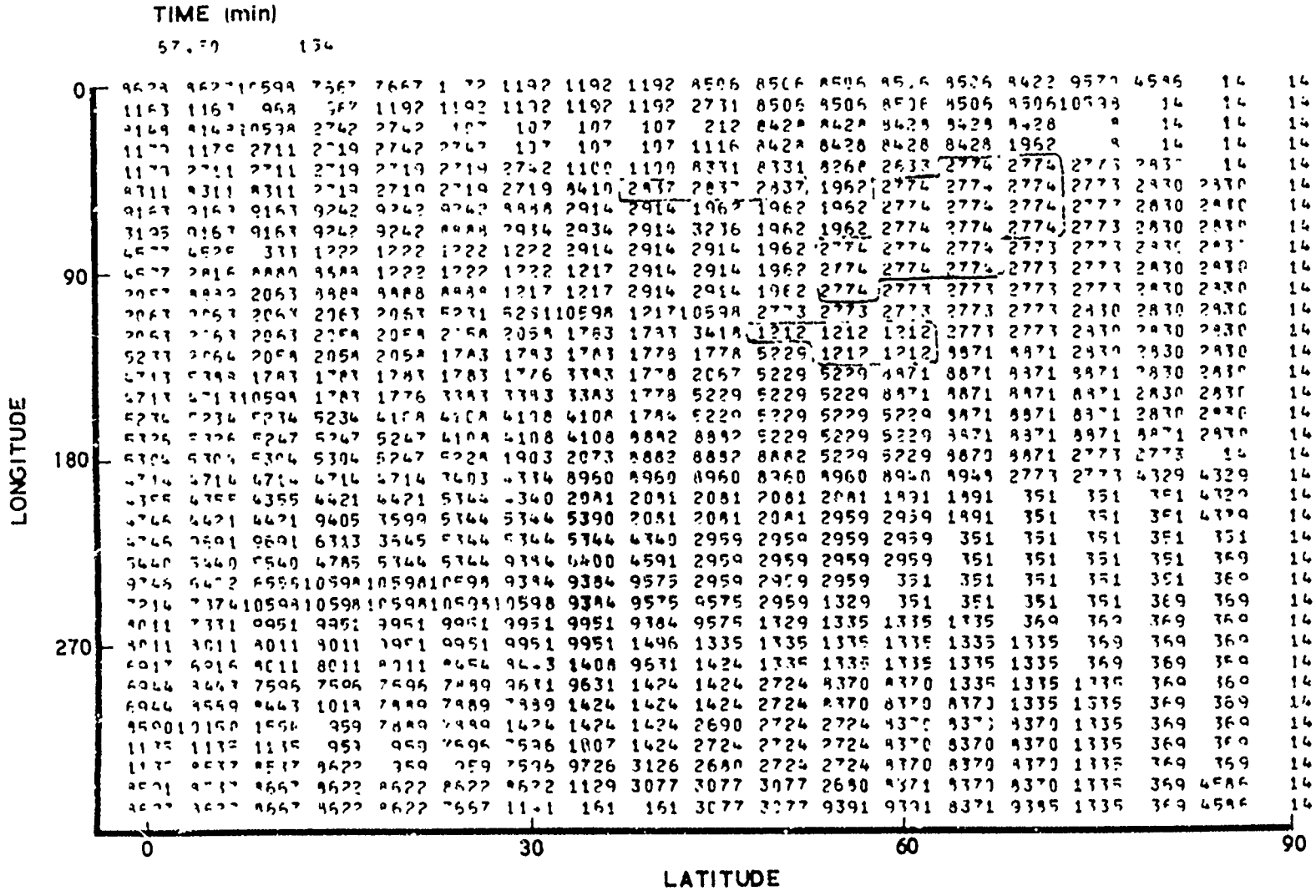

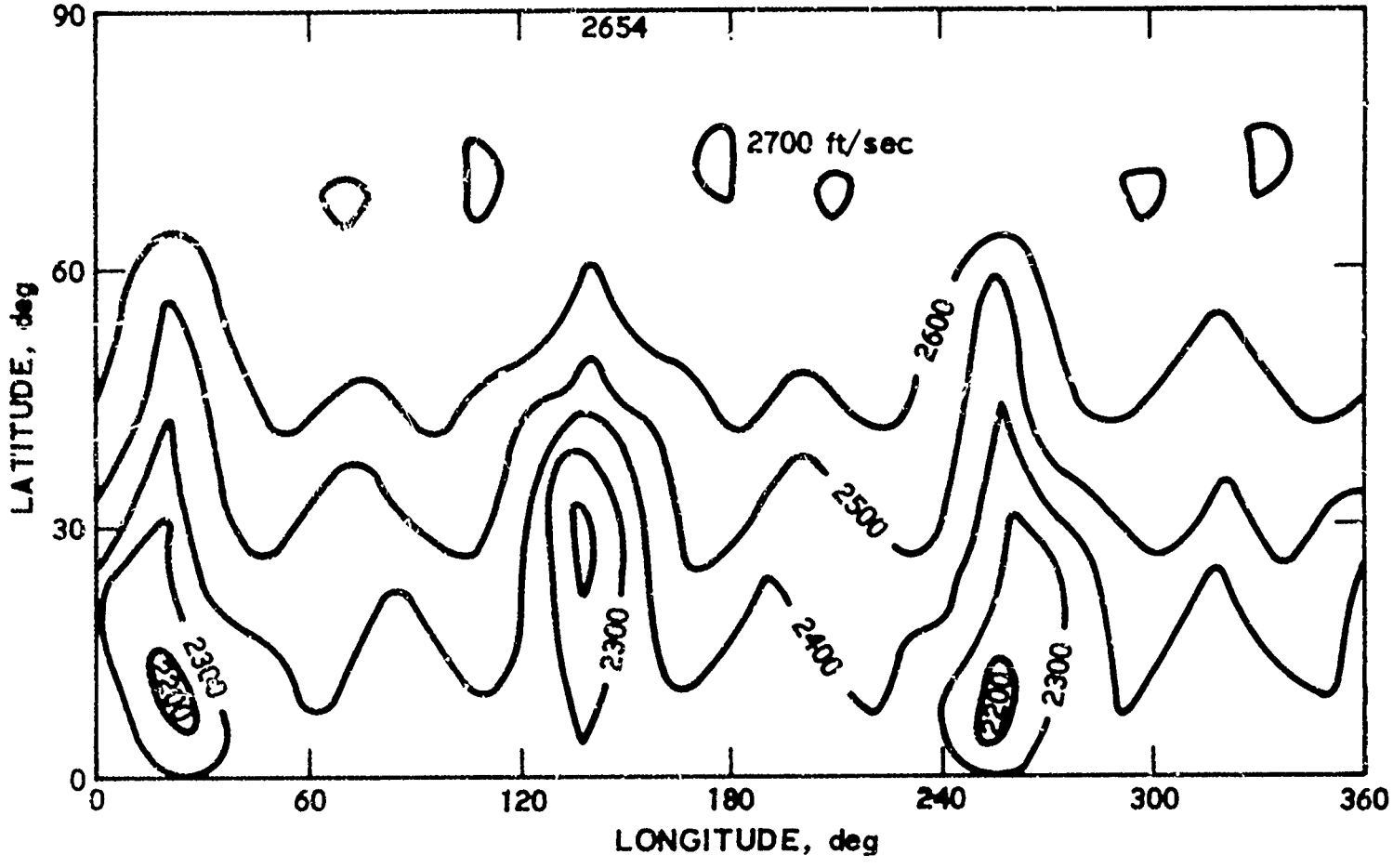

Figure 23. GPS Phase III – 3 × 8 Baseline, Maximum Range Rate (Doppler)

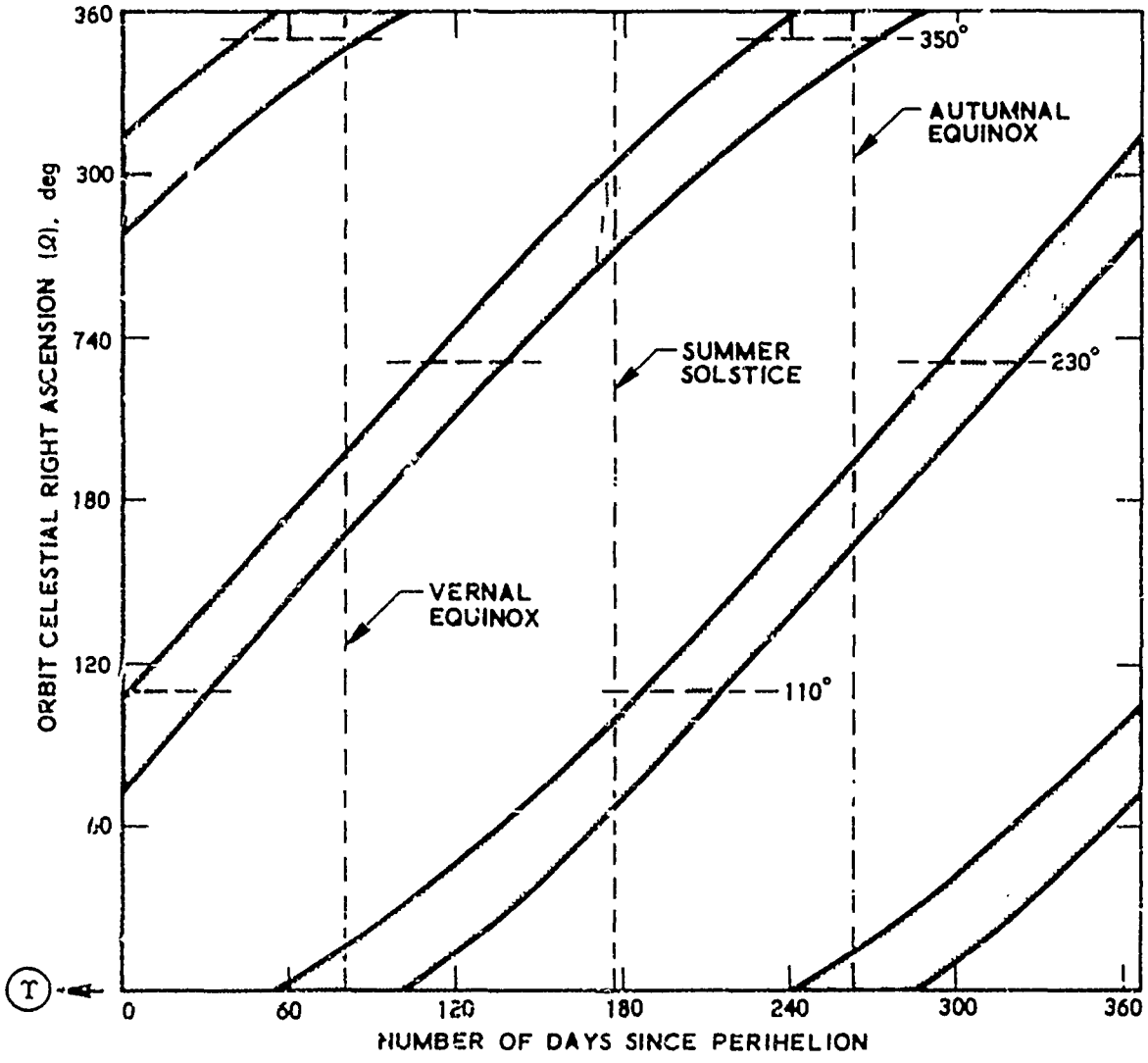

Figure 24. GPS Eclipse Occurrence

5. GPS PHASE I GEOMETRIC PERFORMANCE

The GPS Phase I development configuration is divided into the major segments and operated and controlled in a manner similar to the global operational GPS Phase III. The control segment consists of the MCS, 3 or 4 MS, and a navigation data upload station. The satellite segment consists of 3 navigation development satellites (NDS) and 1 navigation technology satellite (NTS) deployed in subsynchronous circular orbits. The satellite telemetry and command functions are executed by the AFSCF worldwide space-ground link subsystem (SGLS) control net (see Figure 1).

5.1 ORBIT DEPLOYMENT

In the interest of legacy, the Phase I orbit deployment configuration will in time be made part of the Phase II and III system configurations. Because of this, the four orbit elements, eccentricity (e), inclination (i), period (T), and the celestial angular spacing between planes ($\Delta\Omega$) are identical to the Phase III, 24-satellite deployment.

Since a prerequisite for near real-time navigation is the simultaneous observation of four satellites by the user, there are several criteria which dictate the distribution and initial location of the four satellites in the three available orbit planes:

a. Satellite visibility in the test area

b. Duration of satellite visibility

c. Geometric performance during the time of testing

d. Visibility and duration of visibility of single satellites relative to operational ground stations prior to and during testing

e. Visibility and duration of visibility of one (NTS) satellite at the Eastern seaboard subsequent to testing.

The distribution and the search for combinations of the initial locations of the satellites in their respective orbits to comply with these criteria

are virtually infinite. Most of these combinations comply with some of the criteria of the preceding list. The deployment to be described is a compromise relative to the degree with which these criteria can be met simultaneously. There is no absolute solution. Typically, a deployment providing very good performance (GDOP) may not provide good coverage nor extended test time and may not provide a timely opportunity for the vital upload of all satellites prior to testing. The deployments using three orbit planes usually belong in this category.

In order to bound the visibility problem, Figure 25 shows the visibility area-time relationship of two satellites deployed in each of two orbit planes spaced at an angular distance of 120 deg. A systematic search and evaluation of GDOP performance for various combinations of satellite angular distance and angular phasing between planes within the above boundaries reveals several candidate deployments. The orbital parameters of the Phase I deployment are found in Table 4.

It should be emphasized that for the following discussion, the proper inertial location of Ω must be compatible with the GPS Phase III baseline configuration design, launch constraints, seasonal time of day test time considerations, and orbit perturbation effects. No useful purpose is served at this time by introducing these other matters, so the celestial longitude (Ω) is considered only as an arbitrary inertial reference.

5.2 VISIBILITY AND GEOMETRIC PERFORMANCE

Figure 26 shows how the four-satellite area coverage changes with time. Successive areas are indicated at one-hour intervals; it may be noted that as time goes on, the coverage moves north, expands, makes a sweep eastward, starts to shrink, and then proceeds south. At half the orbit period, the process repeats itself and the mirror image of the coverage appears in the Southern Hemisphere. Figure 27 shows the four-satellite coverage of North America at 30-min intervals. The coverage at Yuma, the presently planned test center, starts at 2.5 hours and ends at 5 hours.

Figure 28 shows the ground tracks for each of the satellites. The solid line indicates the satellite travel during the test period in CONUS (defined as PDOP ≤ 8 during the four-satellite coverage). Satellite No. 3 provides the potential for compliance with criterion (e).*

Figure 29 provides the geometric performance within the boundaries of the four-satellite coverage areas as a function of time. Identical performance is obtained at six-hour intervals, when at these intervals the coverage repeats every 90 deg in longitude and alternates between north and south latitudes.

Figure 30 shows the percent of time four-satellite coverage exists in CONUS, and the corresponding navigation performance (PDOP) as a function of time. A more detailed picture is presented in Figure 31 where the performance at Yuma is plotted as a function of time and a comparison is made with the 99.99 percentile performance of the GPS 3 × 8 global deployment. This shows that the GDOP performance for Phase III on a global scale will almost always be better than the GDOP performance demonstrated during Phase I.

Similar to the four-satellite time-coverage sequence discussed above, Figure 32 shows snapshots of the three- and four-satellite coverage in time. Again, mirror images are repeated in the Southern Hemisphere at six-hour intervals displaced 90 deg in relative longitude.

Figure 33 shows the available performance in the three-satellite visibility areas when the user is assumed to have a perfect altimeter; Figure 34 indicates the performance when the user has a perfect clock. Acceptable performance (PDOP levels below 7) is available in these areas immediately adjacent to (surrounding) the four-satellite visibility areas. These areas (sometimes leading, sometimes trailing the four-satellite coverage) sweep across CONUS and provide the opportunity for extended testing both in time and location.

---

*The allowable variation in these ground tracks is specified as a ±2-deg tolerance of the geographic longitude of ascending node in RFP F04701-74-R-0006, Space Vehicle Requirements Document, DNSDP Space Vehicle Systems, No. DNSDP-SVR-101, dated 28 December 1973.

5.3 STATION VISIBILITY

Figures 35 and 36 provide the time-line visibility for 15 different stations for each of the four satellites. Considering Vandenberg, Guam, and Kodiak as primary L-band tracking stations, it is seen that all satellites can be tracked by one of these stations (but not simultaneously) for a minimum of 2 hours each prior to CONUS tests, and for a similar time span 12 hours later. Figure 36 also shows that satellite No. 3 (NTS) is visible to Chesapeake Bay for 3 hours subsequent to the Yuma test time.

Figure 37 shows an expanded form of this time-line and defines the available test time at Yuma to be 2.5 hours (determined by the visibility (5-deg horizon) of satellites No. 1 and 2. If the primary upload station is Vandenberg, more than adequate upload time is available for all satellites, with a minimum time of 10 min for satellite No. 1. Figure 38 shows the elevation angles at Yuma.

5.4 DOPPLER

Figures 39 and 40 provide the range-rate and range acceleration (Doppler and Doppler rate) during the testing at Yuma. Both Doppler and Doppler rates are somewhat less than the maximum observable in the GPS 3 × 8 Baseline.

5.5 ECLIPSES

Figure 24 showed the occurrence of eclipses for the satellites deployed in the orbit planes having celestial right ascension (Ω) of 110 and 230 deg. Figures 41 and 42 detail the two eclipse seasons and the daily variation in eclipse duration for the four satellites. No eclipses occur simultaneously and the maximum duration is about 56 min. In contrast to the GPS 3 × 8 system however (due to the angular spacing between satellites in the same plane), the eclipsing of the satellites in plane 1 occurs 2-1/3 hours apart (or 9-2/3 hours), and for plane 2 eclipsing occurs 1-1/6 hours (or 10-5/6 hours) apart. Some eclipse conditions may be encountered during

nighttime testing once a year. As mentioned previously, the proper inertial value of Ω must be compatible with the effects of Phase III constraints; therefore, the eclipse seasons (dates) discussed here might change.

Table 4. Phase I Orbital Parameters

Satellite No.	Ecc (e)	Inc (i)	A of P (ω)	RA of AN (Ω)	MA (t_o)	Per (T)
1	0	63	0	110	0	12
2	0	63	0	110	70	12
3	0	63	0	230	(-) 30	12
4	0	63	0	230	5	12

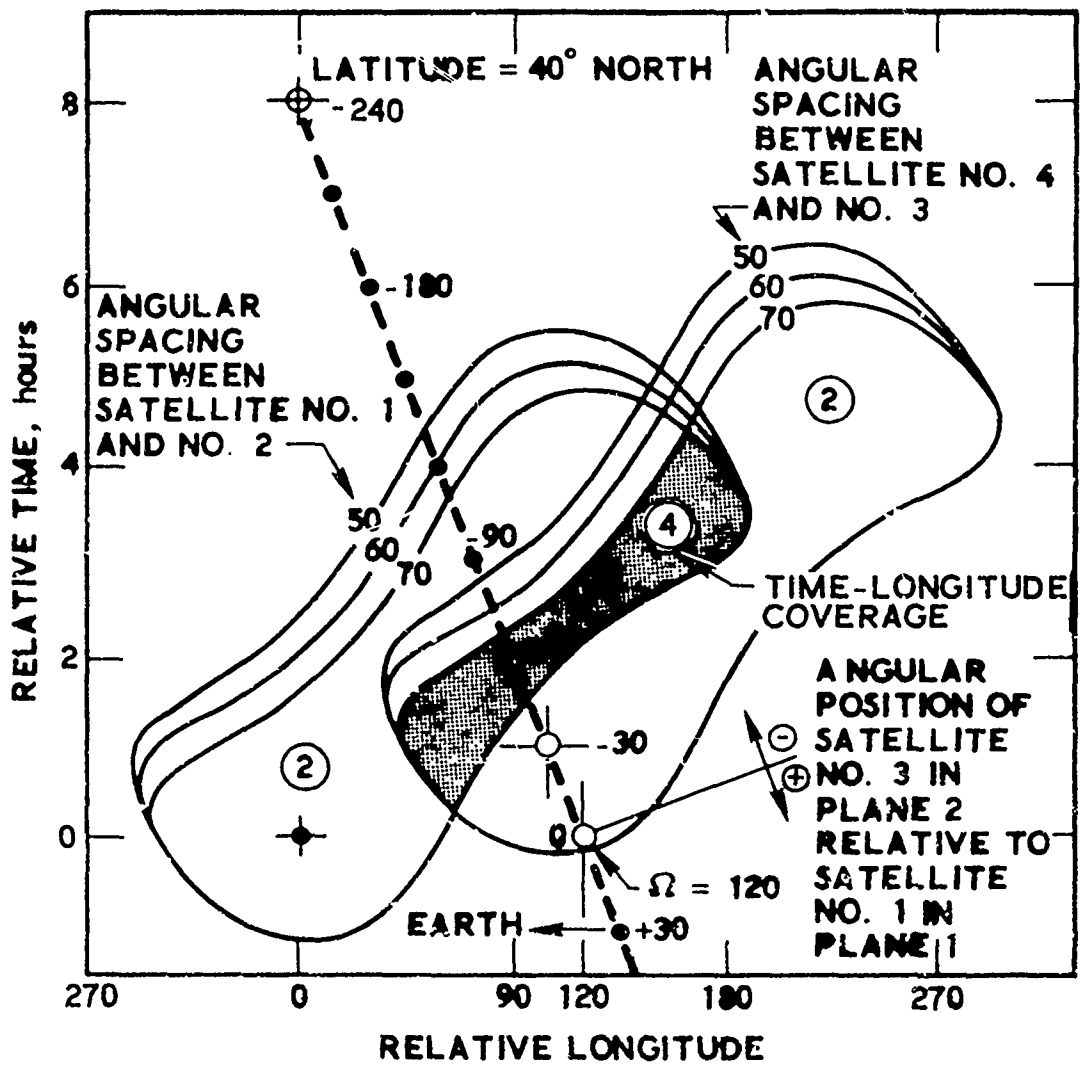

Figure 25. GPS Phase I - Four-Satellite Time-Space Visibility Relationship

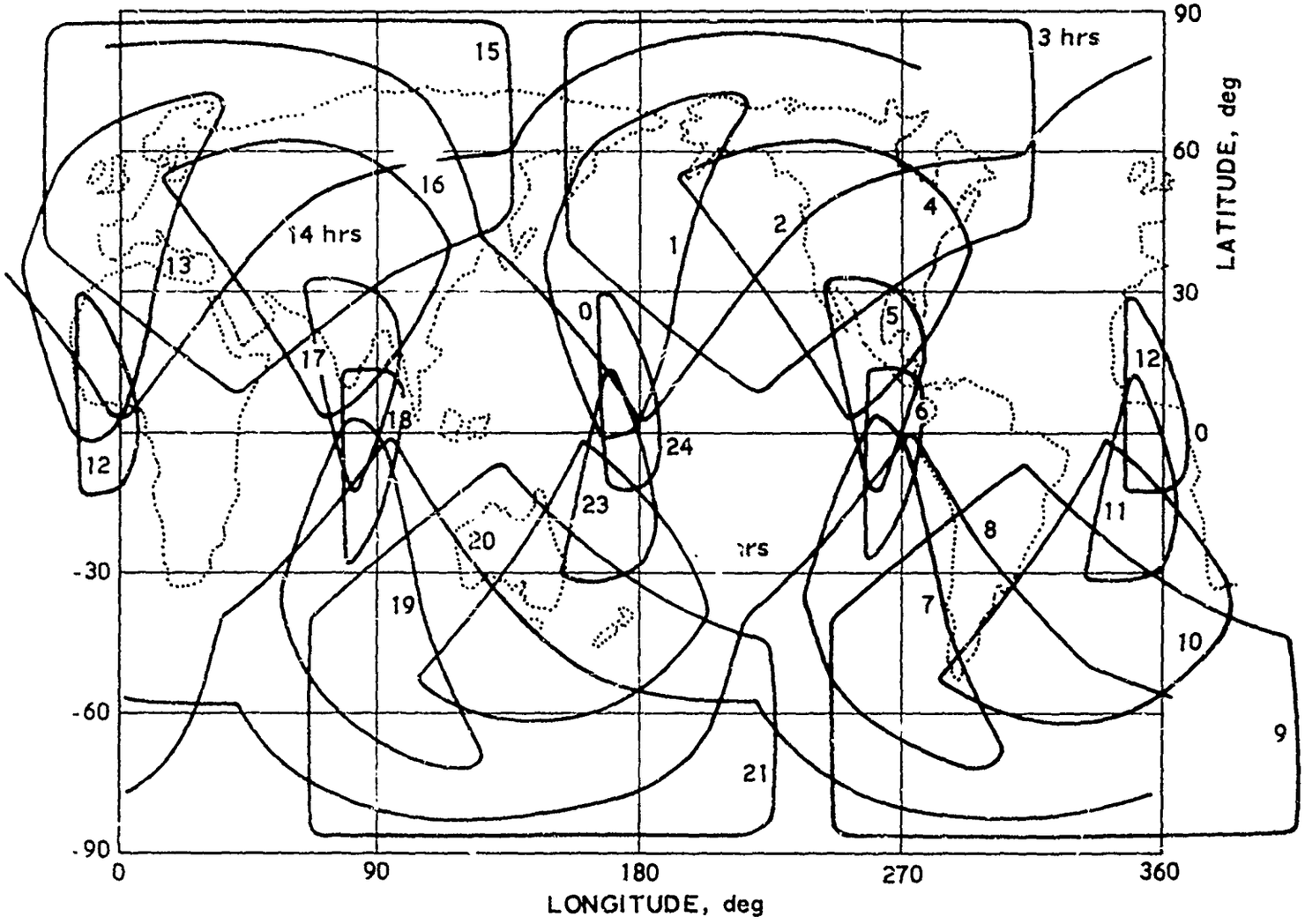

Figure 26. GPS Phase I - Four-Satellite Time-Area Coverage

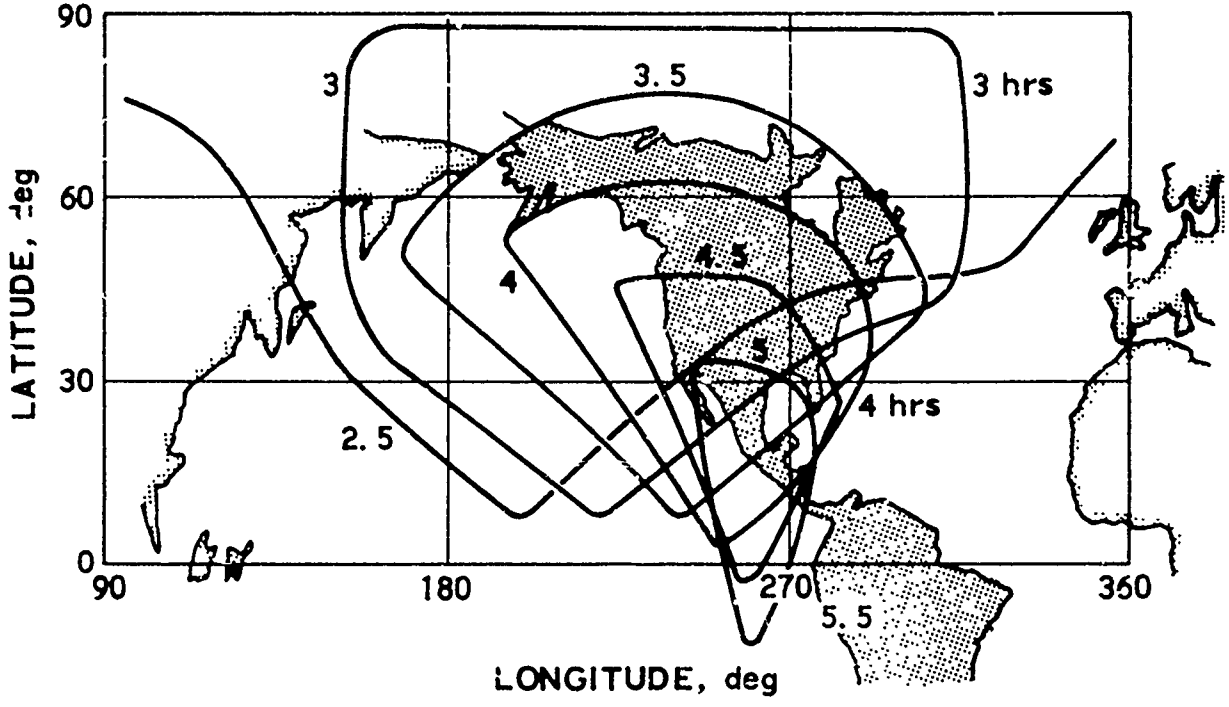

Figure 27. GPS Phase I - Four-Satellite Visibility During CONUS Tests

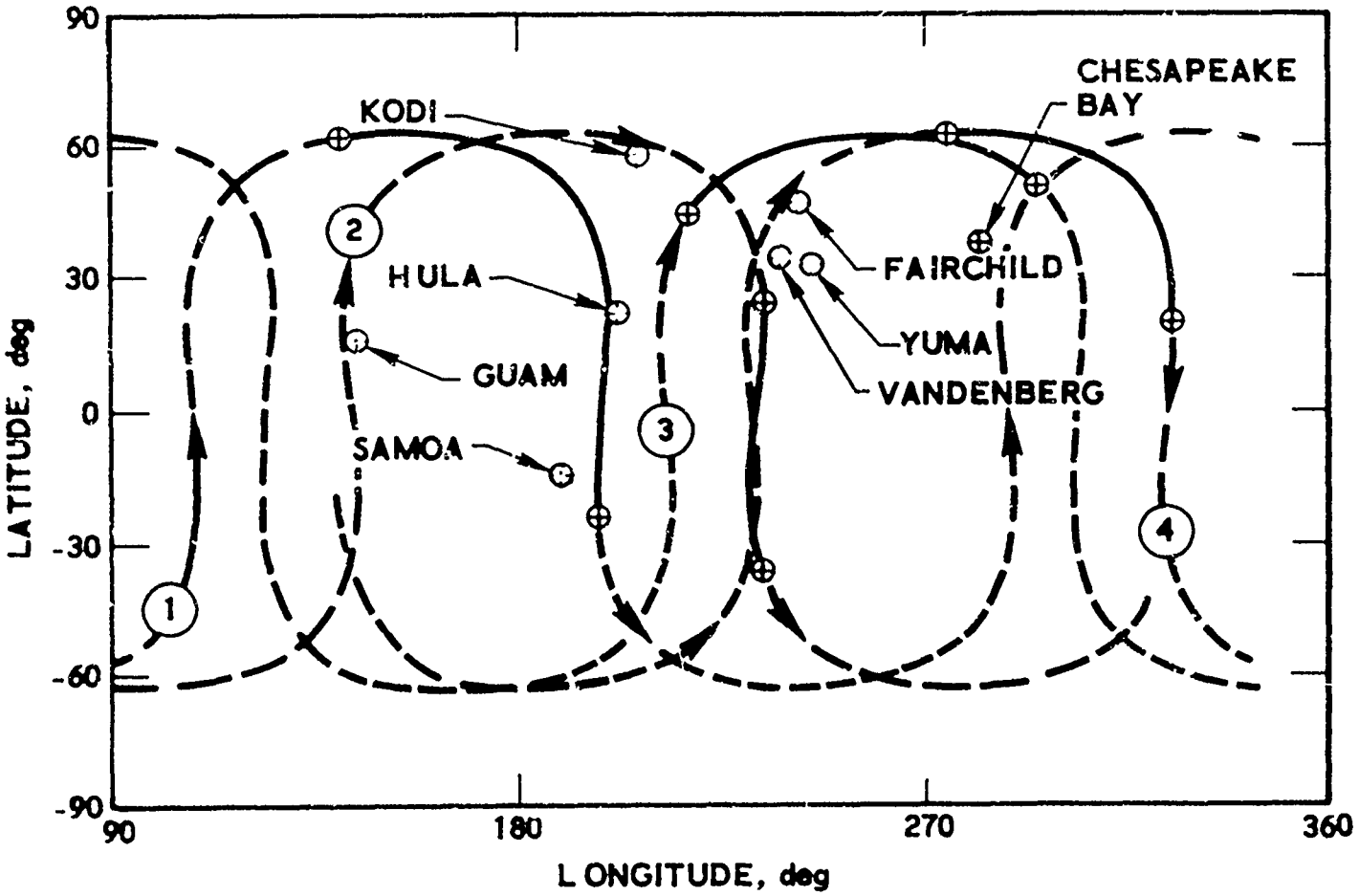

Figure 28. GPS Phase I - Ground Tracks, 2 × 2: 110 (0.70); 230 (-30, 5); 63 deg

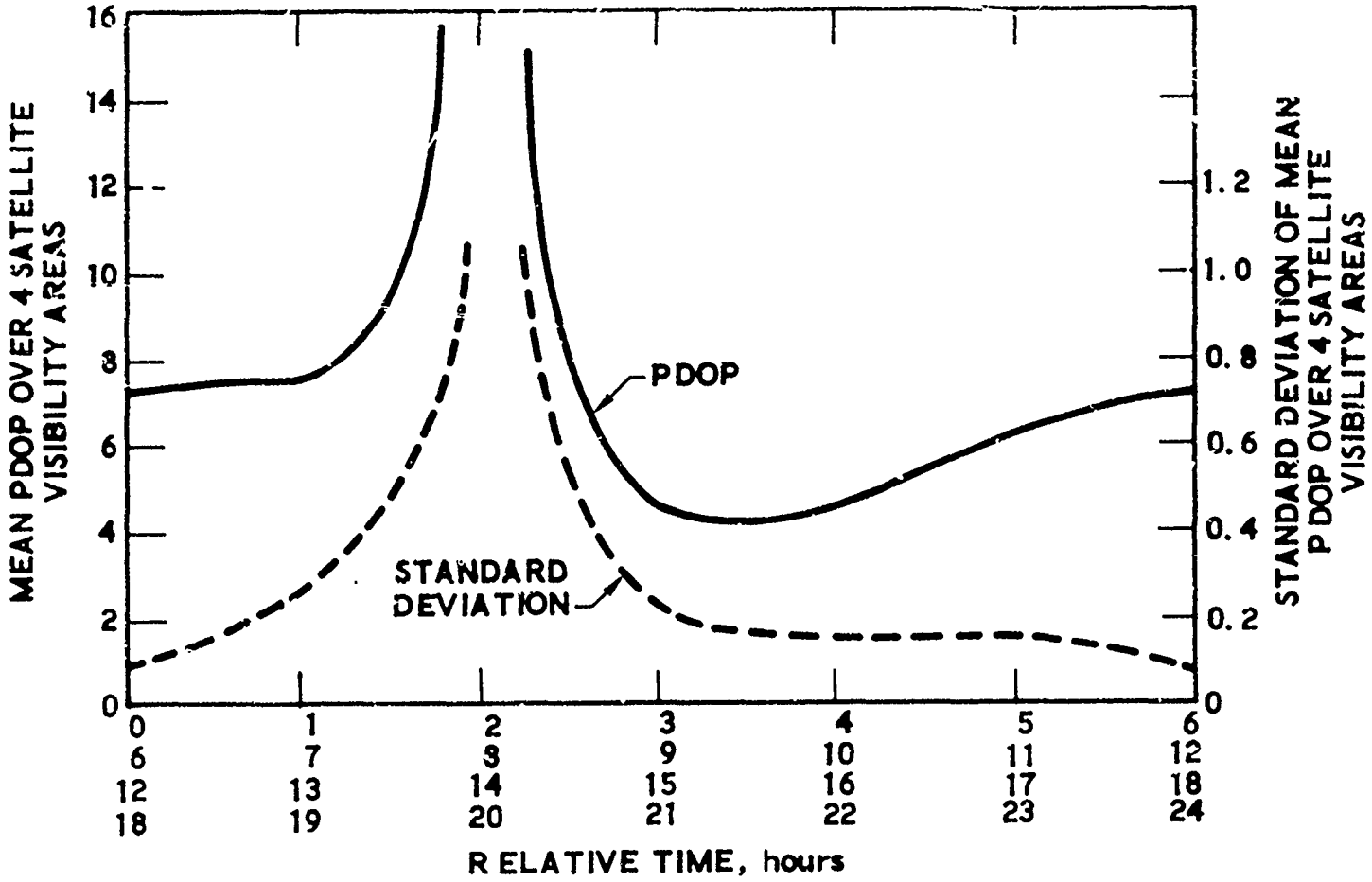

Figure 29. GPS Phase I - 2 × 2, Geometric Performance for Global Coverage Areas

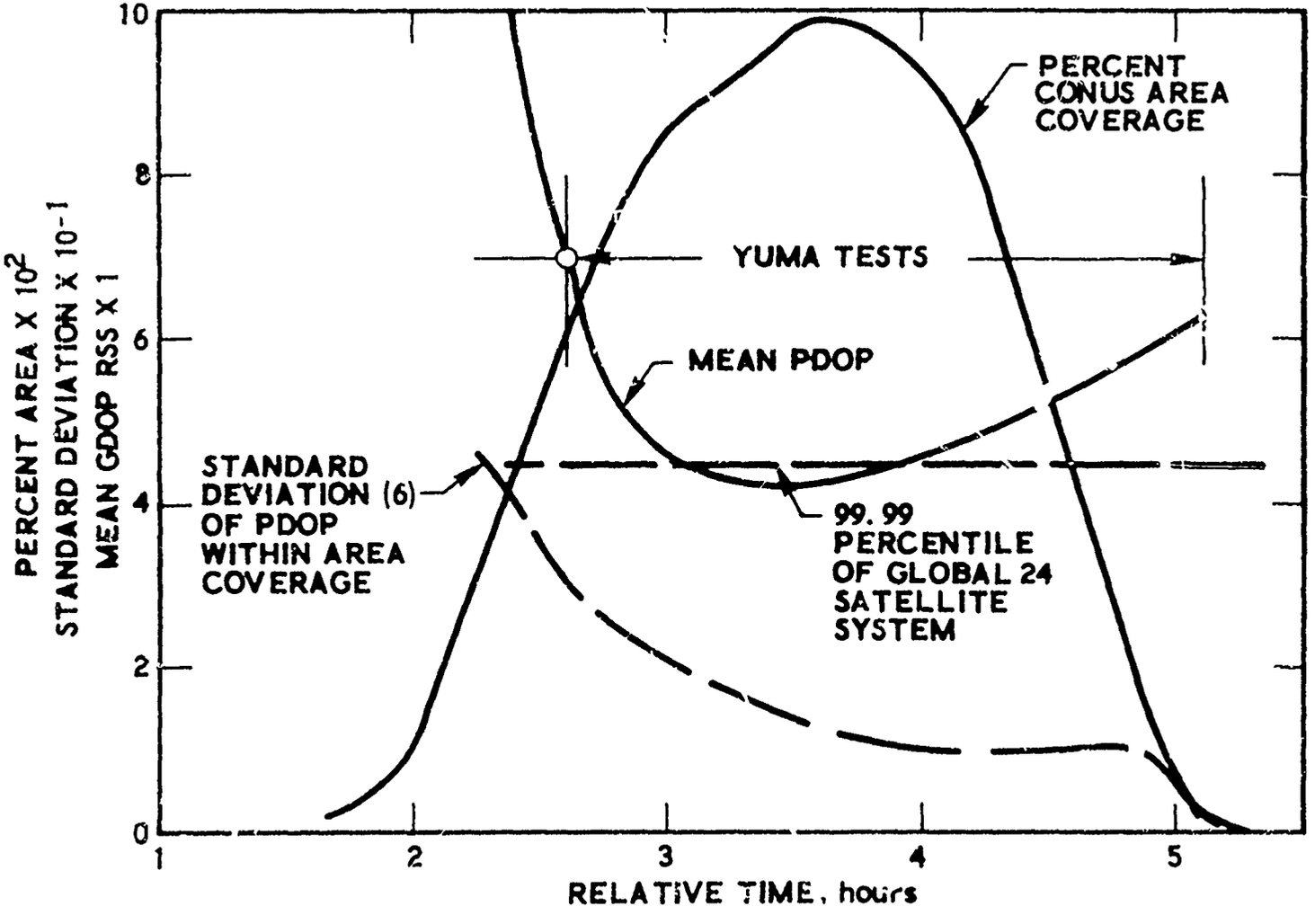

Figure 30. GPS Phase 1 - 2 × 2, Geometric Performance in CONUS

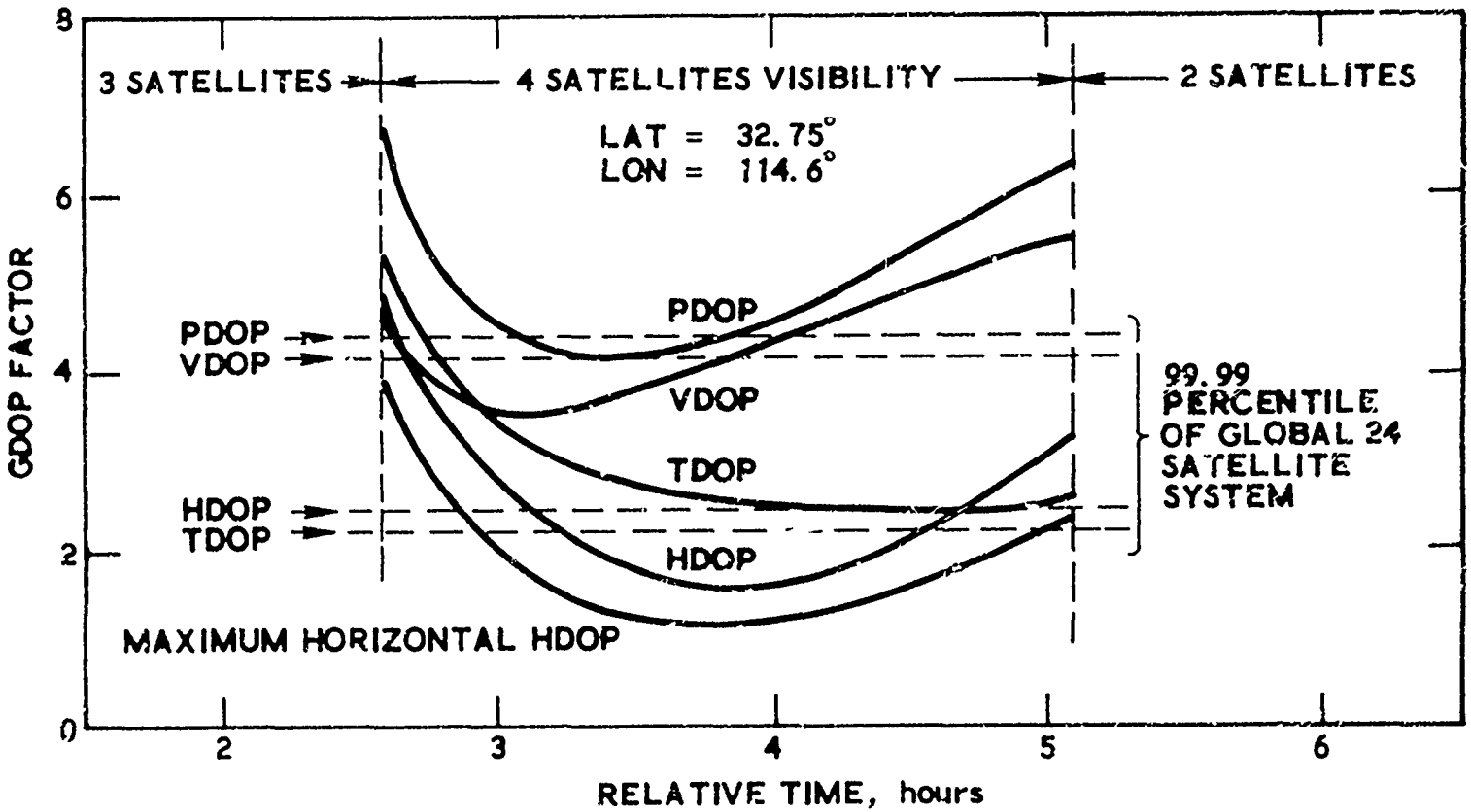

Figure 31. GPS Phase I - 2 × 2, Geometric Performance at Yuma

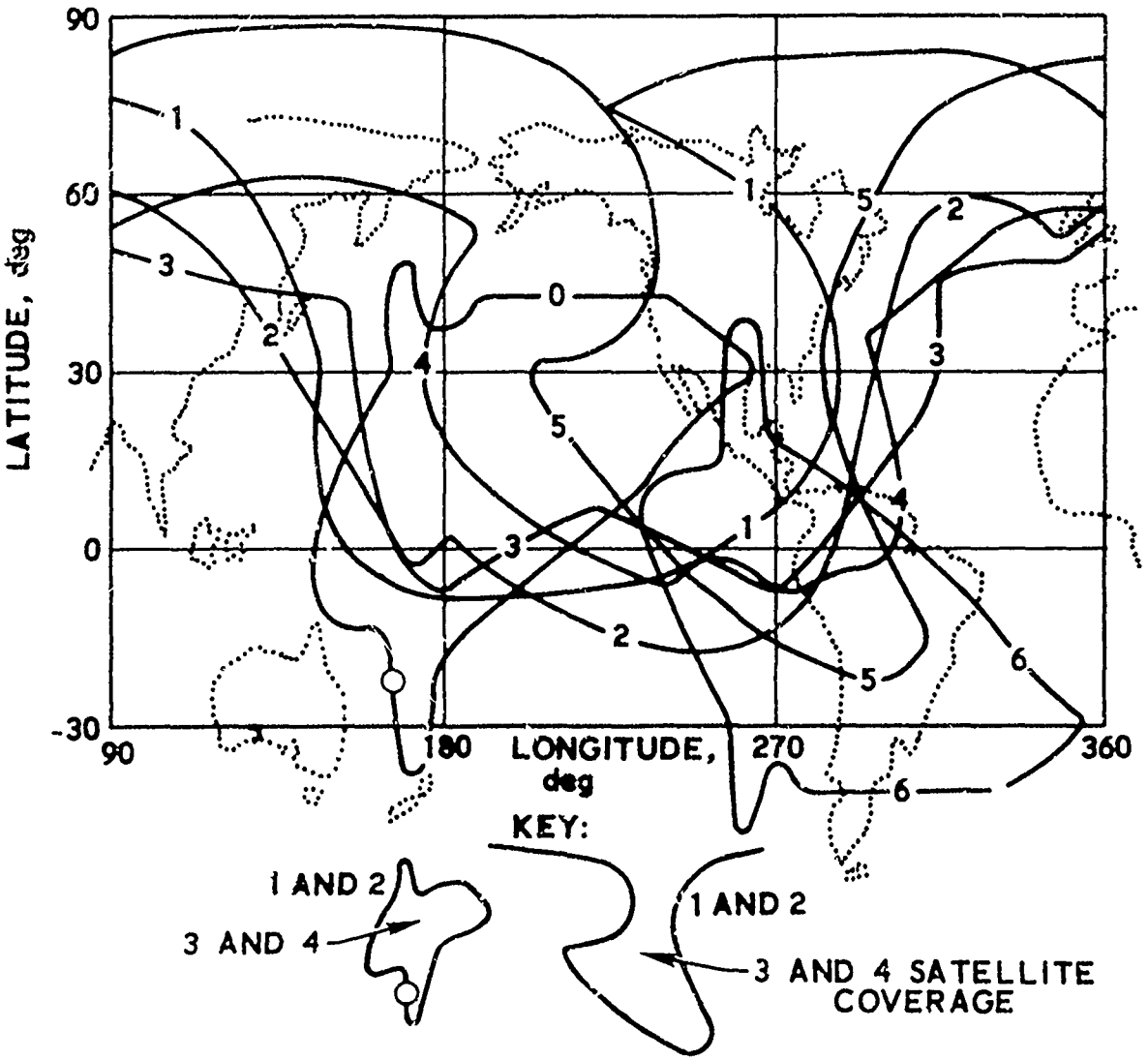

Figure 32. GPS Phase I - 2 × 2, Three- and Four-Satellite Time-Area Coverage

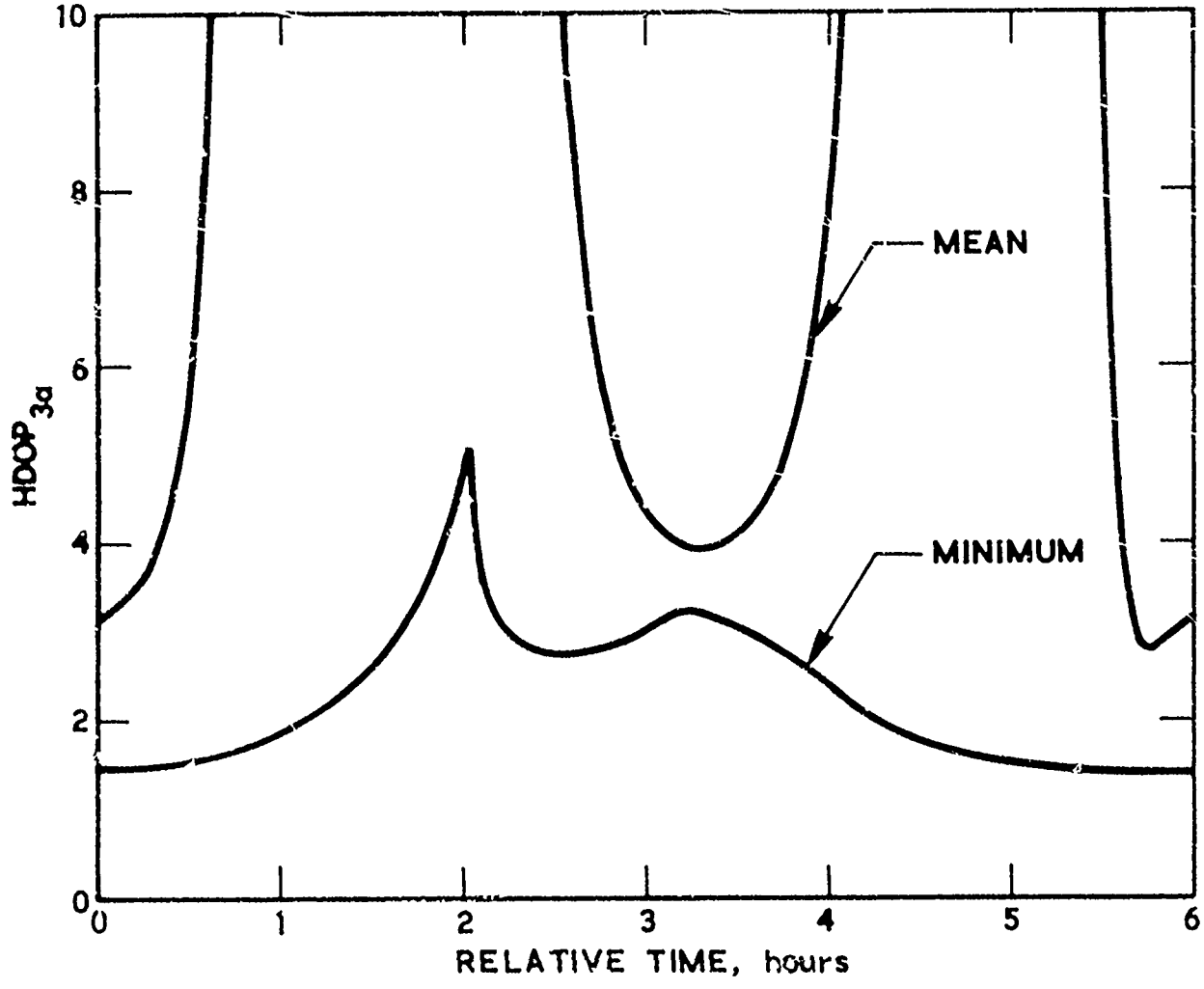

Figure 33. GPS Phase I - 2 × 2, Performance in the Three-Satellite Visibility Areas; Perfect User Altimeter

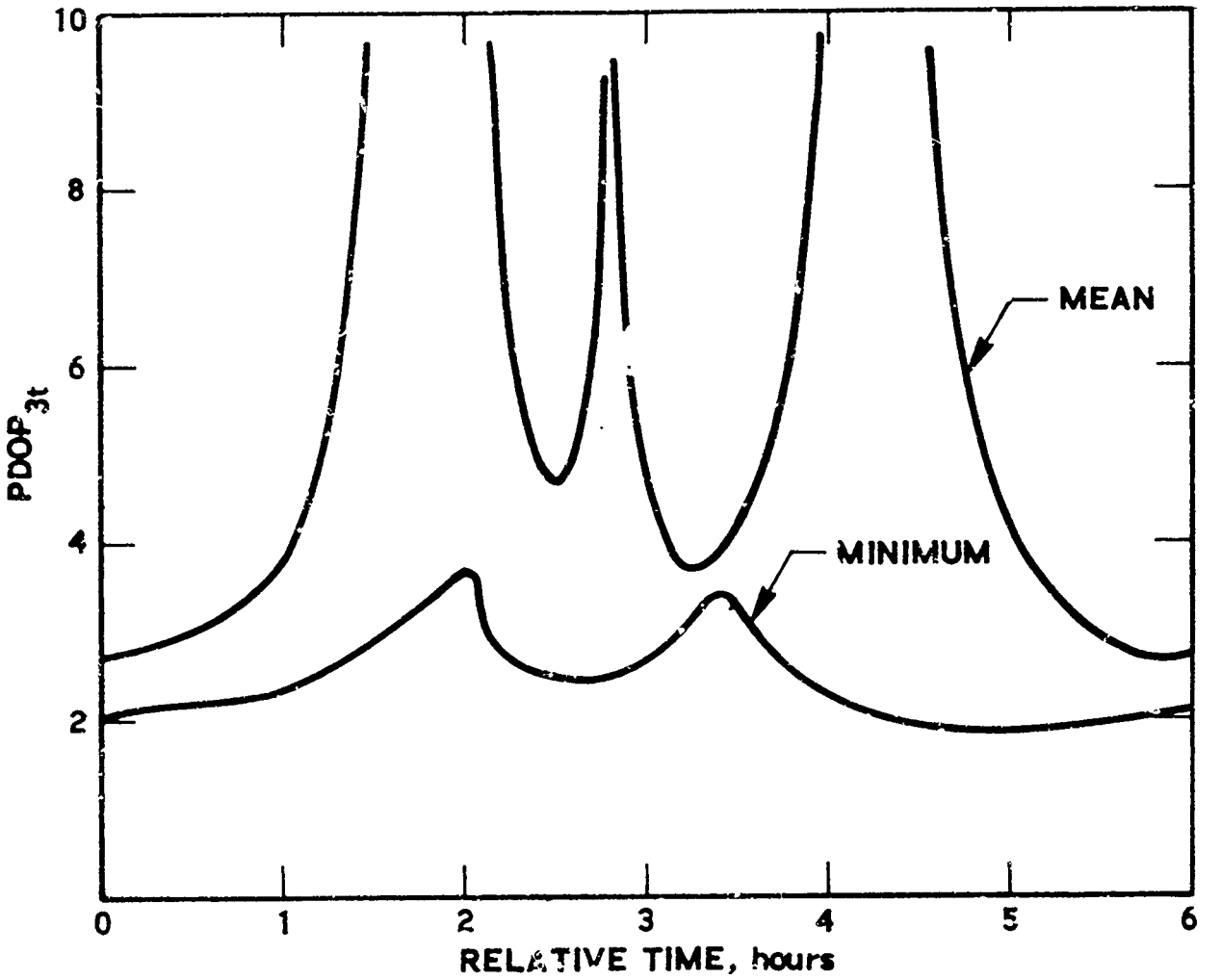

Figure 34. GPS Phase I - 2 × 2, Performance in the Three-Satellite Visibility Areas; Perfect User Clock

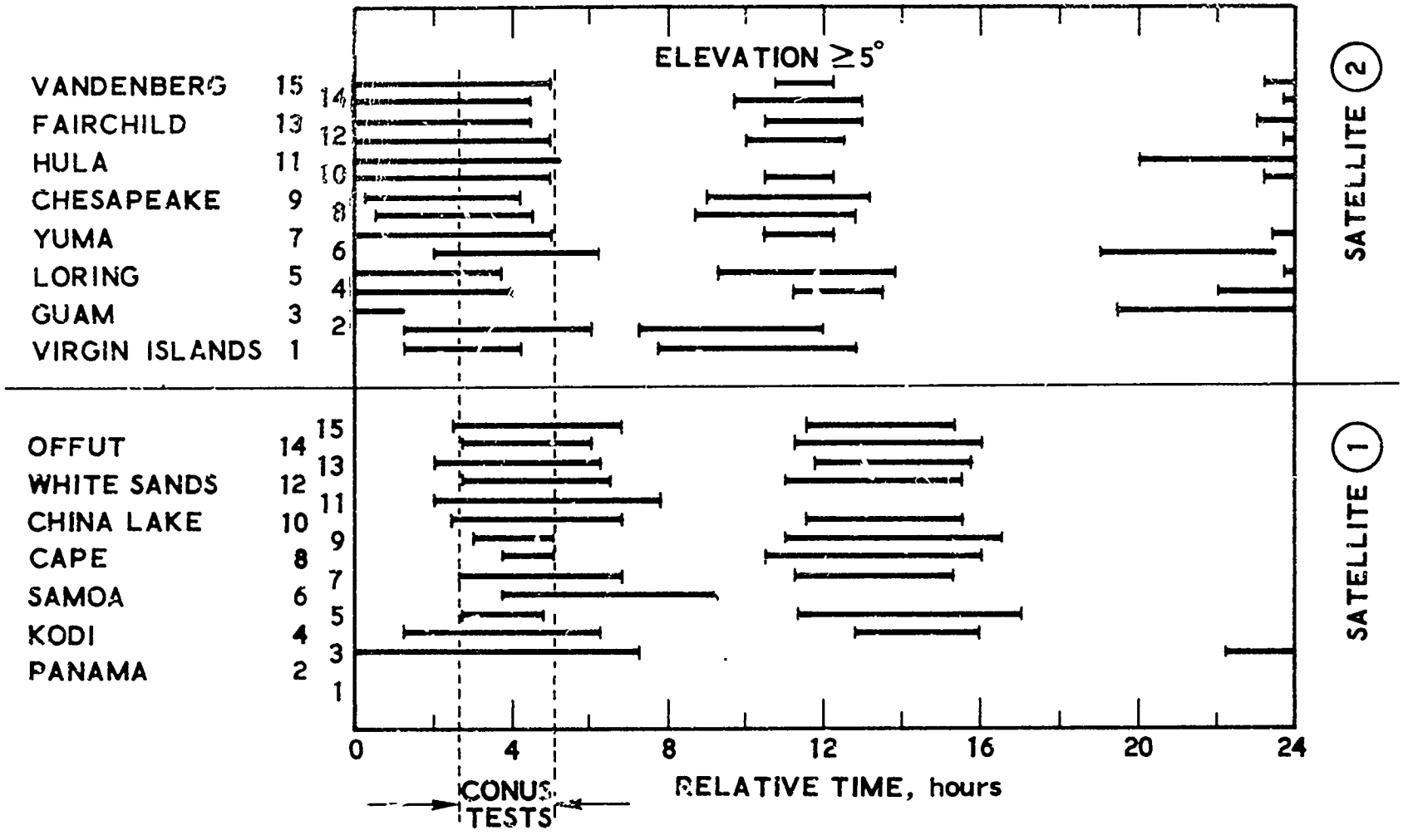

Figure 35. GPS Phase I - 2 × 2, 24-Hour Station Visibility

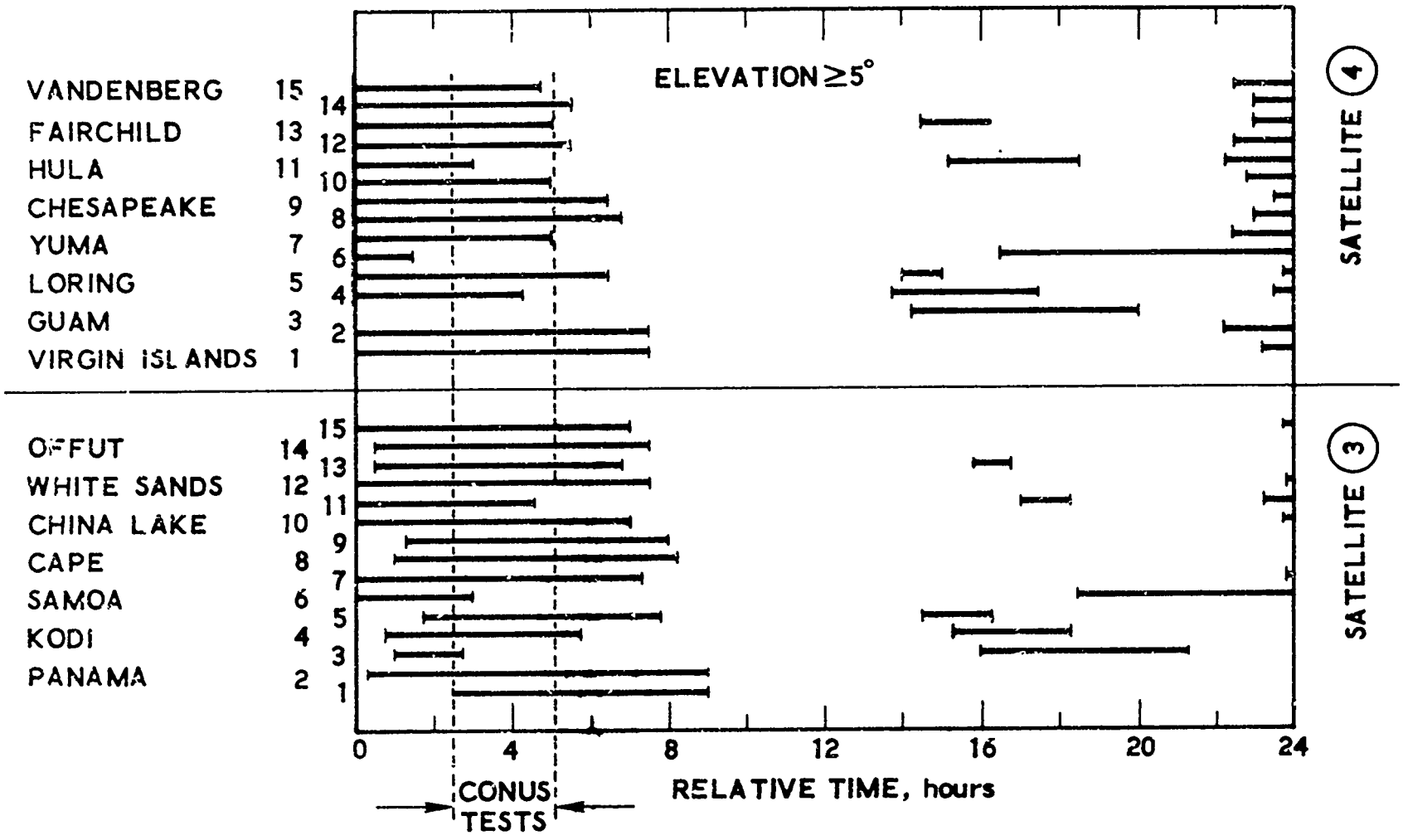

Figure 36. GPS Phase I - 2 × 2, 24-Hour Station Visibility

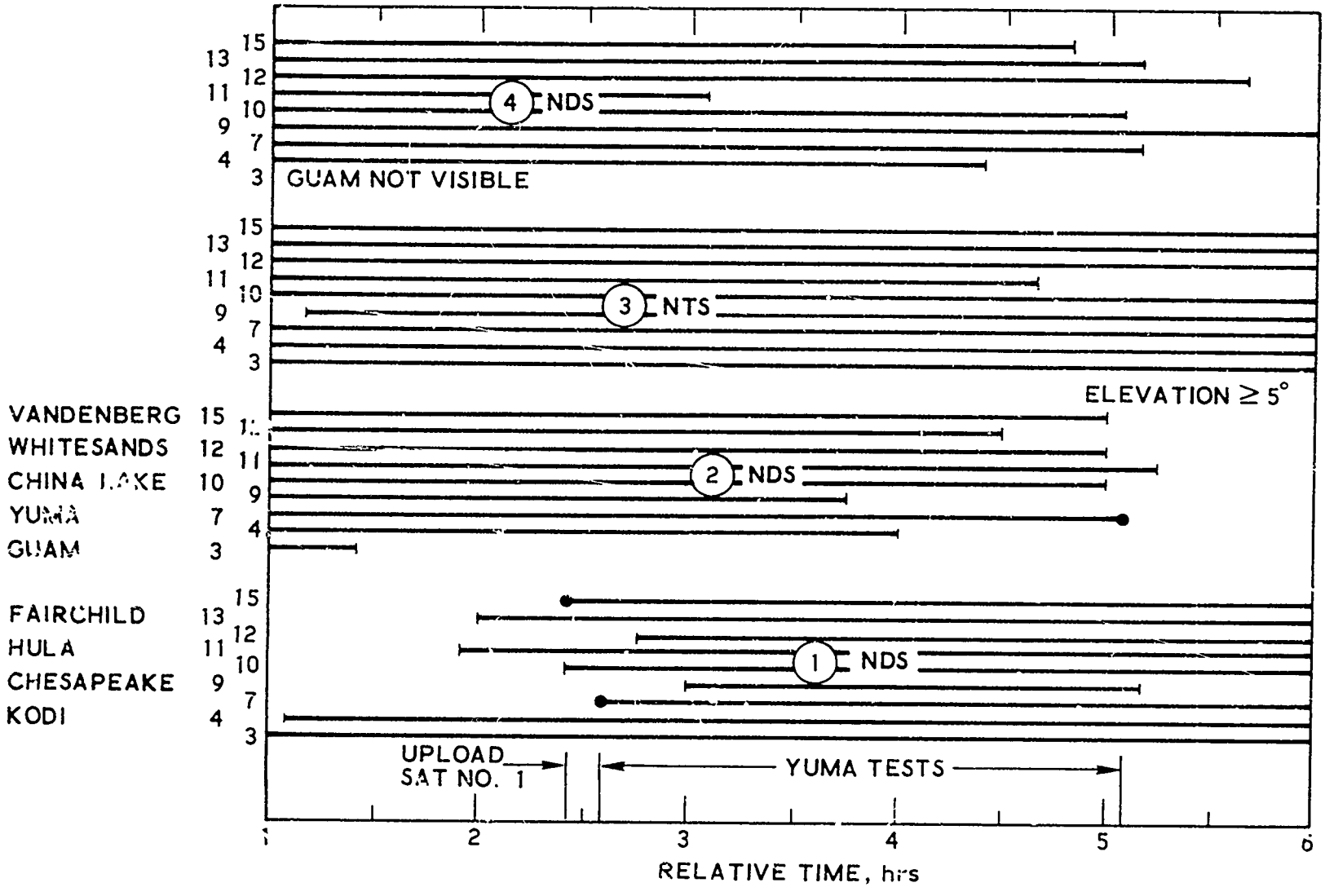

Figure 37. GPS Phase I - 2 × 2, Station Visibility During CONUS Tests

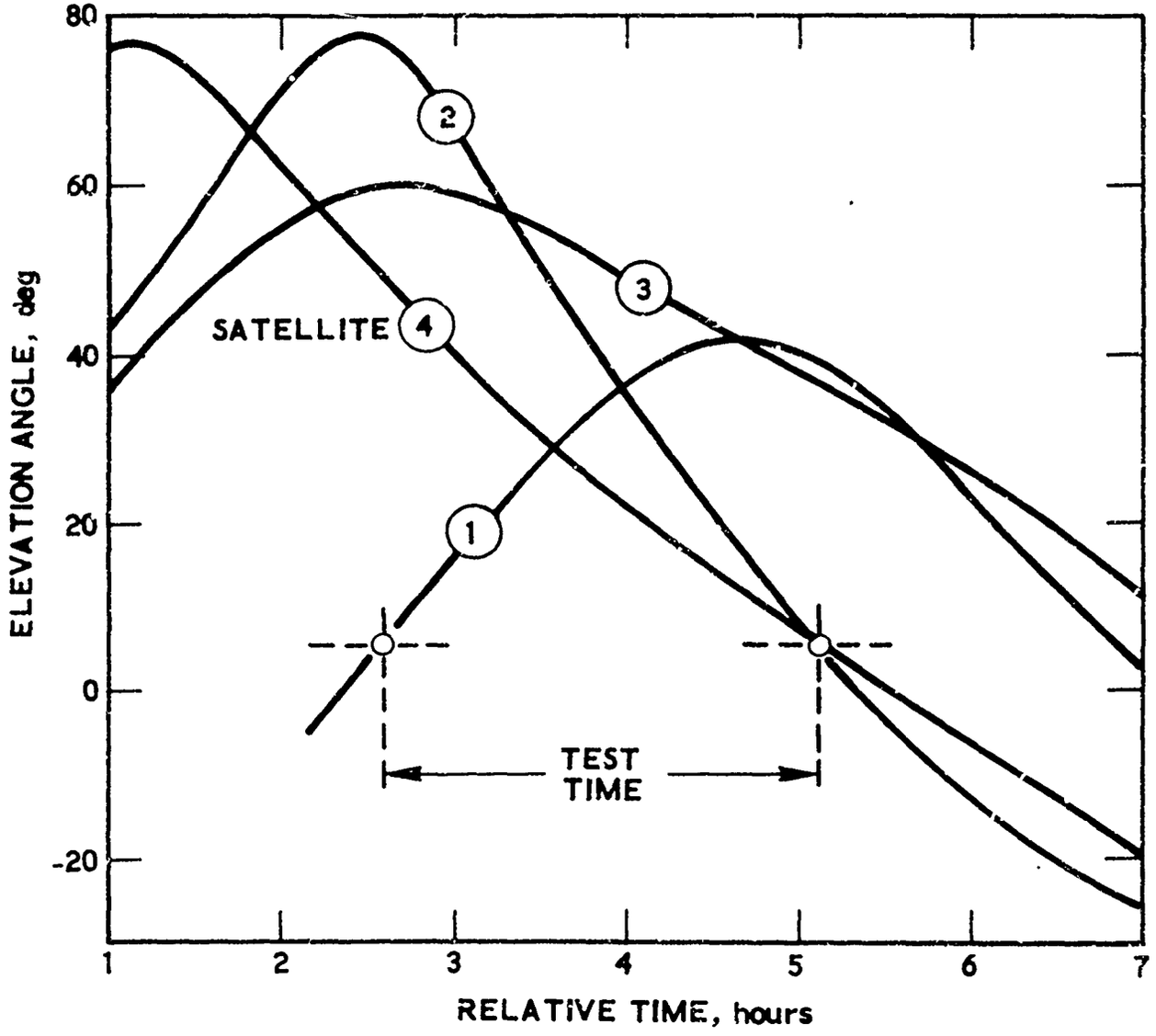

Figure 38. GPS Phase I - 2 × 2, Elevation Angles at Yuma

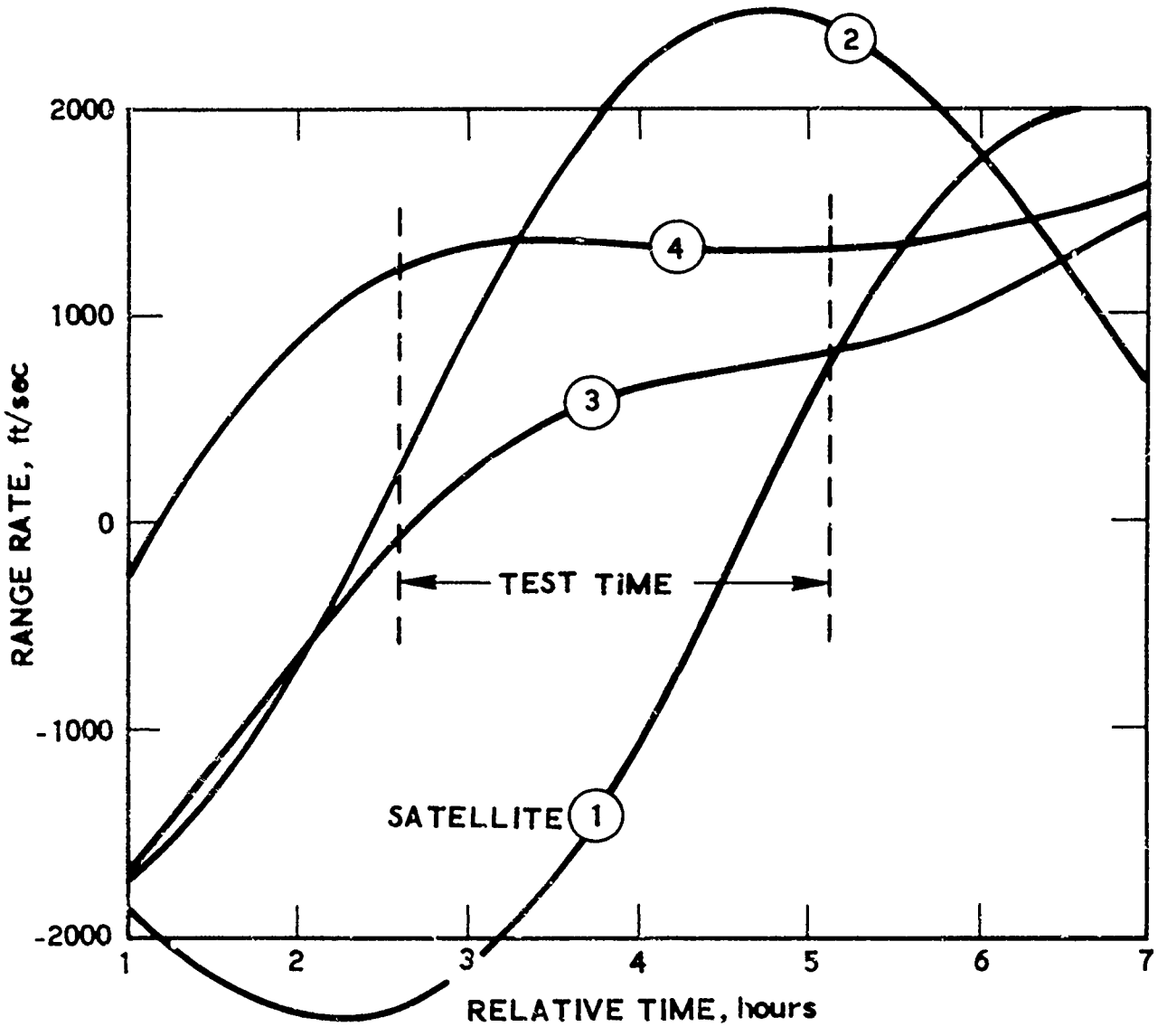

Figure 39. GPS Phase I - 2 × 2, Range-Rate (Doppler) at Yuma

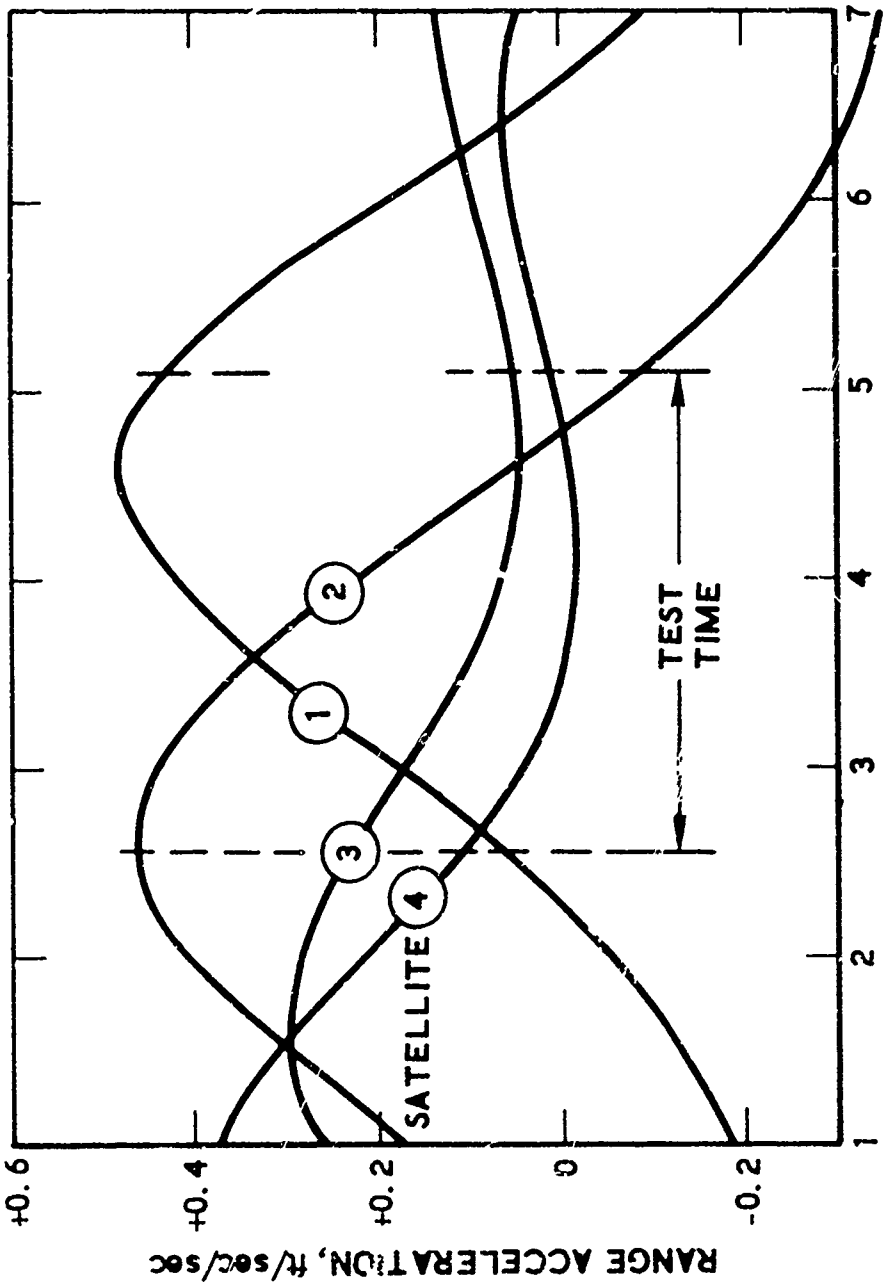

Figure 40. GPS Phase 1 - 2 × 2, Range Acceleration (Doppler Rate) at Yuma

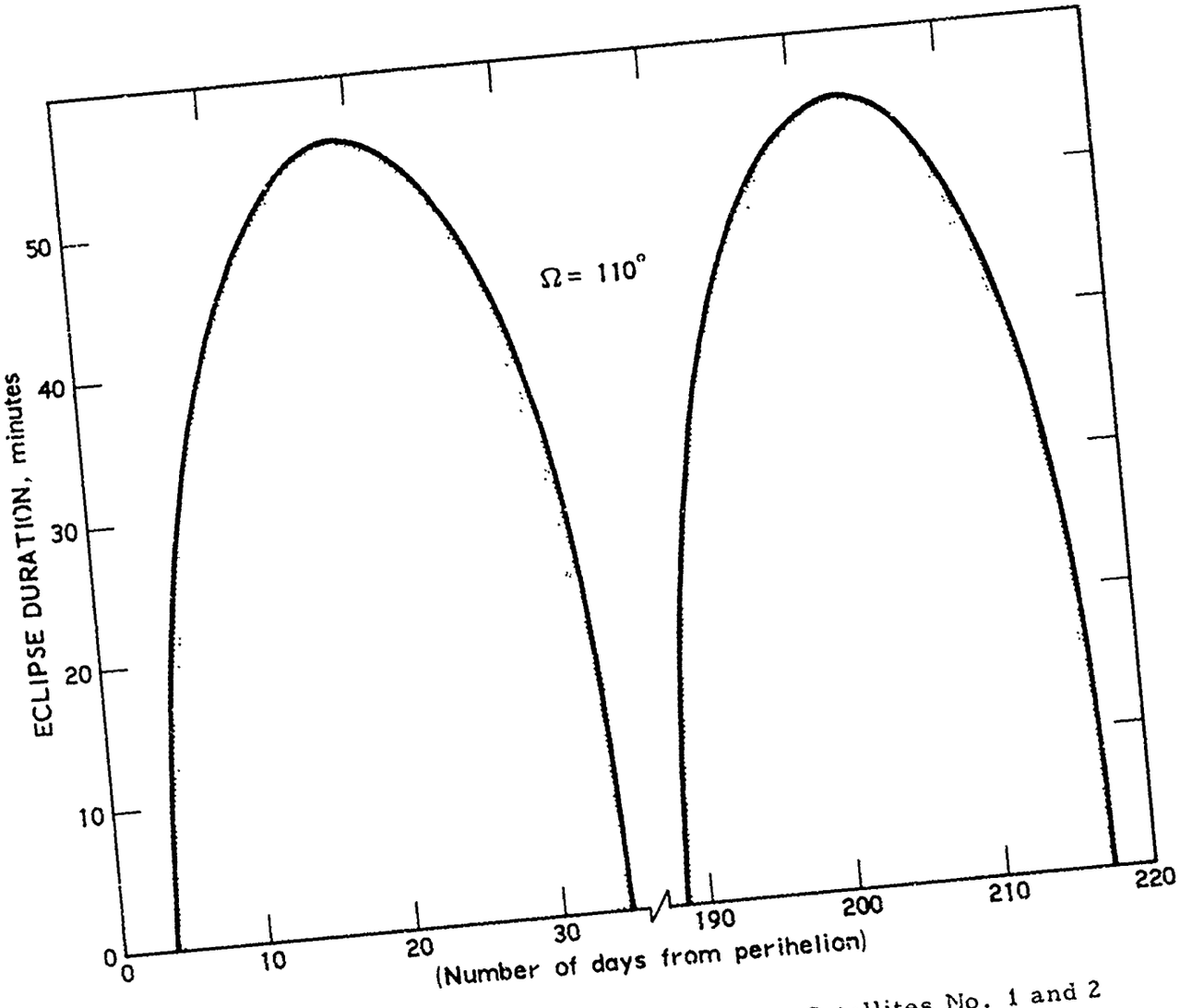

Figure 41. GPS Phase I - Eclipse Occurrence, Satellites No. 1 and 2

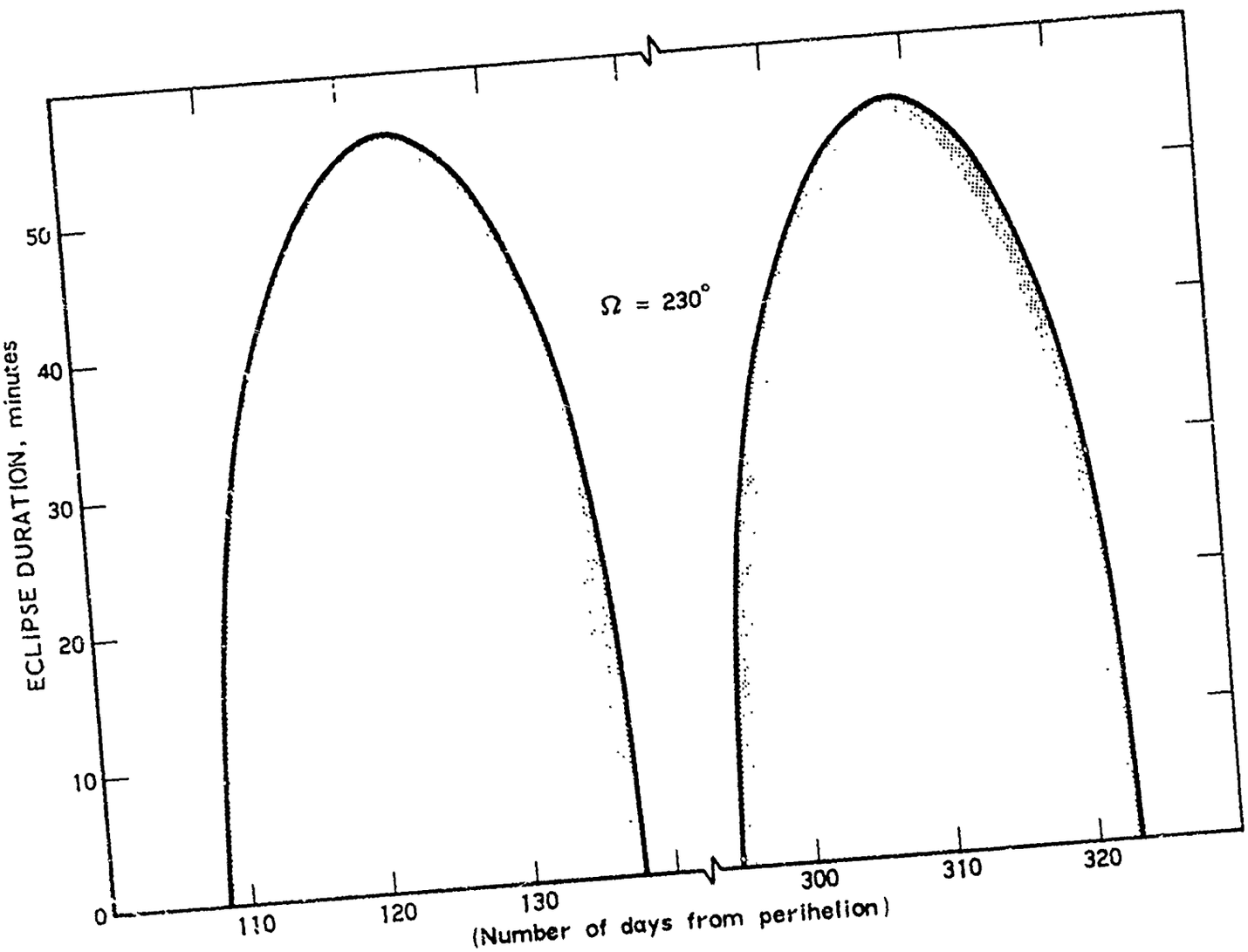

Figure 42. GPS Phase I - Eclipse Occurrence, Satellites No. 3 and 4

6. GPS PHASE II PERFORMANCE

The GPS Phase II control, space, and user system segments are operated in a manner similar to GPS Phase III. Phase II provides the first opportunity for a limited global navigation capability by virtue of its satellite orbit deployment.

6.1 ORBIT DEPLOYMENT

There are two alternative 3 × 3 deployments:

a. Three satellites are distributed uniformly (even) in each of three orbit planes

b. Three satellites are distributed nonuniformly (bunched) in the same orbit planes.

The orbital characteristics of these constellations are defined in Table 5. The characteristics of the first alternative comply with the desire to provide a global navigation capability using a minimum of two satellites on a continuous time basis. The second alternative provides the visibility of the number of satellites representative of the Phase III deployment, part of the time. The exact deployment will be determined at some later date.

6.2 VISIBILITY

Using the identical methods and criteria employed in the analysis given in Section 4.2, Figure 43 shows the percent probability of observing a given number of satellites (or higher) at various latitudes for the even uniformly distributed 3 × 3 constellation. It is seen that on a global scale, a minimum of two satellites are visible for all time-space, and that as many as six are visible 1.04 percent of the time. The distribution indicates that users located at higher latitudes observe more satellites than those at lower latitudes. Tables 6 and 7 provide, on a global basis, the minimum and maximum numbers of satellites seen sometime during the orbit period.

Figure 44 shows the visibility distribution for the bunched 3 × 3 constellation. As would be expected, the number of visible satellites varies greatly. A comparison with the even 3 × 3 configuration (Figure 43) reveals that a user has consistently higher probabilities of observing more satellites at the expense of not seeing any for some time. Tables 8 and 9 show the distribution of the maximum and minimum numbers observed globally.

6.3 PERFORMANCE

Since the evenly-distributed 3 × 3 constellation has less than four satellites visible approximately 20 percent of the time and the bunched 3 × 3 has approximately 40 percent, this time may be utilized by the user equipped with a highly accurate altimeter or highly accurate and synchronized clock, or both.

Figure 45 shows, for the uniformly distributed 3 × 3 configuration, the cumulative GDOP distribution for the global areas where four or more satellites are seen sometime during the orbit period. This distribution is based upon the same criteria as for the global 3 × 8 constellation. The selection of the optimum four satellites using the unit vector volume is identical. If the user is located in the right place at the right time, a 50-50 chance exists that the user will obtain conditions where he can navigate as well as in the 3 × 8 system (PDOP ≤ 4.6 each 50 percentile). Failure to obtain good conditions is attributable to the lack of satellite population, since for all practical purposes, only four or five satellites are available for selection in these areas.

Figures 46 and 47 show, for the even 3 × 3, the GDOP distribution (see Appendix A for definition of GDOP) in the areas where only three satellites are visible. Here the user is either equipped with a perfect altimeter or a highly accurate clock. The ability to navigate is not much different in either case. Figure 48 shows the performance when two satellites are seen and the user has both a perfect altimeter and a perfect clock.

Figures 49 through 52 relate the performance of the bunched 3 × 3 in a similar fashion. For the areas where four or more satellites are seen, the performance relative to the even 3 × 3 is considerably improved. This is due to the greater density of satellites that provide the user with a better selection for the "optimum four."

Table 5. GPS Phase II - 3 × 3 Orbital Characteristics

Satellite Ident	Ecc (e)	Inc (i)	A of P (ω)	RA (Ω)	PER (T)	MA (M)	
						Even	Bunched
1	0	63	0	0	12	15	15
2	0	63	0	0	12	135	75
3	0	63	0	0	12	255	135
4	0	63	0	120	12	(-) 15	(-) 15
5	0	63	0	120	12	105	45
6	0	63	0	120	12	225	105
7	0	63	0	240	12	0	0
8	0	63	0	240	12	120	60
9	0	63	0	240	12	240	120

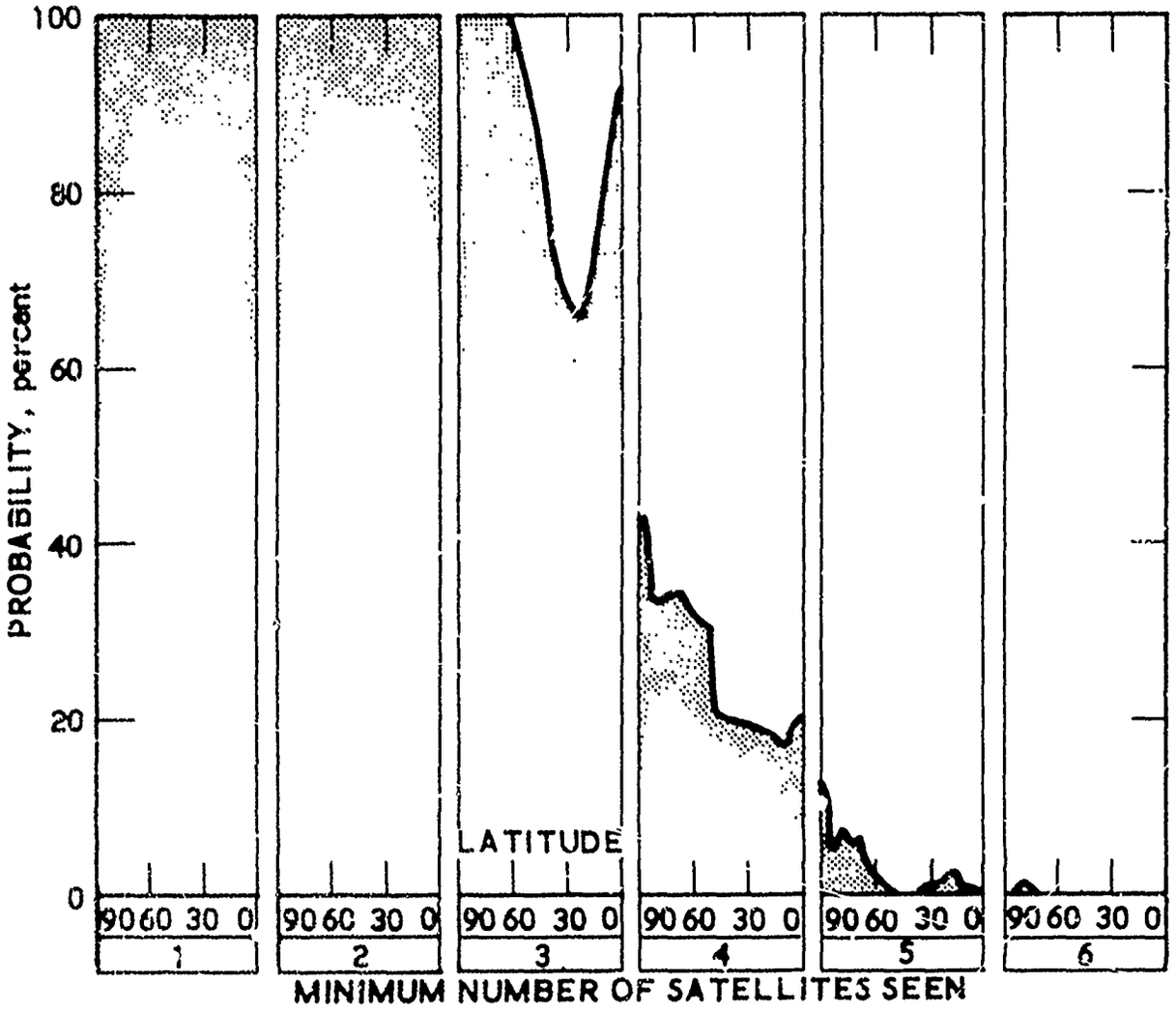

Figure 43. GPS Phase II - 3 × 3 Ever, Global Visibility Distribution

Table 6. GPS Phase II - 3 × 3 Even, Minimum Number of Satellites Seen

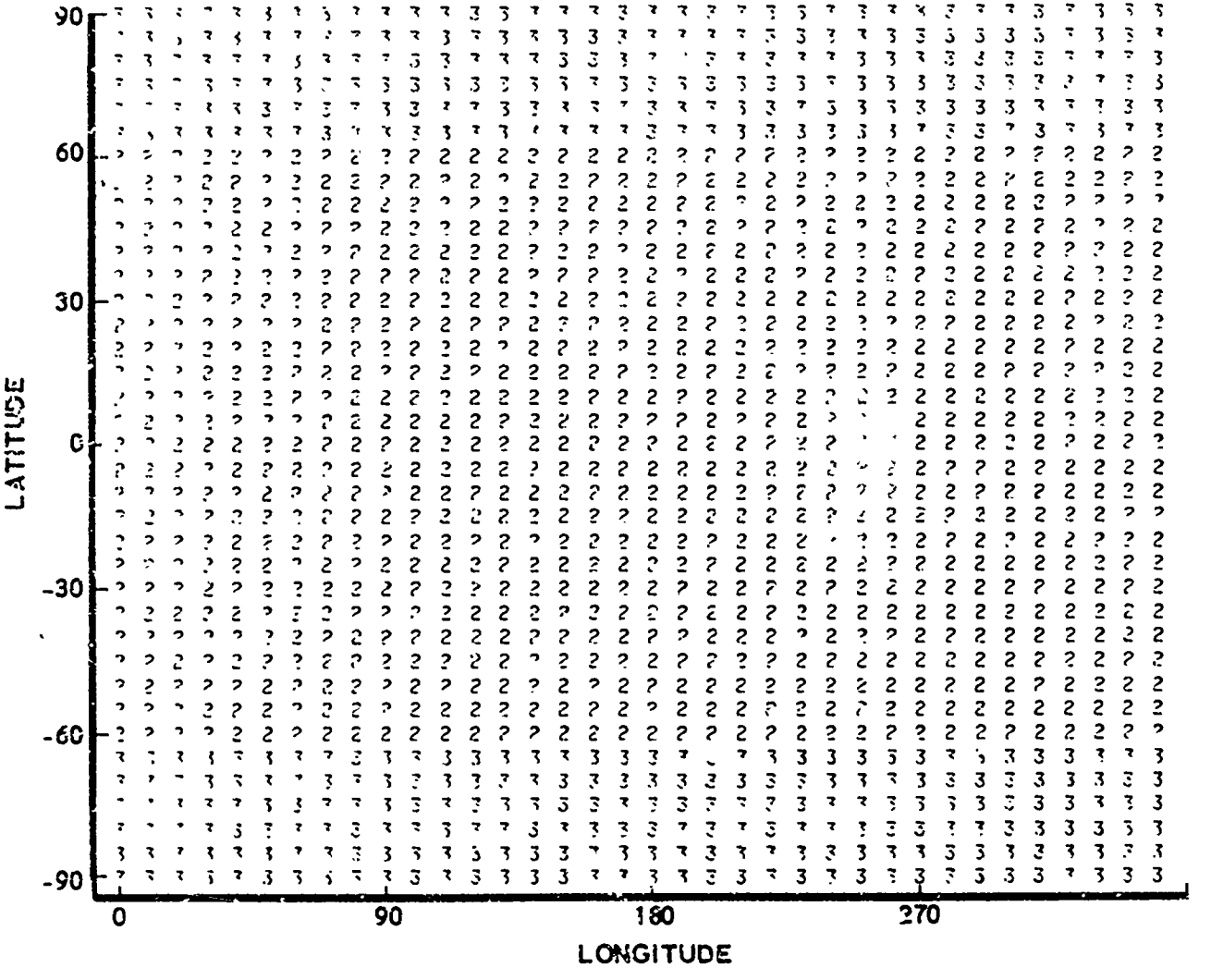

Table 7. GPS Phase II - 3 × 3 Even, Maximum Number of Satellites Seen

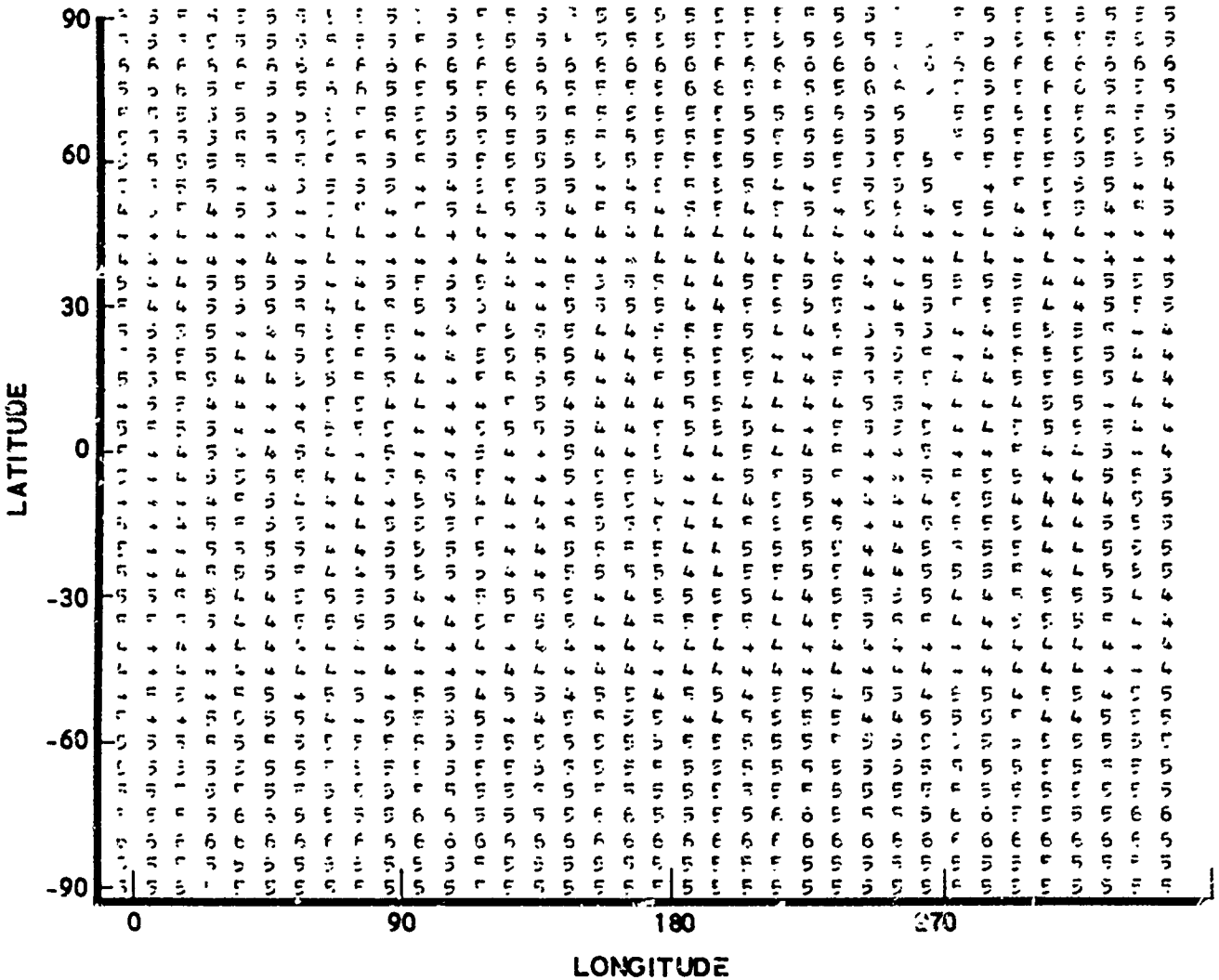

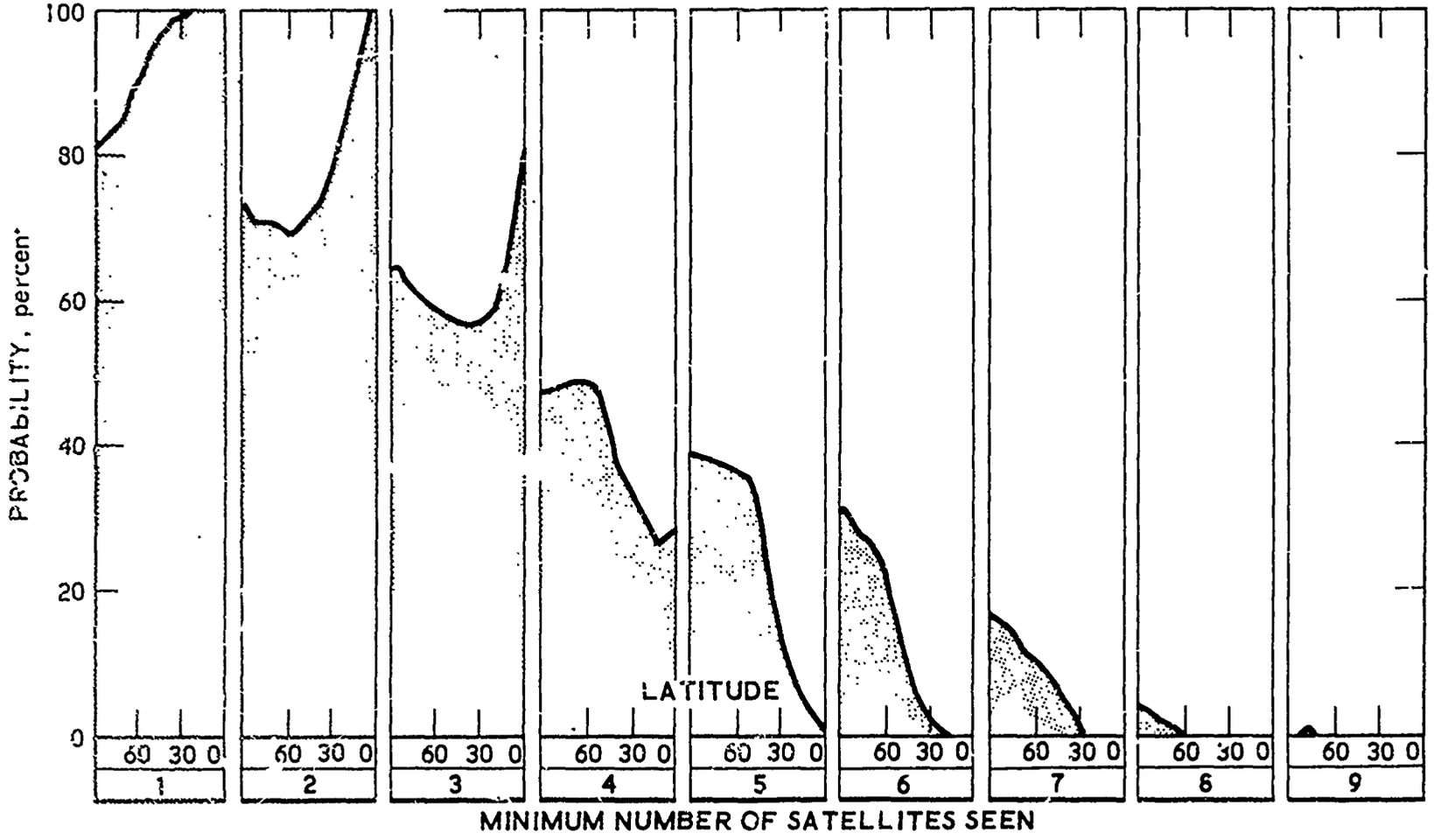

Figure 44. GPS Phase II - 3 × 3 Bunched, Global Visibility Distribution

Table 8. GPS Phase II - 3 X 3 Bunched, Minimum Number of Satellites Seen

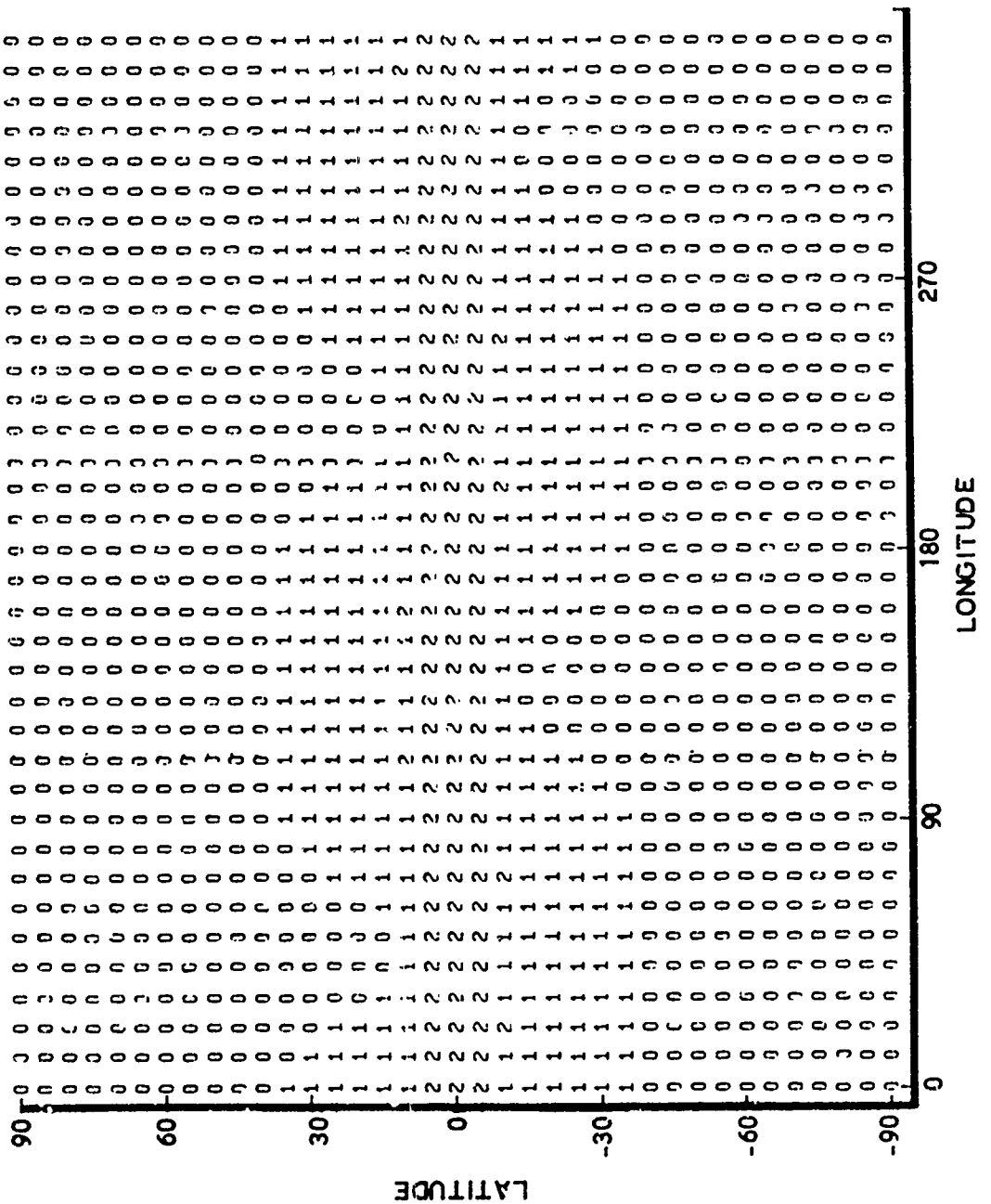

Table 9. GPS Phase II - 3 × 3 Bunched, Maximum Number of Satellites Seen

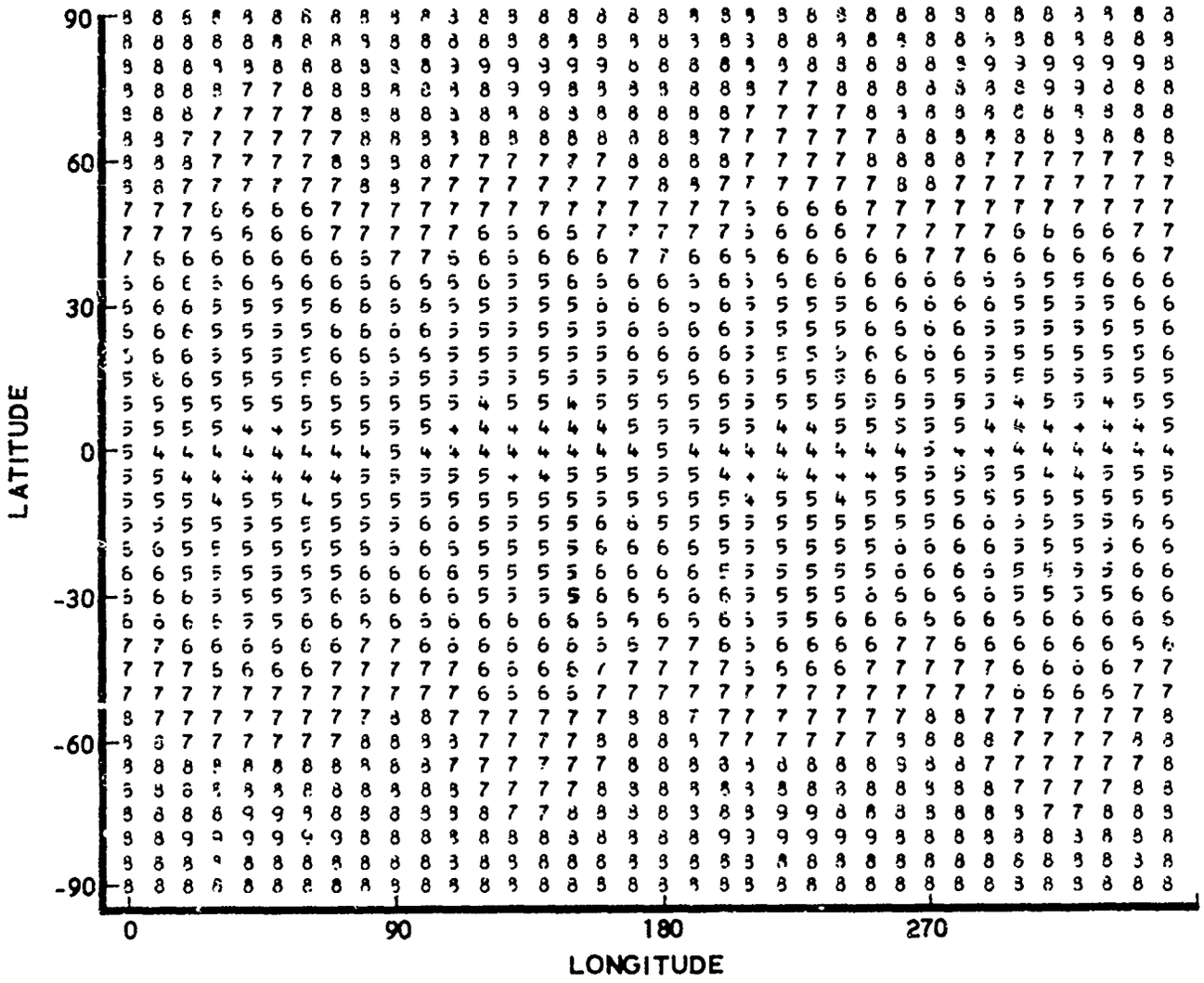

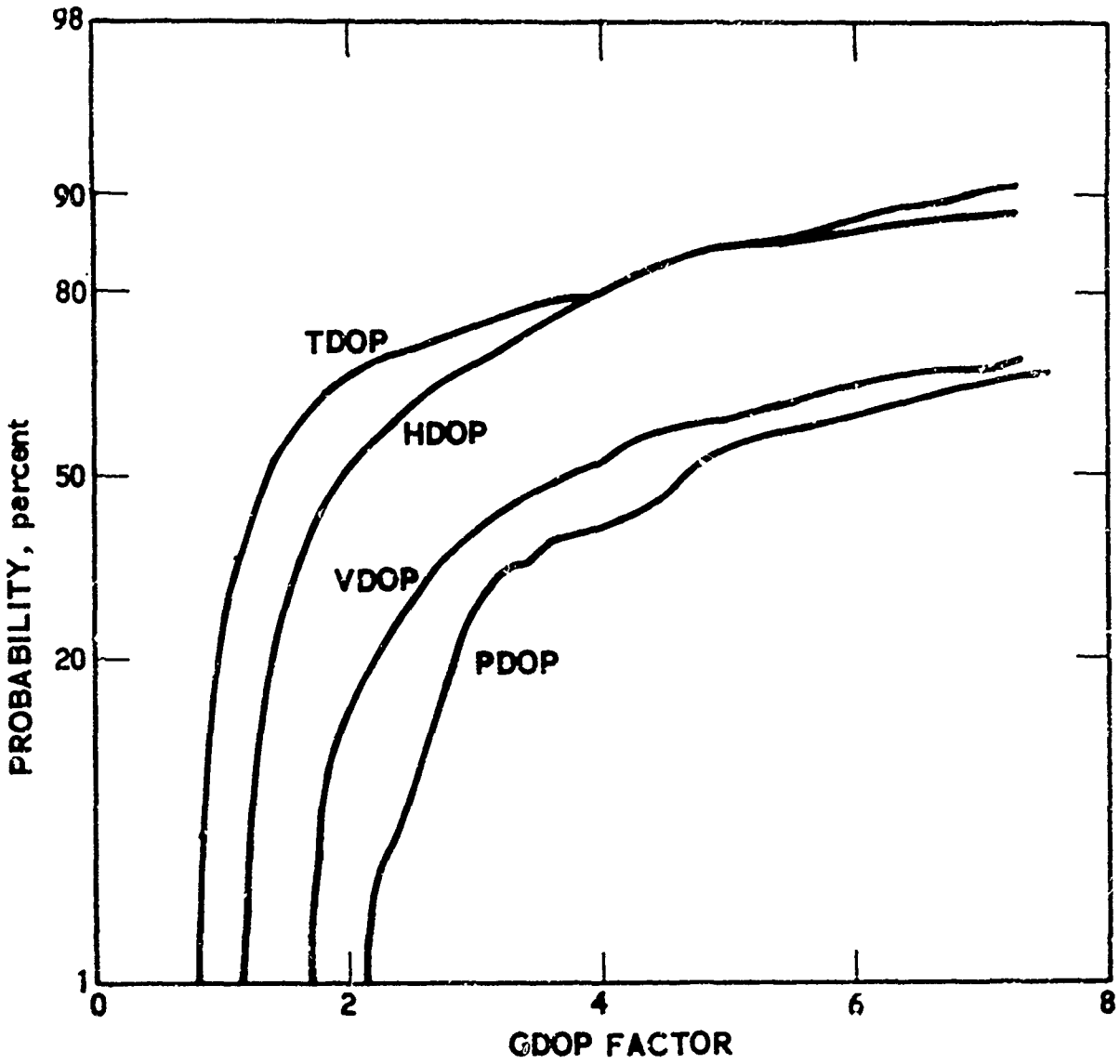

Figure 45. GPS Phase II - 3 × 3 Even, Cumulative GDOP Distribution for the Global Areas Where Four or More Satellites are Visible

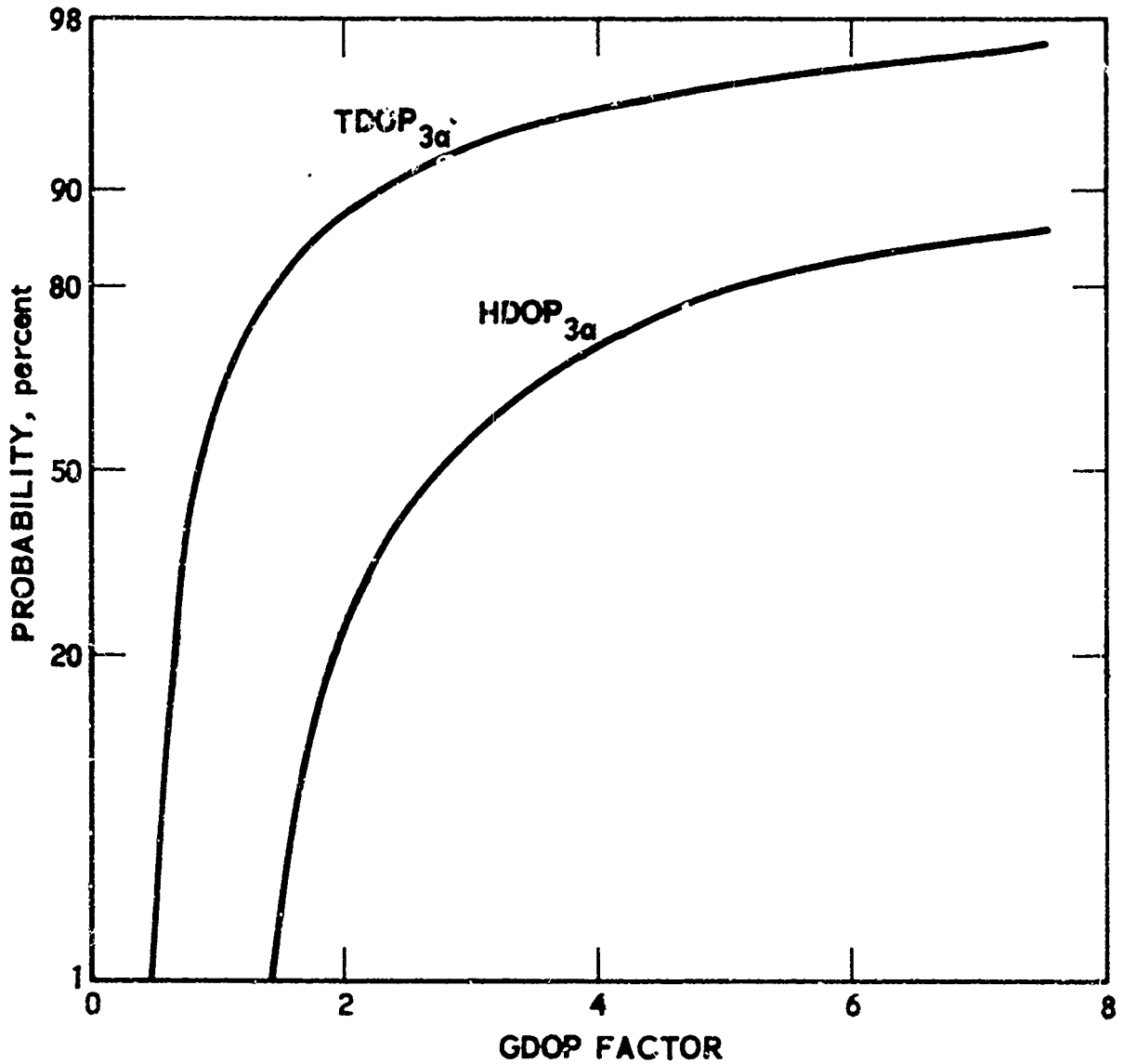

Figure 46. GPS Phase II - 3 × 3 Even, Cumulative GDOP Distribution for the Global Areas Where Three Satellites are Visible (User Has a Perfect Altimeter)

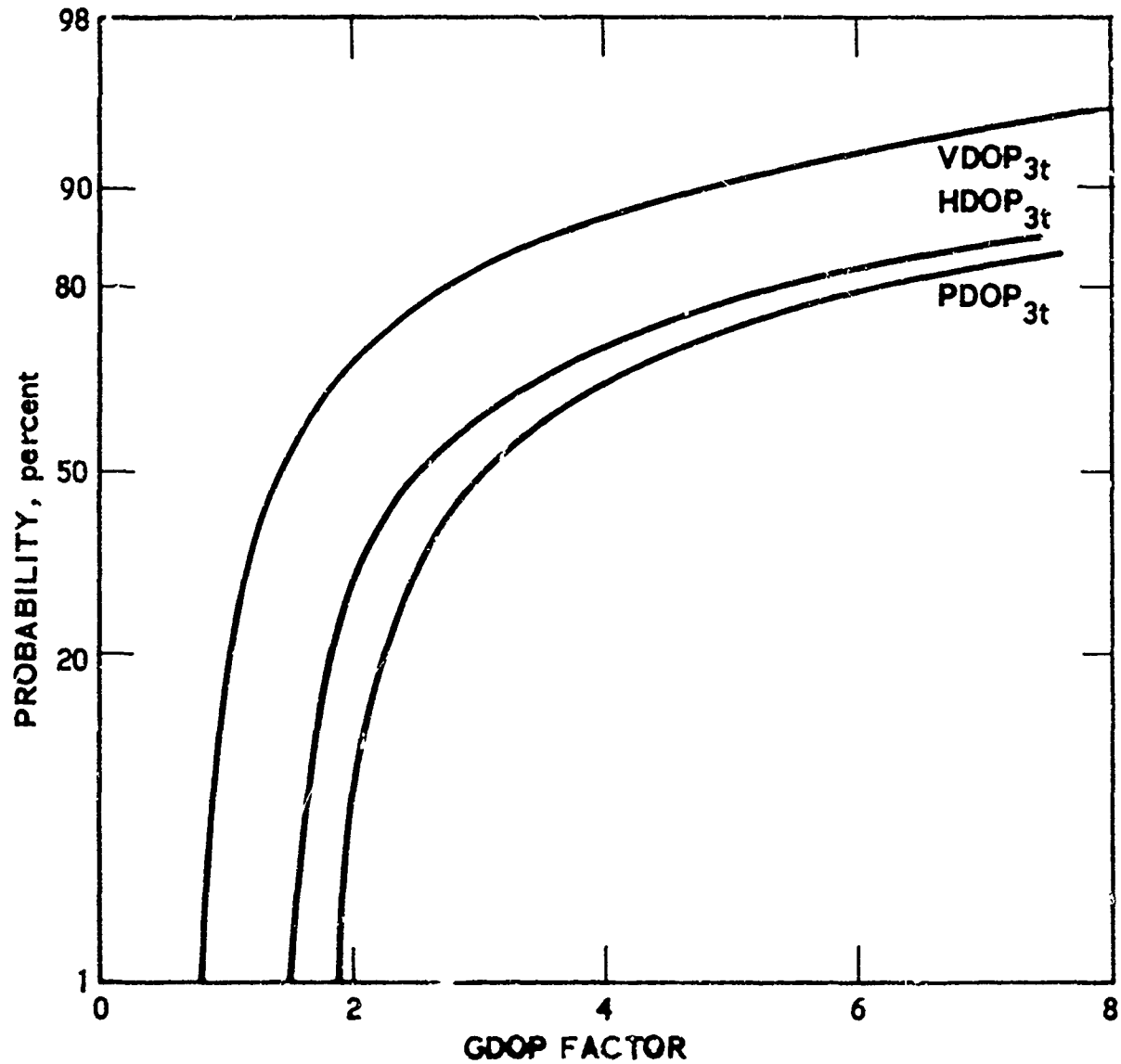

Figure 47. GPS Phase II - 3 × 3 Even, Cumulative GDOP Distribution for the Global Areas Where Three Satellites are Visible (User Has a Perfect Clock)

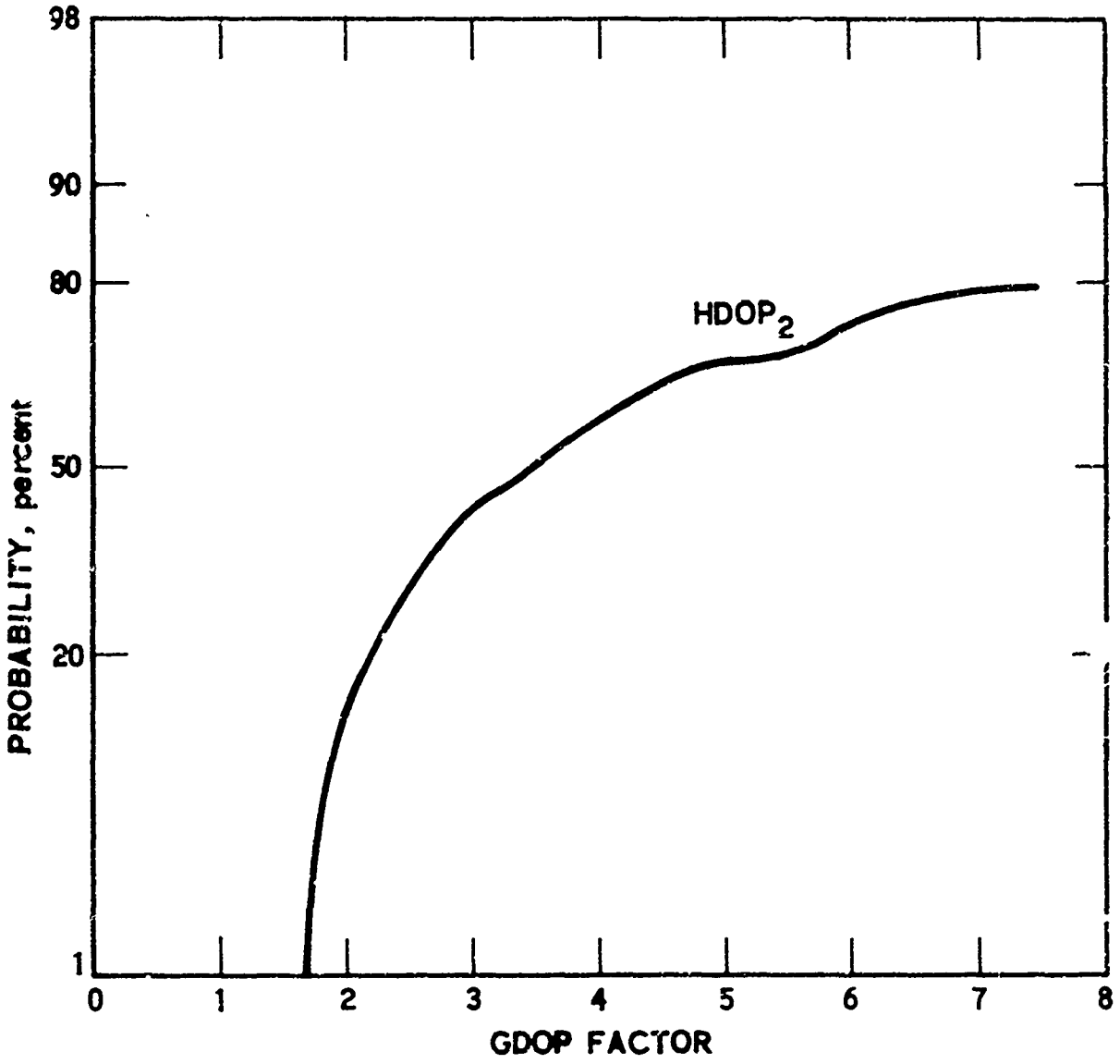

Figure 48 Phase II - 3 × 3 Even, Cumulative GDOP Distribution for the Global Areas Where Two Satellites are Visible (User Has a Perfect Clock and a Perfect Altimeter)

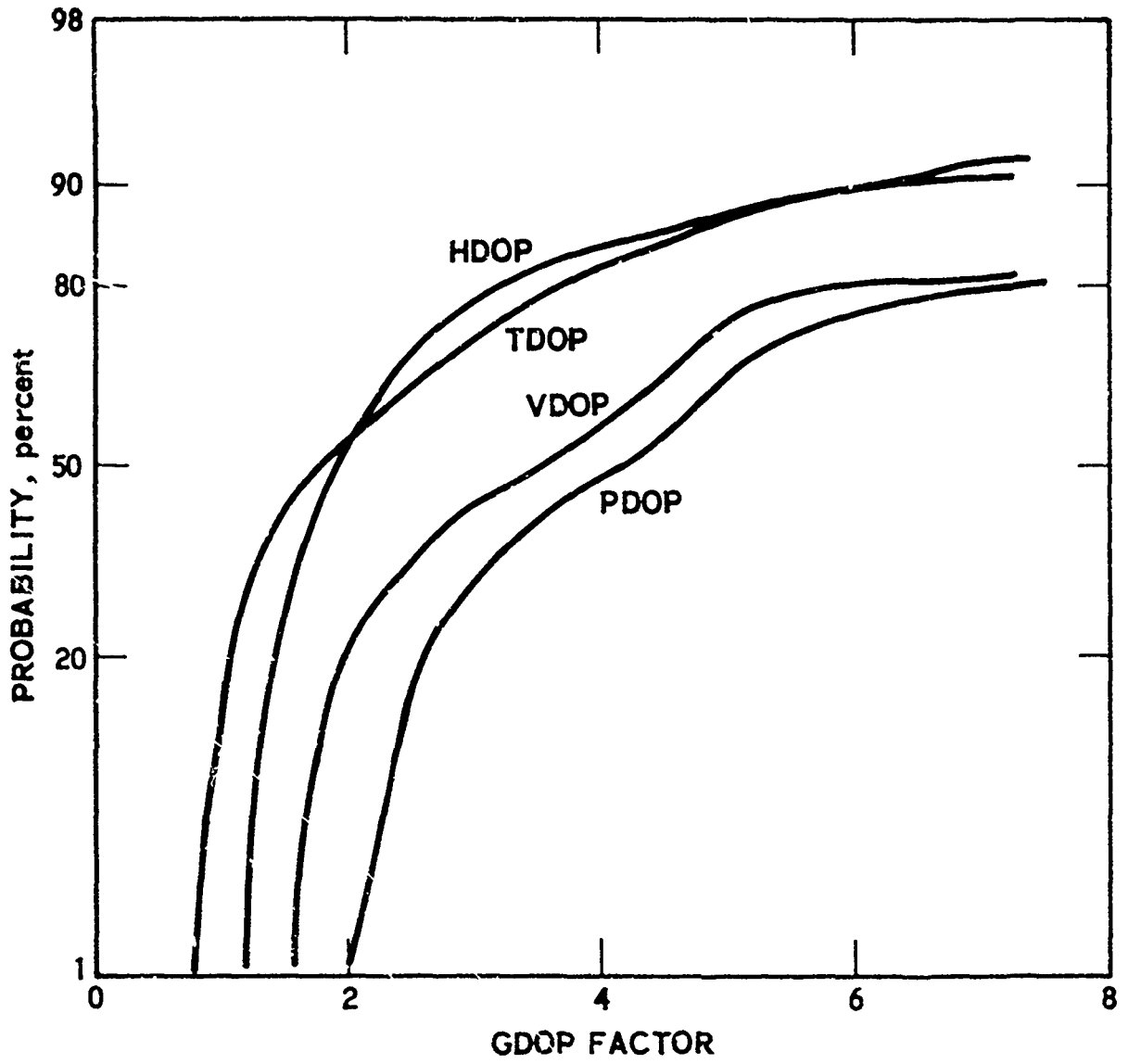

Figure 49. GPS Phase II - 3 × 3 Bunched, Performance for the Global Areas Where Four or More Satellites are Visible

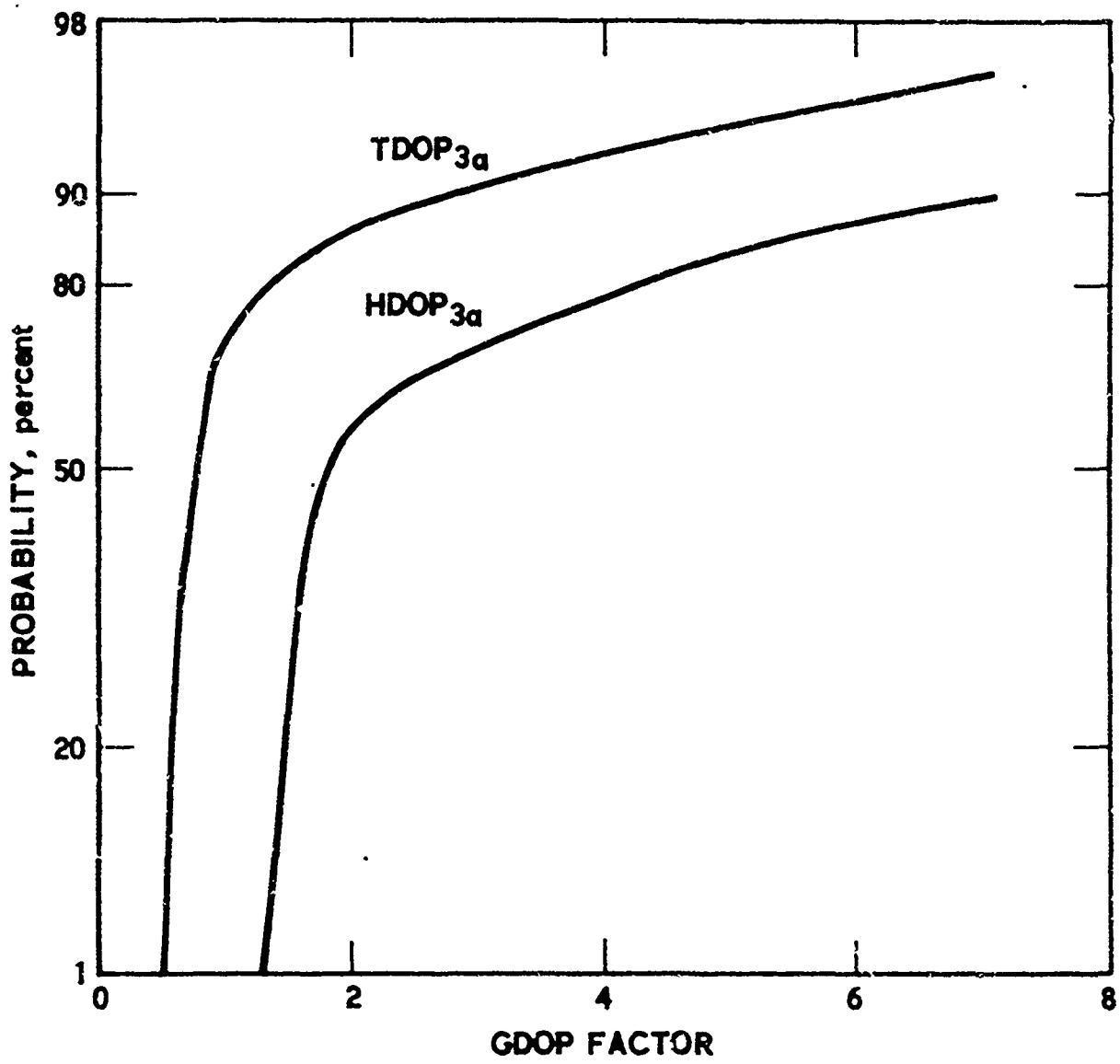

Figure 50. GPS Phase II - 3 × 3 Bunched, Cumulative GDOP Distribution for the Global Areas Where Three Satellites are Visible (User Has a Perfect Altimeter)

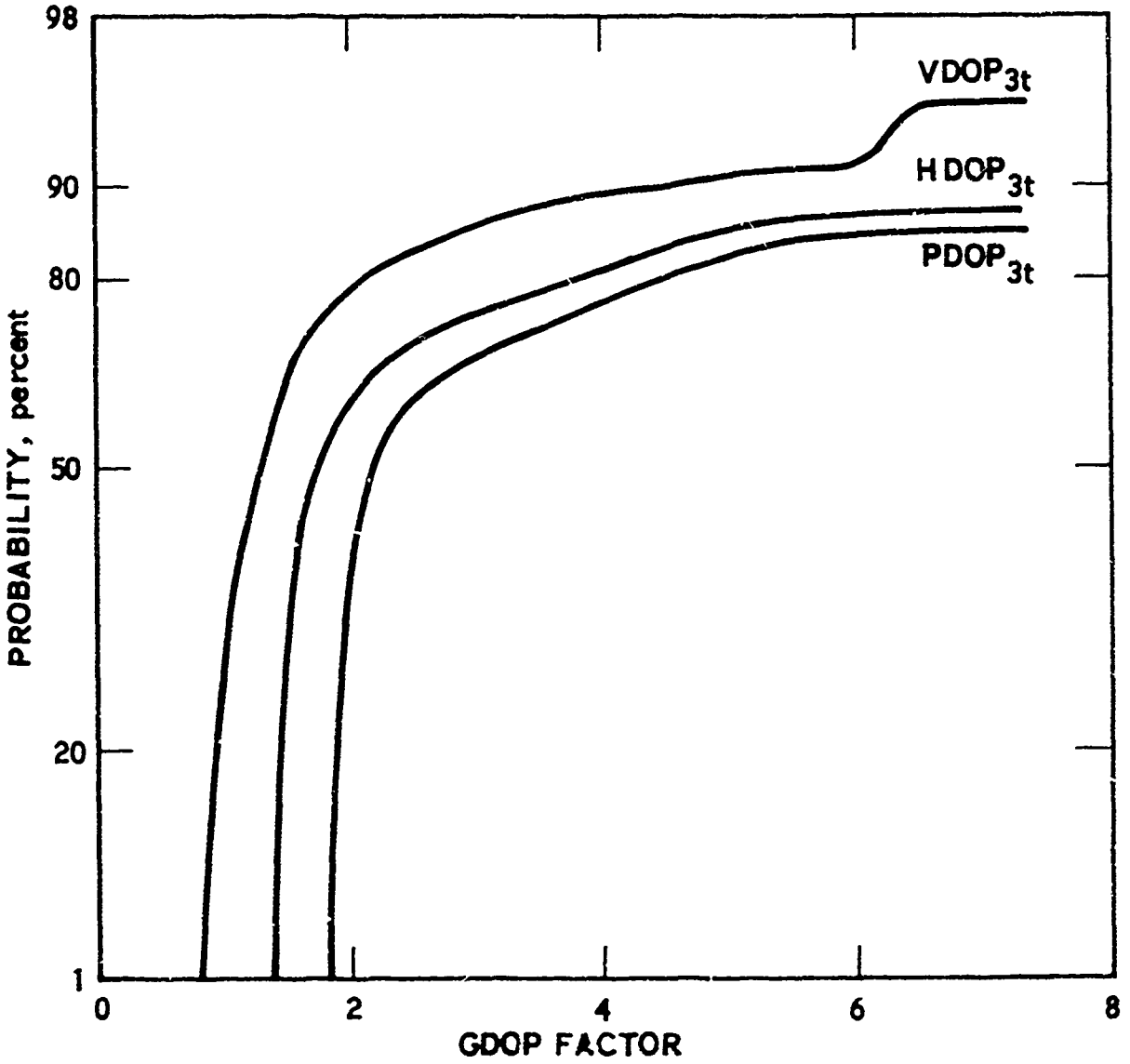

Figure 51. GPS Phase II - 3 × 3 Bunched, Cumulative GDOP Distribution for the Global Areas Where Three Satellites are Visible (User Has a Perfect Clock)

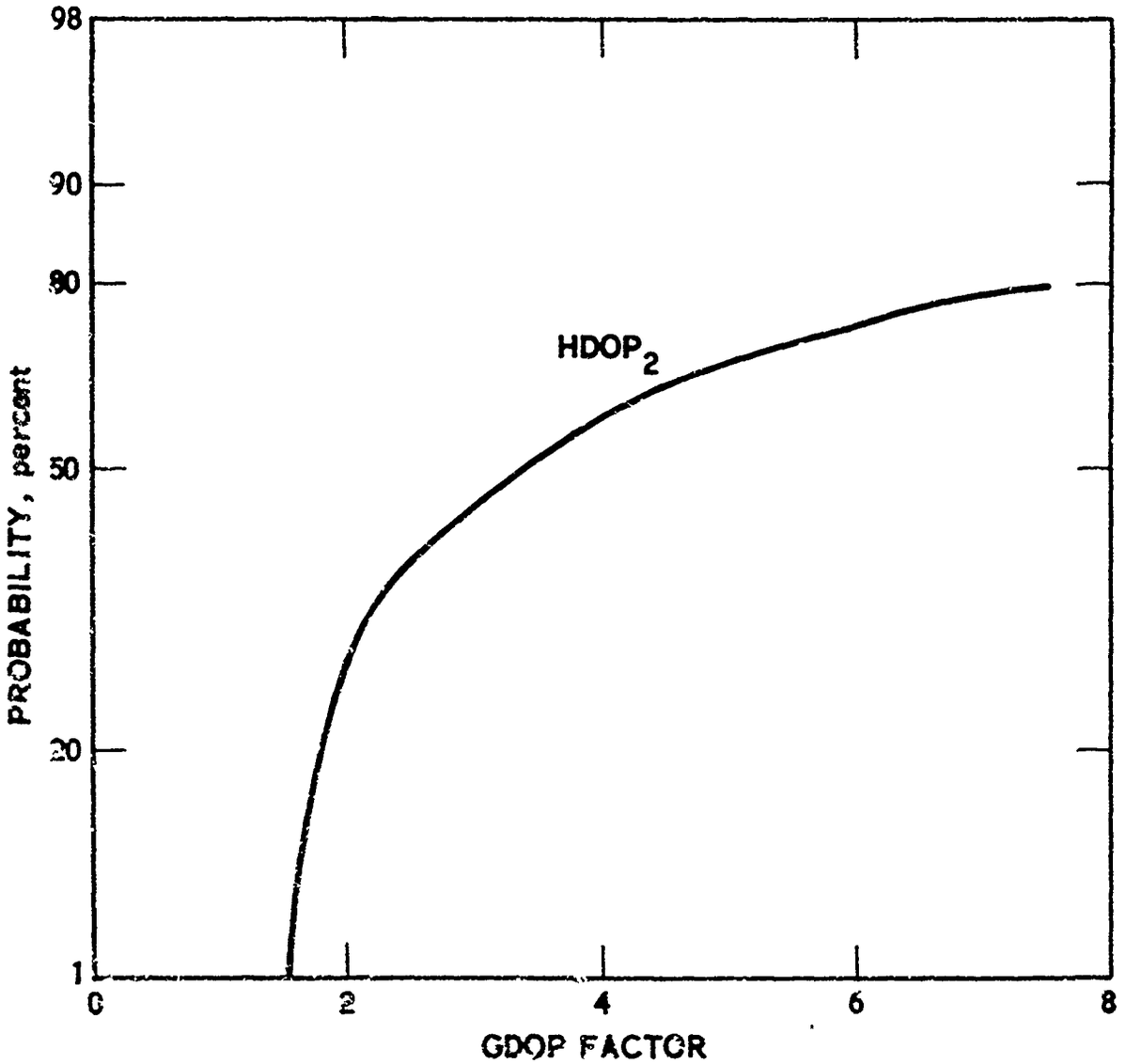

Figure 52. GPS Phase II - 3 X 3 Bunched, Performance for the Global Areas Where Two Satellites are Visible (User Has a Perfect Clock and a Perfect Altimeter)

APPENDIX A

DEFINITION OF THE GEOMETRIC DILUTION OF PRECISION (GDOP)

The equations defining GDOP are derived in this appendix for a pseudoranging user implementation. Under the assumptions introduced regarding pseudoranging error statistics, the results are also applicable to hyperbolic (or range-differencing) implementations. That is, GDOP as here defined is identical for the two implementations.

Consider the vector diagram shown below.

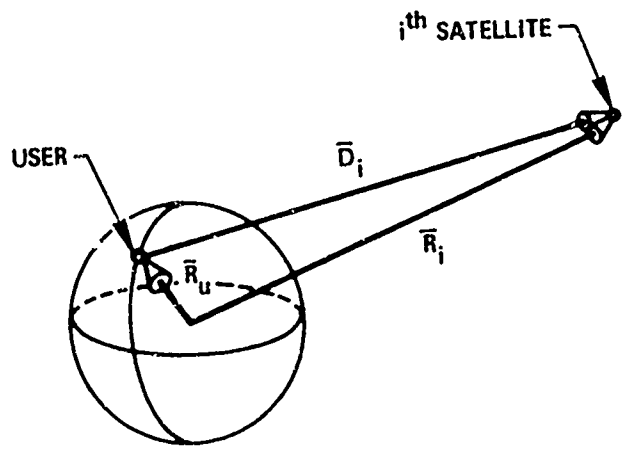

where

$\bar{D}_i$ = Position vector of i^{th} satellite with respect to user

$\bar{R}_i$ = Position vector of i^{th} satellite with respect to origin of an arbitrary coordinate system

$\bar{R}_u$ = Position vector at user with respect to the selected arbitrary coordinate system.

Then, the vector equation corresponding to the above is

$$\bar{R}_u = \bar{R}_i - \bar{D}_i \qquad \text{(A-1)}$$

The magnitude of the range vector $\bar{D}_i$ (the distance from the user to be the i^{th} satellite) can be obtained by dotting $\bar{D}_i$ with its own unit vector $\bar{e}_i$. That is, $\bar{D}_i \triangleq D_i \bar{e}_i$ and therefore $D_i = \bar{D}_i \cdot \bar{e}_i$. Then, dotting $\bar{e}_i$ into both sides of Eq. (A-1)

$$\bar{e}_i \cdot \bar{R}_u = \bar{e}_i \cdot \bar{R}_i - D_i \qquad \text{(A-2)}$$

D_i as it appears in Eq. (A-2) is the actual range of the i^{th} satellite from the user. In the GPS and other pseudoranging systems, the user oscillator is not necessarily synchronized with system time.

If we assume that the user tracks the ranging signal perfectly and that there are no other system biases, the apparent range ρ_i to the i^{th} satellite is

$$\rho_i = D_i + c\Delta t_u = D_i + B_u \qquad \text{(A-3)}$$

where c is the assumed speed of light and Δt_u is the time bias between the user's oscillator and system time. However, there will in general be a fairly well known bias in the satellite oscillator-derived time relative to system time. Call this bias B_i. Then, the perfectly measured apparent range ρ_i, called a pseudorange, is given by

$$\rho_i = D_i + B_u + B_i \qquad \text{(A-4)}$$

The fundamental user pseudoranging equation is obtained from Eq. (A-2) and Eq. (A-4)

$$\bar{e}_i \cdot \bar{R}_u - B_u = \bar{e}_i \cdot \bar{R}_i - \rho_i + B_i; \qquad i = 1,2,\ldots,n \qquad \text{(A-5)}$$

Equation (A-5) summarizes the information on n satellites which is required for the calculation of user position and time bias ($\bar{R}_u$ and B_u). The n equations represented by Eq. (A-5) can be written in expanded matrix form as

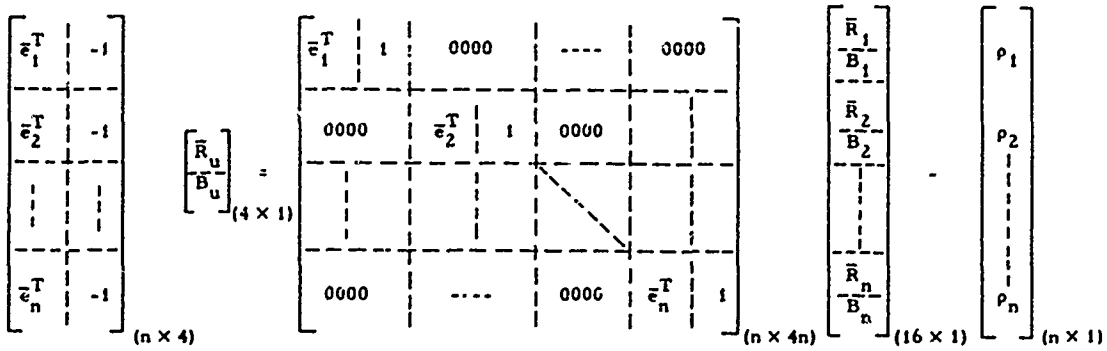

(A-6)

This redundant system of n equations can be solved for the four unknowns represented by $\bar{R}_u$ and B_u.

It will be convenient to write Eq. (A-6) in a more compact form as

$$G_{u_{(n \times 4)}} \bar{X}_{u_{(4 \times 1)}} = A_{u_{(n \times 4n)}} \bar{S}_{(4n \times 1)} - \bar{\rho}_{(n \times 1)} \qquad \text{(A-7)}$$

where $\bar{X}_u$ is the user position and time bias vector, $\bar{S}$ is the satellite position and time bias vector, $\bar{\rho}$ is the n-vector of user pseudoranges, and the matrices G_u and A_u are comprised of satellite-user line-of-sight direction cosines as inferred from Eq. (A-6). Note that $A_u \bar{S}$ is an n-vector of the projections of the satellite position vector $\bar{S}$ on to lines between the user and each i^{th} satellite.

For convenience, represent the right-hand side of Eq. (A-7) by $\bar{\rho}^*$

$$A_u \bar{S} - \bar{\rho} = \bar{\rho}^*$$

and then

$$G_u \bar{X}_u = \bar{\rho}^* \qquad \text{(A-8)}$$

Equation (A-8) is a system of n linear equations with four unknowns (the elements of $\bar{X}_u$). The measurement vector $\bar{\rho}^*$ in general contains

measurement errors due to ephemeris modeling, ionosphere modeling, troposphere modeling, multipath, receiver noise, etc. All sources are included. Then, if $COV(\delta\bar{\rho}^*)$ represents the covariance matrix for the n-vector of errors corresponding to the n-vector $\bar{\rho}^*$, the minimum variance unbiased estimate of $\bar{X}_u$ is given by[1]

$$\hat{\bar{X}}_u = \left[G_u^T \, COV^{-1}(\delta\bar{\rho}^*) \, G_u\right]^{-1} G_u^T \, COV^{-1}(\delta\bar{\rho}^*) \, \bar{\rho}^* \qquad \text{(A-9)}$$

and the covariance of the corresponding error in the estimate of $\bar{X}_u$ is given by

$$COV(\delta\bar{X}_u) = \left[G_u^T \, COV(\delta\bar{\rho}^*) \, G_u\right]^{-1} \qquad \text{(A-10)}$$

Equation (A-10) gives the covariance of the errors in position and time ($\delta\bar{X}_u$) that a user would have if he accurately knew his measurement error characteristics [represented by $COV(\delta\bar{\rho}^*)$] and he made n simultaneous (or almost simultaneous) pseudorange measurements to n satellites. Thus, in Eq. (A-10) $COV(\delta\bar{\rho}^*)$ reflects the instrumentation performance of the system, whereas the factors G_u and G_u^T only reflect the geometry of the system. Although there are some geometrical effects contained in $COV(\delta\bar{\rho}^*)$ (the effect of elevation angle on ionosphere modeling errors, for example), as a good first approximation the geometric performance can be measured by computing $COV(\delta\bar{X}_u)$ in Eq. (A-10) with $COV(\delta\bar{\rho}^*)$ set equal to the identity matrix. This is a fundamental assumption in the calculation of GDOP. The GDOP calculations are therefore defined by

$$COV(\delta\bar{X}_u) = \left(G_u^T \, G_u\right)^{-1} \qquad \text{(A-11)}$$

---

[1] P. B. Liebelt, An Introduction to Optimal Estimation, Addison-Wesley, 1967.

Then the various GDOPs are simply formed from the appropriate elements of COV ($\delta\bar{X}_u$) obtained from Eq. (A-11).

Depending upon the number of satellites seen, the following conventions for calculation of the various GDOPs are used here:

A.1 FOUR OR MORE SATELLITES SEEN

The user solution includes the XYZ position and the user clock bias

$$[G^T G]^{-1} = \begin{array}{c} \begin{matrix} X & Y & Z & t \end{matrix} \\ \begin{vmatrix} \sigma_{11} & \sigma_{12} & \sigma_{13} & \sigma_{14} \\ \sigma_{21} & \sigma_{22} & \sigma_{23} & \sigma_{24} \\ \sigma_{31} & \sigma_{32} & \sigma_{33} & \sigma_{34} \\ \sigma_{41} & \sigma_{42} & \sigma_{43} & \sigma_{44} \end{vmatrix} \end{array}$$

$$\text{PDOP} = \sqrt{\sigma_x^2 + \sigma_y^2 + \sigma_z^2}$$

$$\text{HDOP} = \sqrt{\sigma_x^2 + \sigma_y^2}$$

$$\text{VDOP} = \sqrt{\sigma_z^2}$$

$$\text{TDOP} = \sqrt{\sigma_t^2}$$

A.2 THREE SATELLITES SEEN

The user solution includes the XYZ position when the user has a perfect clock.

$$[G^T G]^{-1} = \begin{array}{c} \begin{matrix} X & Y & Z \end{matrix} \\ \begin{vmatrix} \sigma_{11} & \sigma_{12} & \sigma_{13} \\ \sigma_{21} & \sigma_{22} & \sigma_{23} \\ \sigma_{31} & \sigma_{32} & \sigma_{33} \end{vmatrix} \end{array}$$

$$PDOP_{3t} = \sqrt{\sigma_x^2 + \sigma_y^2 + \sigma_z^2}$$

$$HDOP_{3t} = \sqrt{\sigma_x^2 + \sigma_y^2}$$

$$VDOP_{3t} = \sqrt{\sigma_z^2}$$

The user solution includes the XY position and time bias when the user has a perfect altimeter.

$$[G^T G]^{-1} = \begin{array}{c} \begin{matrix} X & Y & t \end{matrix} \\ \begin{vmatrix} \sigma_{11} & \sigma_{12} & \sigma_{13} \\ \sigma_{21} & \sigma_{22} & \sigma_{23} \\ \sigma_{31} & \sigma_{32} & \sigma_{33} \end{vmatrix} \end{array}$$

$$HDOP_{3a} = \sqrt{\sigma_x^2 + \sigma_y^2}$$

$$TDOP_{3a} = \sqrt{\sigma_t^2}$$

A.3 TWO SATELLITES SEEN

The user solution includes the XY position when the user has a perfect clock and a perfect altimeter.

$$[G^T G]^{-1} = \begin{vmatrix} & X & Y \\ X & \sigma_{11} & \sigma_{12} \\ Y & \sigma_{21} & \sigma_{22} \end{vmatrix}$$

$$HDOP_2 = \sqrt{\sigma_x^2 + \sigma_y^2}$$

It turns out that the GDOP equation for COV $[\delta(d\bar{x}_u/dt)]$, (velocity components), is identical to Eq. (A-11).

B.1 ALGORITHMS ASSOCIATED WITH THE SATELLITE SELECTION PROCESS

The selection of satellites which provide optimum navigation performance over a specified time interval (Δt) requires that a simple form of ephemerides or equivalent information for all satellites be stored in the user computer. This could be in terms of the six classical orbit elements (i, e, ω, Ω, t_o, T). The signal codes identifying all satellites must also be stored.

In addition, based upon the present estimate of user position and/or time, proper algorithms and other software to perform the selection process must be available. These include:

a. Calculation of all satellite position vectors and velocity vectors

b. Calculation of the user position vector

c. Calculation of unit vectors along the user-to-satellite line of sight

d. Identification of the candidate population of satellites which complies with the visibility criteria of being above a given elevation angle after a certain length of time

e. Identification of the highest satellite in the sky and all satellite combinations amongst the available population (minus one satellite) taken three at a time, using the highest in the sky to form the combinations of four

f. Calculation of the volume of the tetrahedron formed by the four unit vectors to each satellite for all combinations and the volume rate of change

g. Calculation of the mean geometric volume for all combinations based upon the present time and some future time

h. Selection logic to ensure that volumes do not have zero value transitions during the time interval considered

i. A comparison of all volumes to identify the maximum mean volume for the satellite combination providing the best navigation performance, the identity of the four satellites, and the signal codes.

Pages 106, 107 & 108 are Blank

Figure B-1 provides a flow chart of the computation processes. For the basic navigation determination process, many of the algorithms to perform the above computations are available in the user computer. A few are described in more detail to acquaint the reader with the process.

B.2 ELEVATION RATE OF CHANGE

Consider the vectors depicted below.

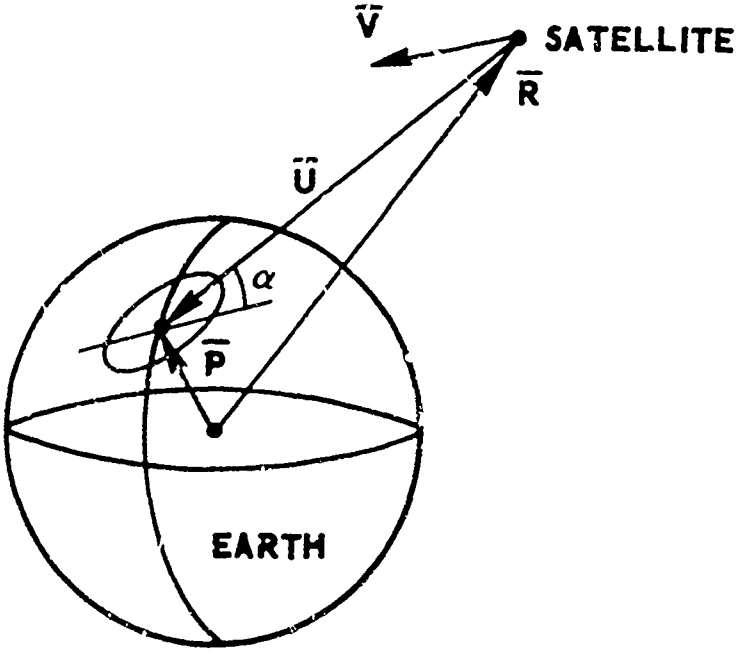

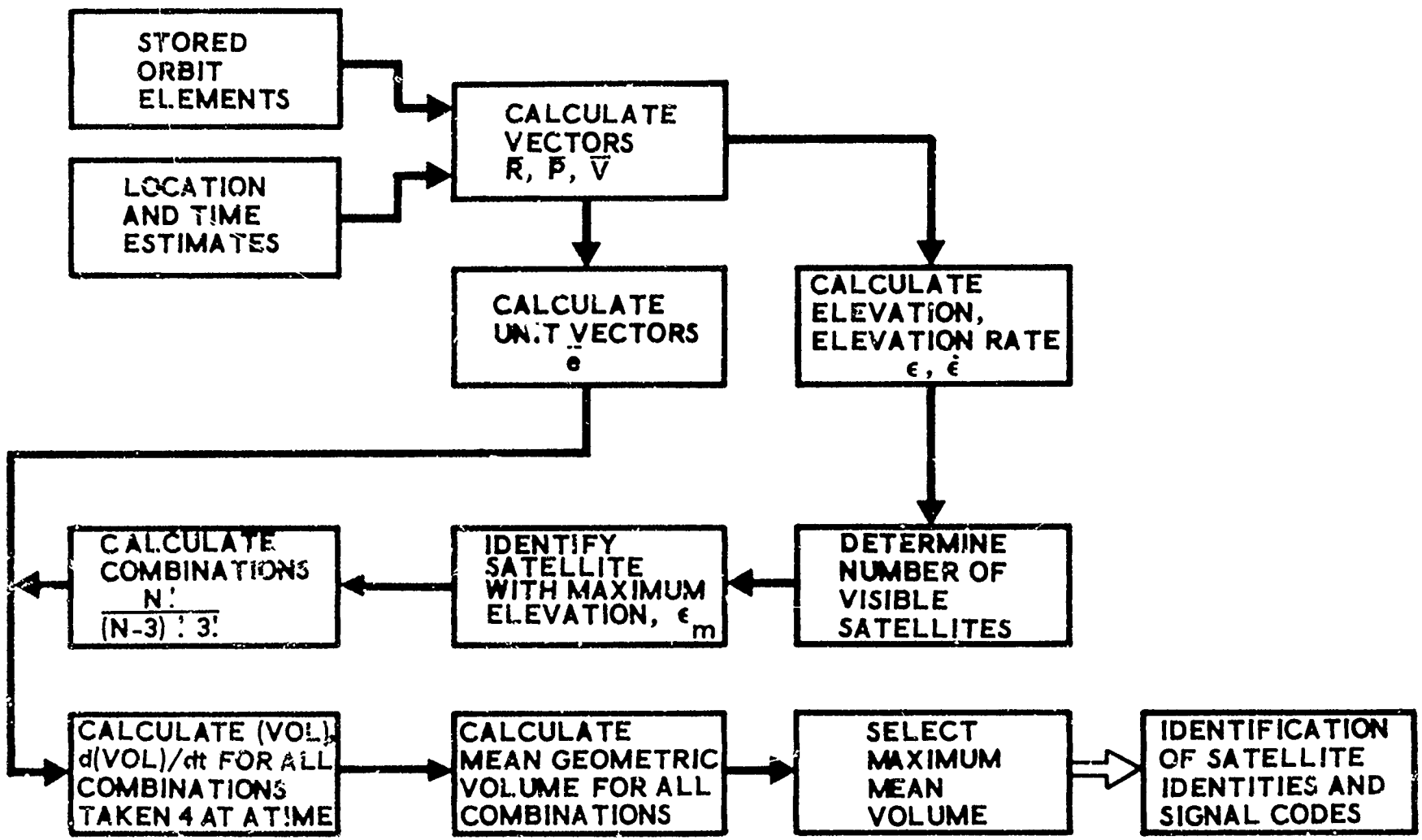

Figure B-1. Satellite Selection Method Flow

Based upon the stored orbit elements and the estimate of user position and time, the following vectors can be determined:

$\overline{R}$ satellite position vector

$\overline{V}$ satellite velocity vector

$\overline{P}$ user position vector

$\overline{U}$ satellite-to-user vector

From algebra,

$$\tan\alpha = -\frac{\overline{P}\cdot\overline{U}}{|\overline{P}|\,|\overline{U}|} \Big/ \frac{|\overline{P}\times\overline{U}|}{|\overline{P}|\,|\overline{U}|} = -\frac{\overline{P}\cdot\overline{U}}{|\overline{P}\times\overline{U}|} \tag{B-1}$$

By differentiation,

$$\sec^2\alpha\,\dot{\alpha} = -\frac{|\overline{P}\times\overline{U}|\,(\overline{P}\cdot\dot{\overline{U}} + \dot{\overline{P}}\cdot\overline{U}) - \overline{P}\cdot\overline{U}\,(\overline{P}\times\dot{\overline{U}} + \dot{\overline{P}}\times\overline{U})\cdot\overline{e}_b}{|\overline{P}\times\overline{U}|^2} \tag{B-2}$$

where $\overline{e}_b$ = unit vector of $\overline{P}\times\overline{U}$.

Since by definition $\dot{\overline{P}}$ equals zero and $\dot{\overline{U}} = -\overline{V}$, the elevation rate of change is

$$\dot{\alpha} = \frac{|\overline{P}\times\overline{U}|\,(\overline{P}\cdot\overline{V}) - \overline{P}\cdot\overline{U}\,(\overline{P}\times\overline{V})\cdot\overline{e}_b}{|\overline{P}|^2\,|\overline{U}|^2} \tag{B-3}$$

The allowable rate of change of elevation angle ($\dot{\alpha}$) for the time interval Δt is simply determined from

$$\alpha + \dot{\alpha}\,\Delta t \geq 5 \text{ deg} \tag{B-4}$$

Candidate satellites to be considered for the visibility population statistics are, therefore, those satellites whose elevation angle α [Eq. (B-1)] and elevation rate $\dot{\alpha}$ [Eq. (B-3)] satisfy the condition of Eq. (B-4).

B.3 UNIT VECTOR VOLUME

Consider the vectors depicted in Figure B-2a. Based upon the previous calculation, the following vectors are known:

$\overline{R}_n$ satellite position vector

$\overline{V}_n$ satellite velocity vector

$\overline{P}_n$ user position vector

$\overline{U}_n$ user-to-satellite vector (LOS)

$\overline{e}_n$ unit vector from user to satellite

All unit vectors by definition must be contained within the unit sphere centered at the user location as depicted in Figure B-2b for any combination of the four satellites taken from the population of visible satellites.

If lines are drawn between the four unit vector points (Figure B-2b), a tetrahedron is formed.

Depending upon the directions of the unit vectors, the shape of this tetrahedron may take many forms. As an example, the volume may be at its maximum value when the three lower unit vectors are 120 deg apart, or the volume will be zero when all four unit vectors lie in one plane.

It can be shown that there is an extremely high correlation between the volume of the tetrahedron and GDOP.

Consider the vectors $\overline{A}$, $\overline{B}$, and $\overline{C}$ defined in Figure B-2c. These vectors can be obtained by the proper subtraction of the unit vectors $\overline{e}_1$, $\overline{e}_2$, $\overline{e}_3$, $\overline{e}_4$. As a consequence, the volume of the tetrahedron is found from the triple scalar product of the vectors $\overline{A}$, $\overline{B}$, and $\overline{C}$: i.e.,

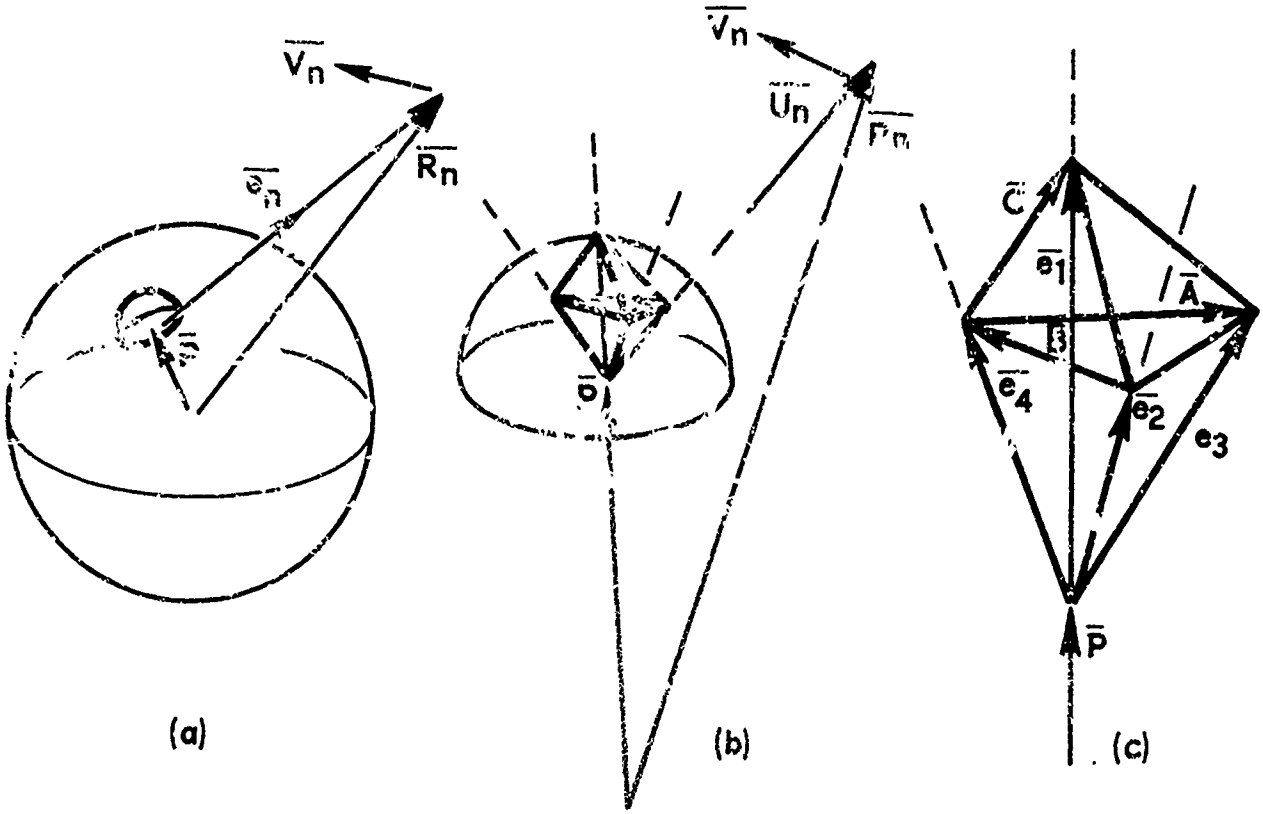

Figure B-2. Unit Volume Vectors

$$V = \frac{1}{6}\,\overline{C}\cdot(\overline{A}\times\overline{B}) \tag{B-5}$$

By differentiation,

$$\dot{V} = \frac{1}{6}\,\overline{C}\cdot(\overline{A}\times\dot{\overline{B}}) + \overline{C}\cdot(\dot{\overline{A}}\times\overline{B}) + \dot{\overline{C}}\cdot(\overline{A}\times\overline{B}) \tag{B-6}$$

By definition it is known that

$$\left|\overline{U}_n\right|\overline{e}_n = \overline{R}_n - \overline{P} \tag{B-7}$$

and hence

$$\left(\dot{\overline{U}}_n\cdot\overline{e}_n\right)\overline{e}_n + \left|\overline{U}_n\right|\dot{\overline{e}}_n = \dot{\overline{R}}_n - \dot{\overline{P}} \tag{B-8}$$

Since $\dot{\overline{R}}_n = \overline{V}_n$ (see Figure B-2a) and $\dot{\overline{P}} = 0$,

$$\dot{\overline{e}}_n = \frac{\overline{V}_n - \left(\overline{V}_n\cdot\overline{e}_n\right)\overline{e}_n}{\left|\overline{U}_n\right|} \tag{B-9}$$

$\dot{\overline{A}}$, $\dot{\overline{B}}$ and $\dot{\overline{C}}$ can now be found by the proper subtraction of the unit vector derivatives $\dot{\overline{e}}_n$ ($n = 1, 2, 3, 4$) and substituted into Eq. (B-9) from which the instantaneous rate of change of the unit vector volume can be calculated.

The volume (V_t) at some future time (t) can be found from the present volume (V_o) by

$$V_t = V_o + \dot{V}_o\,(t - t_o) \tag{B-10}$$

Hence the mean geometric volume (V_m) in this time interval is

$$V_m = 2\left(\frac{1}{V_o} + \frac{1}{V_t}\right)^{-1} \qquad \text{(B-11)}$$

Since negative and positive volumes are defined by Eq. (B-5), the simple logic

$$V_o\, V_t > 0 \qquad \text{(B-12)}$$

ensures that zero volume transitions are not included in the selection process comparing $|V_m|$ for all combinations.